

Cover Page



Universiteit Leiden



The handle <http://hdl.handle.net/1887/21009> holds various files of this Leiden University dissertation.

**Author:** Guérolé, Aude

**Title:** Dissection of DNA damage responses using multiconditional genetic interaction maps

**Issue Date:** 2013-06-25

*Dissection of DNA  
damage responses using  
multiconditional genetic  
interaction maps*

Aude Guénoilé

Dissection of DNA damage responses using multiconditional genetic interaction maps  
Aude Guénolé

Thesis, Leiden University  
June 25, 2013

Cover front page: "Inextricable matière" by Simon Guieu  
Cover rear page: "The end eventually" by Samuel Guénolé  
layout: Aude Guénolé  
Printing: Ipskamp Drukkers, Enschede, The Netherlands

ISBN: 978-94-6191-780-5

© 2013, Aude Guénolé

All right reserved. No parts of this thesis may be reprinted or reproduced or utilized in any form or by electronic, mechanical, or other means, now known or hereafter invented, including photocopying and recording, or in any information storage or retrieval system without written permission of the author.

Dissection of DNA  
damage responses using  
multiconditional genetic  
interaction maps

ter verkrijging van  
de graad van Doctor aan de Universiteit Leiden,  
op gezag van Rector Magnificus Prof. Mr. C.J.J.M. Stolker,  
volgens besluit van het College voor Promoties  
te verdedigen op dinsdag 25 juni 2013  
klokke 08.45 uur

door

Aude Guénoilé  
geboren te Léon, Frankrijk in 1983

## **Promotiecommissie**

### **Promotor:**

Prof. Dr. L. Mullenders

### **Co-promotor:**

Dr. H. van Attikum

### **Overige Leden:**

Prof. Dr. P. J. J. Hooykaas

Prof. Dr. J. T. den Dunnen

Dr. D. van Gent (Erasmus Medical Center Rotterdam)

The research described in the thesis was performed at the department of Toxicogenetics at the Leiden University Medical Center (LUMC) and was financially supported by Dutch NWO.

*"Where there is a will there is a way"*  
Henry Hudson  
(1565-1611)

## ABBREVIATIONS

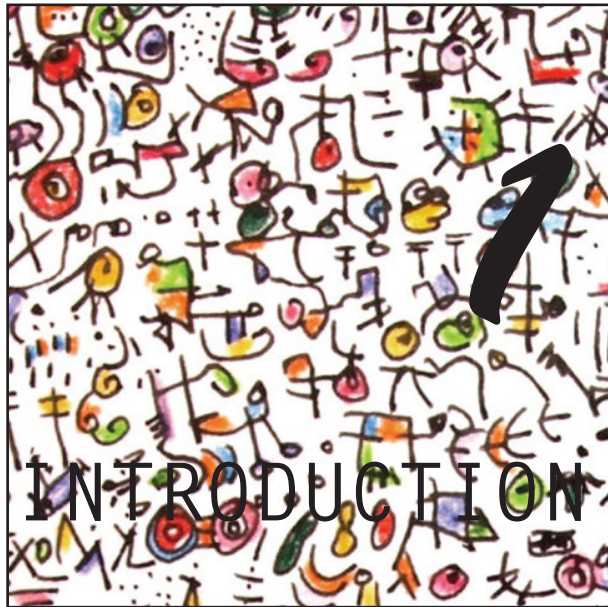
DNA	Deoxyribonucleic acid
IR	Ionizing radiation
UV	Ultra violet
DDR	DNA damage response
AT	Ataxia telangectasia
ATM	Ataxia telangectasia mutated kinase
PI3K	Phosphatidylinositol 3-kinase-related kinase
ATR	Ataxia telangectasia and Rad3 related kinase
ssDNA	single strand DNA
DNA-PKcs	DNA-dependent protein kinase catalytic subunit
DSB	Double-strand break
RPA	Replication protein A
APC	Anaphase promoting complex
FHA	Forkhead-associated
RNR	Ribonucleotide reductase
dNTP	Desoxyribonucleotides
MMS	Methyl methanesulfonate
HU	Hydroxyurea
H2AX	Histone H2A.X
H3	Histone H3
K56R	Lysine on position 56 replaced by an arginine
6-4PP	6-4 Photoproduct
CPD	Cyclobutane pyrimidine dimer
NER	Nucleotide excision repair
XP	Xeroderma pigmentosum
RNA	Ribonucleic acid
BER	Base excision repair
SSB	Single-strand break
MMR	Mismatch excision repair
PCNA	Proliferating cell nuclear antigen
E1	Ubiquitin-activating enzyme
E2	Ubiquitin-conjugating enzyme
E3	Ubiquitin-ligating enzyme
PRR	Post-replication repair
TLS	Translesion synthesis
NHEJ	Non-homologous end joining
HR	Homologous recombination
SUMO	Small Ubiquitin-like Modifier
CRL	Cullin-RING ligase
EMAP	Epistatic mini-array profiling
dE-MAP	differential epistasis mapping
CPT	Camptothecin
ZEO	Zeocin
DDC	DNA damage checkpoint
GCR	Gross chromosomal rearrangement

## TABLE OF CONTENTS

<b>Abbreviations</b>		7
<b>Chapter 1</b>	Introduction and outline of this thesis	9
<b>Chapter 2</b>	A Multi-Conditional Genetic Interaction Map to Dissect DNA Damage Response Pathways	29
<b>Chapter 3</b>	Rtt109 chromatin modifier regulates mutagenic DNA damage bypass	51
<b>Chapter 4</b>	Neddylation affects cell cycle control and genome integrity	67
<b>Chapter 5</b>	Irc21 is a general response factor in checkpoint control, repair and genome stability	81
<b>Chapter 6</b>	Sae2 and Pph3 cooperate to promote DNA repair and checkpoint recovery	95
<b>Chapter 7</b>	General discussion	109
<b>Appendix</b>	Nederlandse samenvatting	119
	English summary	123
	Résumé en français	127
	Acknowledgments	131
	Curriculum Vitae	133
	Publications	135







**DNA damage**

The genetic information contained in the DNA dictates the structure, the organization and function of the cell. Thus, it is of major importance for every cell in a tissue or organ that compose an organism to protect the integrity of its genetic information. Especially due to its chemical composition, DNA is a fragile molecule, susceptible to DNA damage formation, when exposed to various genotoxic threats. In the environment, ionizing and ultraviolet radiation (IR and UV) as well as certain chemicals are examples of such genotoxic threats corrupting the chemical structure of DNA. Additionally, byproducts of normal cellular metabolic reactions such as oxygen radicals can interact with and damage the DNA molecule. As a consequence of these numerous attacks, the frequency of DNA damage induced in human cells is estimated to be around 1,000 to 1,000,000 lesions per cell per day [1, 2]. If left unrepaired or repaired inaccurately these lesions can lead to chromosomal aberrations and mutations, which in turn can lead to genome instability, cancer development or cell death [3]. In addition, during replication, DNA duplication by polymerases, although tightly regulated, leaves errors that modify the original information and can also result in mutations.

**DNA damage responses**

To combat DNA damage, cells have evolved an intricate system known as the DNA damage response (DDR), which senses DNA lesions and activates downstream pathways such as chromatin remodeling, cell cycle checkpoints and DNA repair [4]. Primarily, the DDR was defined as a cascade of reactions transmitting the signal from sensor proteins to downstream effectors via transducers that altogether coordinate gene expression, cell cycle progression and repair. However, it becomes apparent that this signaling pathway is not as linear as thought. Sensors can be part of effector

or transducer complexes (e.g component of replication fork) or repair factors can feedback to sensors and thus play roles of transducer.

Importantly, dysfunctions in the DDR have been linked to human diseases. For example, defects in repair and signaling were found to result in chromosome aberrations that are hallmarks of multiple cancers such as lymphomas or osteosarcomas [5]. Human syndromes such as Ataxia telangiectasia (AT and AT-like) and Nijmegen breakage syndrome are caused by mutations in the central checkpoint kinase, ATM and Nbs1 respectively. The latter is a component of the MRN complex involved repair of DNA double stranded breaks. These are examples that stress the importance of the DDR for human health.

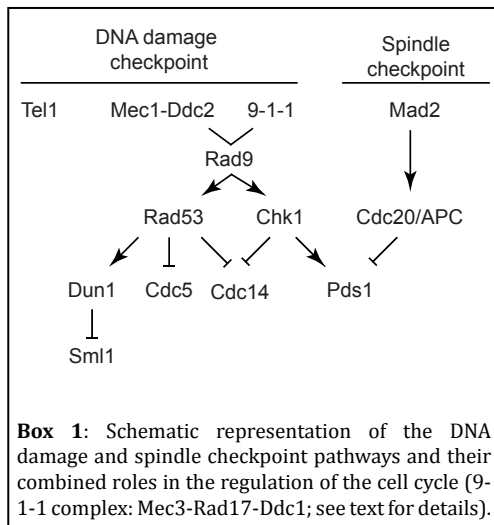
Most of these DDR pathways and factors are conserved from yeast to mammals. Since my thesis work dealt with the budding yeast *Saccharomyces cerevisiae*, I will focus on this model organism to give an overview of the different processes composing the DDR and will occasionally refer to the mammalian DDR.

**Checkpoint signaling pathways**

One essential and early component of the DDR is the DNA damage checkpoint. Its role is to delay the G1/S transition, arrest cells at the G2/M boundary or slow down S-phase progression upon induction of DNA damage to allow time for repair. In S-phase, in addition to the DNA damage checkpoint, the replication checkpoint operates to slow down replication and inhibit firing of late origins of replication when cells experience a replicative stress.

*Mec1 and Tel1 kinases activate checkpoint-signaling cascades*

The key components of these checkpoint pathways are the two phosphoinositol-3-kinase related (PI3K) kinases Mec1 and Tel1 (Box 1). ATM and ATR are the mammalian



homologues of Tel1 and Mec1, respectively. Mec1/ATR is crucial for signaling ssDNA at DNA lesions and stalled replication forks while mainly Tel1/ATM signals DSBs. DNA-PKcs, another mammalian PI3K kinase, which has no homologue in yeast, is involved in the detection and repair of DSB by non-homologous end-joining [6].

Recruitment of Tel1 and Mec1 to sites of DNA damage is essential for the activation of downstream signal transduction pathways. The recruitment of these kinases involves different complexes that recognize the DNA lesions. Mec1 binds to its partner Ddc2, which recognizes ssDNA coated with replication protein A (RPA) complex at stalled or collapsed forks and DSBs [7]. On the other hand, Tel1 is recruited to sites of DSB by the Mre11-Rad50-Xrs2 (MRX) complex, which tethers the ends [8].

Another group of proteins is required for the Ddc2-independent recruitment of Mec1 to sites of DNA damage [9, 10]. The Rad24-RFC complex, normally sliding on the DNA during replication, loads the Mec3-Rad17-Ddc1 complex (9-1-1 complex;

Box 1) upon detection of aberrant DNA structures [11]. The 9-1-1 complex was then suggested to attract and stimulate Mec1 activity at the lesion by direct interaction with the 9-1-1 component, Ddc1 [12].

At last, the replication initiation and S-phase checkpoint factor Dpb11 was also found to physically and genetically interact with Ddc2-Mec1 [13]. The current evidence suggests that Dpb11 and the 9-1-1 complex independently recruit and activate Mec1 at DNA lesions.

#### *Chk1 and Rad53 kinases control DNA damage-induced cell cycle arrest*

Mec1 and Tel1 are the two kinases that are at the top of checkpoint signaling cascade. They activate by phosphorylation a number of downstream DDR factors. Two of these are the downstream checkpoint-transducing kinases, Chk1 and Rad53 (Box 1). Chk1 and Rad53 form two parallel pathways that amplify the checkpoint signal and promote cell cycle arrest by phosphorylation of a multitude of DDR and cell cycle regulators.

Chk1 becomes only activated by Mec1 in a process that necessitate the adaptor kinase Rad9 [14] (Box 1). Its main target is the anaphase inhibitor Pds1. Hyperphosphorylated-Pds1 is stabilized and provokes cell cycle arrest before anaphase. Indeed, Pds1 phosphorylation prevents its ubiquitylation by the anaphase promoting complex in conjunction with Cdc20 (Cdc20/APC) and its subsequent degradation which is needed for sister chromatid separation during normal cell cycle [15, 16]. Chk1 also contributes to the inhibition of mitotic exit by inactivating the Cdc14 early anaphase release (FEAR) pathway (Box 1). Cdc14 desphosphorylates the targets of the cyclin-dependent kinase 1 (Cdk1) and thereby allows mitotic exit [17]. Thus, it is thought

that Chk1 either directly or via stabilization of Pds1 prevents release of the phosphatase Cdc14 from the nucleolus.

Although both Tel1 and Mec1 can activate Rad53, Mec1 seems to be the prime kinase for this process. Rad53 activation depends on two adaptor proteins Rad9 and Mrc1 that are also phosphorylated by Mec1 and Tel1. Rad53 has two FHA domains (FHA1 and FHA2), which mediate the interactions with the phosphorylated adaptor protein leading to activation and autophosphorylation of Rad53 [18]. Mrc1 and Rad9 are partially redundant in transducing replication stress signals [19]. However, Mrc1 as part of the replisome functions in the replication checkpoint while Rad9 signals DNA damage in S-phase [20].

Rad53's most-studied target is the Dun1 kinase (Box 1). Dun1 also has an FHA domain that mediates its interaction with phosphorylated-Rad53 leading to Dun1 activation [21]. Dun1 is required for the DNA damage-induced transcription of numerous genes, some of which promote cell cycle arrest in G2/M. Sml1, the ribonucleotide reductase (RNR) transcription inhibitor, is Dun1's best-characterized target. Upon phosphorylation, Sml1 is targeted for degradation, which results in increased RNR-dependent dNTP synthesis [22, 23]. Rad53 also affects Pds1 stability by preventing the Cdc20-Pds1 interaction thereby inhibiting recruitment of the APC complex as well as Pds1 degradation [24]. Finally, Rad53 was also proposed to inhibit the mitotic exit network (MEN) in two ways. First, similar to Chk1, it prevents Cdc14 release from the nucleolus and dephosphorylation of Cdk1 targets required for mitotic exit. Secondly, it inhibits the Cdc5 polo-like kinase, which consequently suppresses the MEN [16] (Box 1). However, the exact mechanism by

which Rad53 abolishes the MEN is unclear and needs further investigation.

*The spindle checkpoint collaborates with the DNA damage checkpoint to regulate cell cycle progression.*

The spindle checkpoint controls the accurate segregation of the chromosomes by inspecting the attachment of microtubules to the kinetochores that are complexes of proteins associated with the centromeres. This checkpoint seems to sense the tension present at the kinetochores upon bipolar attachment [25]. Normally activated upon microtubule damage, the spindle checkpoint also contributes to DNA damage checkpoint-induced G2/M arrest. The spindle checkpoint stabilizes Pds1 by inhibiting the APC complex (Box 1). However, it is not known whether the spindle checkpoint is activated upon DNA damage induction. Nevertheless, cells deleted for the spindle checkpoint protein Mad2 are sensitive to DNA damaging agents (MMS and HU). Moreover, loss of Mad2 in *rad53Δchk1Δ* double mutant eliminates residual cell-cycle arrest after UV treatment suggesting that the spindle and the DNA damage checkpoints work redundantly [26]. On the other hand, Rad9 and Rad53 were also found regulated by the spindle checkpoint. They are both phosphorylated after nocodazole-induced microtubule damage in Mad2-dependent and Mec1-independent fashions, which means that the DNA damage and the spindle checkpoints interplay with each other [27]. Yet, the exact roles of Rad9 and Rad53 in the spindle damage checkpoint are not clear.

*Checkpoint recovery and adaptation*

Cells need to inactivate the DNA damage checkpoint in order to re-enter the cell cycle. Conceivably, checkpoint inactivation

should occur either when repair of the DNA damage has been completed or when cells adapt to an irreparable lesion.

Checkpoint inactivation due to completion of repair is called checkpoint recovery and is initiated by the disappearance of DNA lesions. Then, constitutive inhibitors of the checkpoint can revert each step of the signal transduction cascade. For example, work from Keogh and coworkers showed that the phosphatase complex Pph3-Psy2 dephosphorylates  $\gamma$ H2AX, a histone phosphorylated by Mec1 and Tel1 during the early steps of the DDR. Indeed, persistent  $\gamma$ H2AX results in prolonged checkpoint activation even when repair has occurred [28]. Moreover, Pph3-Psy2 and two other phosphatases, Ptc2 and Ptc3 were also found to dephosphorylate Rad53 thereby allowing cell cycle resumption after completion of repair [29, 30]. In human cells, on the other hand, Wip1 and the phosphatase PP2A were found to dephosphorylate both Chk1 and Chk2 (the mammalian homolog of Rad53).

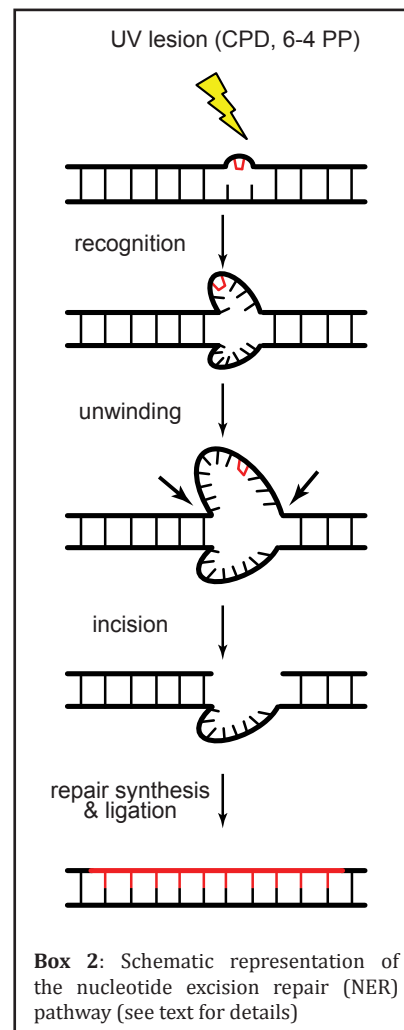
In yeast, inactivation of the checkpoint due to an irreparable DSB is called adaptation. Cells restart progression through the cell cycle while the damage persists. Many factors involved in repair (e.g Rad54, Rad51, Sae2, yKu70, Srs2), cell cycle regulation (e.g CKII, Cdc5) or checkpoint inhibition (Ptc2, Ptc3, Pph3) have been implicated in adaptation. Whereas adaptation is a process that leads to genomic instability [31], it appears to promote viability in cells carrying an irreparable DSB. Importantly, under these conditions, mammalian cells likely activate senescence or apoptosis. However, work from Yoo et al. showed that in xenopus egg extracts treated with the replication inhibitor aphidicolin, Chk1 is deactivated and the nuclei enter in mitosis while DNA

replication is incomplete [32]. This suggests that other organisms than yeast may adapt to irreparable DNA damage.

## DNA repair

### *Nucleotide excision repair*

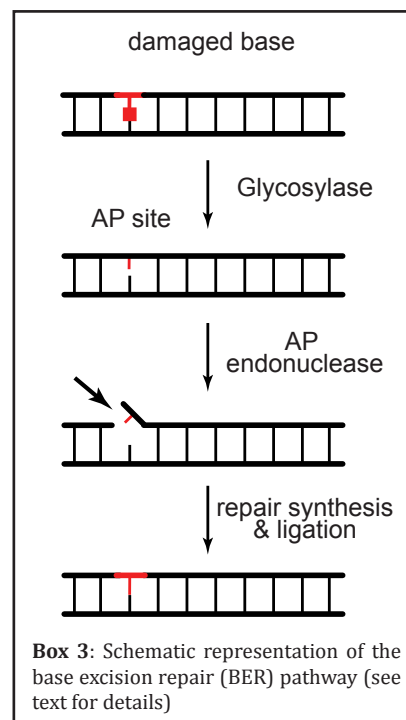
UV induces two main types of photoproducts: 6-4 photoproducts (6-4 PP) and cyclobutane pyrimidine dimers (CPDs), which are repaired by nucleotide excision repair (NER). In humans, mutations in NER factors result in Xeroderma Pigmentosum (XP) and Cockayne syndrome (CS) diseases.



XP patients show an extreme sensitivity towards sunlight and develop skin cancers in sun-exposed parts of the body with an abnormally high incidence. CS patients also display photohypersensitivity (which does not give rise to cancer development) but more prominently mental and psychomotor retardation among other severe developmental and neurological disorders. NER is composed of two sub-pathways called transcription-coupled (TC-NER) and global genome repair (GG-NER). While the first pathway operates on lesions in transcribed strands and is activated by stalling of RNA polymerase II, GG-NER takes care of removing UV lesions from the rest of the genome. Generally, TC-NER and GC-NER follow a 3-steps mechanism starting from the detection of the photolesion followed by excision of the oligonucleotide-containing lesion and completion of repair by a gap-filling step recovering the lost information (Box 2) [33]. Although they differ at the DNA damage recognition step, the two pathways remove the lesion by a common mechanism using a core set of repair factors. In yeast Rad4/Rad23 (XPC/hRad23), Rad7/Rad16 (functional equivalent of mammalian UVDDDB1/2) and Rad26-RNA Pol II (CSB/RNA pol II) are the factors that detect helix-distorting lesions during GG-NER and TC-NER respectively. The Rad4/Rad23 complex works in both GG-NER and TC-NER while Rad7/Rad16 is specific to GG-NER. Rad14-RPA (XPA/RPA) is another complex that acts in the two NER subpathways. TFIIH helicases subunits Rad3 and Rad25 help to unwind the DNA before the incision step, which is carried out by the two structure dependent endonucleases Rad1-Rad10 and Rad2 at the 5' and 3' side, respectively, of the damage. The DNA binding complexes Rad14-RPA and Rad4-Rad23 are also essential for the incision of the damage. In the last step, the replication machinery fills the gap and completes repair [34].

### Base excision repair

Base-excision repair (BER) removes damaged bases such as 8-Oxoguanine or apurinic/pyrimidinic sites (AP) from the DNA (Box 3). First, the damage is recognized by enzymes called N-glycosylases each having specific substrates, that cleave the DNA to remove the damaged bases from the DNA backbone leaving an AP site. Next, cleavage of AP sites by AP endonucleases or AP lyases lead to the formation of 5' and 3' blocked single strand break (SSB), respectively. In most cases, BER reactions are initiated by 5' incision of the AP site by either Apn1 or Apn2 AP endonuclease. Then, Polymerase  $\epsilon$  can use the 3' end to fill the gap, which generates a 5' single strand overhang further removed by the flap endonuclease Rad27. The final step is the ligation by the Cdc9 ligase [35]. This long-patch BER pathway is the most common in yeast. Higher eukaryotes possess the multifunctional DNA polymerase  $\beta$ , which



favors a short-patch repair mechanism. This polymerase is able to insert one nucleotide and removes the 5' extremity through lyase activity. The following ligation step is performed by XRCC1-Lig3 [36]. In the case of 3' blocked SSBs, resulting from 3' incision of the AP site by AP lyases such as Ntg1, Ntg2 or Ogg1, the BER reaction involves the Rad1-Rad10, a structure-specific flap endonuclease that cleaves the 3' extremity of the AP site.

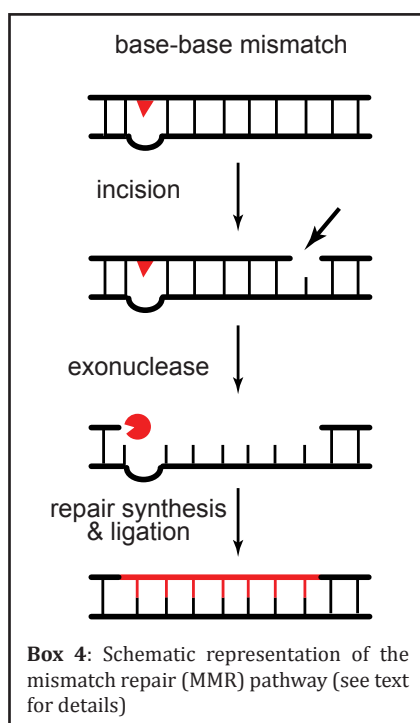
#### Mismatch repair

Mismatch repair (MMR) is particularly important to correct errors that arise from mispairing during replication such as base mismatches, small insertions or deletions (Box 4). In humans, defects in mismatch repair lead to microsatellite instability, which is notably observed in hereditary non-polyposis colorectal cancer (HNPCC) [37]. Msh2, together with Msh3 or Msh6 forms two heterodimers that recognize the

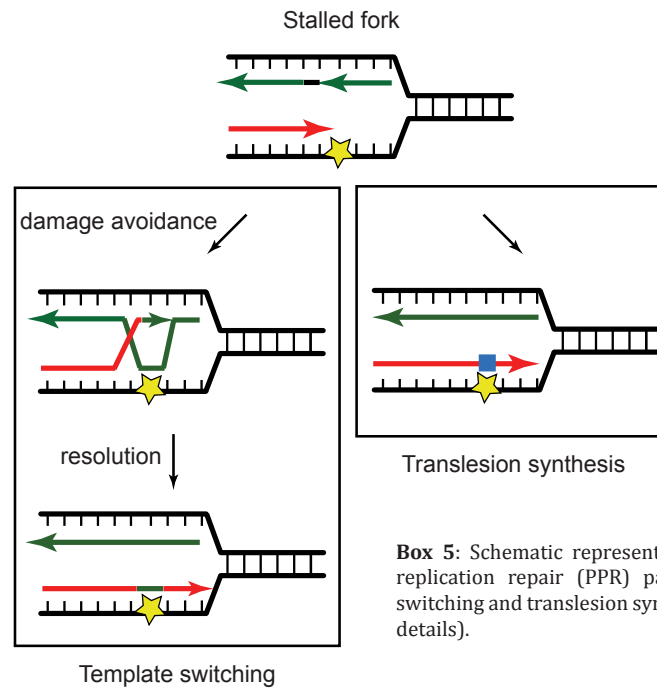
errors in the DNA. Msh2-Msh6 recognizes base mismatches and insertions (1-2 nucleotides) or deletion loops while Msh2-Msh3 detects insertion/deletion loops only. The binding of either of the two complexes induces a conformational change that attracts the Mlh1-Pms1 complex to the lesion. A nick on either side of the mismatch allows further processing by exonucleases such as Exo1. To date, no process has been found responsible for this nick. Whereas, in the lagging strand, nicks are likely due to the formation of Okazaki fragments, it is not clear how they are introduced in the leading strand. The 5' to 3' exonuclease activity was suggested to be performed by Exo1 and Rad27 while the only 3' to 5' exonucleases activity have been associated with the replication polymerases  $\delta$  and  $\epsilon$ . In fact, the proliferating nuclear cell antigen (PCNA) binds multiple components of the recognition complexes and likely recruits Pol $\delta$  and  $\epsilon$  to the mismatch [38]. Then, the polymerases are thought to complete the repair process by performing the DNA synthesis and ligation steps [39]. It is important to note that NER and BER factors genetically and physically interact with MMR components, which suggests extensive crosstalks between these pathways.

#### Post-replication repair

Lesions that are not removed by the earlier mentioned repair pathways before resumption of DNA replication, can interfere with the replication machinery and block its progression (Box 5). Two post-replication repair (PRR) mechanisms can bypass these lesions namely translesion synthesis (TLS) and template switching. PCNA is responsible for the initiation of PRR and for the choice of the bypass pathway. When replication forks are blocked by DNA lesions, PCNA is ubiquitinated by the Rad6-Rad18, an ubiquitin E2 conjugating-E3 ligating enzyme complex. Monoubiquitilation of







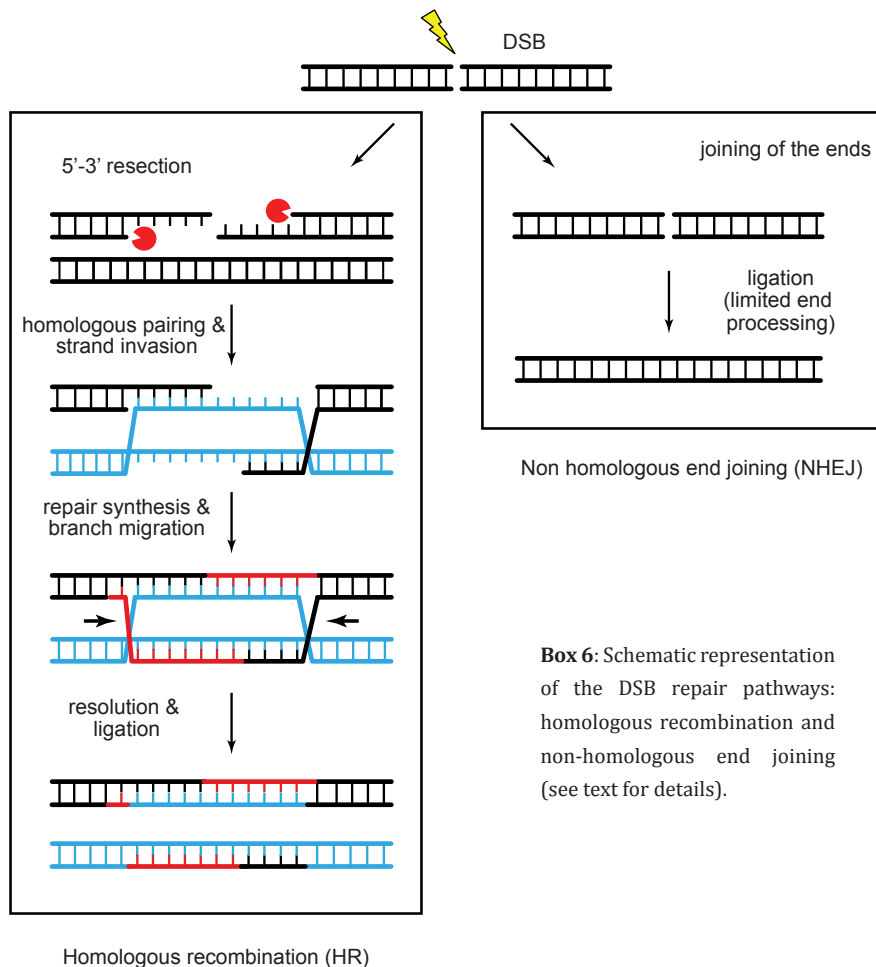
**Box 5:** Schematic representation of the post-replication repair (PPR) pathways: template switching and translesion synthesis (see text for details).

PCNA promotes bypass by TLS, while its polyubiquitination by the ubiquitin Mms2-Ubc13 E2-conjugating and the Rad5 E3-ligase complex favors the template switching pathway. TLS involves specialized polymerases such as Rev1, Pol $\zeta$  or Pol $\eta$  that can incorporate correct or incorrect nucleotides opposite the lesion and as such may be mutagenic.

On the other hand, template switching, a largely unknown mechanism for DNA damage bypass, is thought to be error-free. One of the accepted models starts with reinitiation of replication downstream the blocking lesion and is followed by a gap-filling event that uses the newly synthesized complementary strand as template in a recombination-like reaction (Box 5). Although Rad52 is possibly involved in this process, the other factors implicated remain to be discovered [40].

#### *Double stranded break repair*

Double stranded breaks are repaired by two mechanisms, homologous recombination (HR) and non-homologous endjoining (NHEJ)(Box 6). The choice of these two repair pathways depends on the phase of the cell cycle. HR occurs mainly in S and G2 phase due to the fact that it uses a sister-chromatid to copy the information required to seal the break. NHEJ on the other hand, is active during the whole cell cycle but is predominantly used in G1 phase. The key step of HR is the 5' to 3' resection of the DSB, which is initiated by the Mre11-Rad50-Xrs2 (MRX) complex and its associated partner Sae2. Then, the exonuclease Exo1 or the helicase Sgs1 and the helicase/nuclease Dna2, in a second resection step called long-range resection, further process the ends. The resulting 3' single strand overhangs (ssDNA) are rapidly coated by replication protein A (RPA). Next, RPA proteins are replaced by Rad51 proteins in a Rad52 and



**Box 6:** Schematic representation of the DSB repair pathways: homologous recombination and non-homologous end joining (see text for details).

Rad51 paralogs Rad55-Rad57 dependent manner, to form the Rad51 filament. This filament in concert with the Swi/Snf Rad54 protein catalyzes the search for a homologous sequence and proceeds with strand invasion. Annealing of the filament with the homologous template initiates DNA synthesis and branch migration that leads to formation of a joint molecule and structures called Holiday junctions (HJ). In the end of HR, the Sgs1-Top3-Rmi1 complex resolves both the joint molecule and the HJ, a step that is followed by a final ligation step [41, 42].

NHEJ involves the direct religation

of the broken ends. The yKu70-yKu80 and MRX complexes form the core set of NHEJ proteins. Human Ku is part of a complex of which catalytic subunit DNA-PKcs is required for efficient NHEJ. Yeast cells lack a functional DNA-PKcs homolog. MRX appears early after DSB formation to tether the ends. Although it is not clear which of the two complexes is the first to bind, it seems likely that the yKu complex occupy these extremities of the ends while the MRX complex can bind further away from the extremities. Then, DNA ligase IV and its associated partner Lif1 are recruited to the DSB through direct interaction with the MRX and Ku complexes and proceed with ligation

of the ends. In the context of clean breaks, ligation can occur without end-processing thereby being an error-free mechanism. However, in some cases, end-processing events must occur before ligation and necessitate the activity of enzymes such as the flap endonuclease Rad27, Polymerase Pol4 or lyases [43]. This type of NHEJ is thus error-prone.

1

### DDR-induced chromatin modifications

In eukaryotic cells, DNA is packaged together with histone proteins into a sophisticated structure called chromatin. This structure acts as a natural barrier that restricts the access to DNA. To enable enzymes that function in DNA metabolic processes such as replication, transcription or DNA repair to access DNA, chromatin has to be highly dynamic. Histone proteins are the main components regulating chromatin flexibility. They are modified by various post-translational modifications that alter DNA packing and as such ease or limit its accessibility. Here are examples of histone modifications and their functions in the DDR.

#### *Phosphorylation*

Tel1/Mec1 kinases phosphorylate many DDR substrates preferentially on a consensus SQ motif. Tel1/Mec1 dependent phosphorylation of the C-terminal SQ motif of histone H2AX ( $\gamma$ H2AX) is an important and conserved event during the DDR [44]. This modification spreads around and up to 100 kilobases away from a DSB. H2A-S129A mutants that cannot be phosphorylated by Tel1 or Mec1 are sensitive to DNA damaging agents and have a mild DSB repair defect [45]. In addition,  $\gamma$ H2AX helps the recruitment of chromatin remodelers to DSB sites such as NuA4, INO80 or SWR1. These complexes respectively, acetylate histones at the damaged site, facilitate end-resection by the MRX complex

or favor the binding of the Ku complex thus stimulating repair by NHEJ [46, 47].

#### *Methylation*

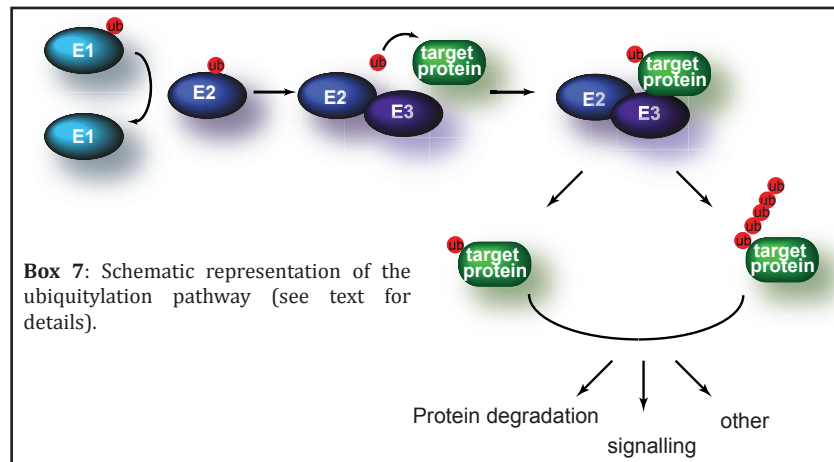
Methylation of lysine 79 on histone H3 (H3-K79me) also contributes to checkpoint activation and DNA repair. Dot1 is the histone methyltransferase responsible for the H3K79 mono-, di- or tri-methylation. Moreover, Rad9 is thought to be recruited to the DNA damage through its tudor domain, which recognizes and binds such methylated histones. Deletion of Dot1 causes defects in the G1/S and DNA intra-S damage-induced checkpoints. It was proposed that Dot1 loss perturbs Rad9 recruitment and subsequent Rad53 activation [48]. In addition, mutations in Rad9 tudor domain or failure to methylate H3K79 lead to a G1/S and intra-S checkpoint defect [48].

#### *Acetylation*

Acetylated histones H3 on lysine 56 (H3K56ac), by the histone H3 acetyltransferase Rtt109, are deposited during S-phase. In late S and G2 phases, the acetyl-groups on H3K56 are removed by the histone deacetylases (HDACs) Hst3 and Hst4 to allow cells to progress through mitosis. While H3K56ac is a mark for completion of S-phase, it was also found to affect checkpoint signaling in response to a DSB [49]. H3K56 acetylation by Rtt109 at site of DSB signals that repair has been completed; in turn H3K56ac removal is required for checkpoint recovery [49].

#### *Ubiquitylation*

Ubiquitylation is a cascade of reactions that results in the covalent attachment of a small peptide called ubiquitin to targeted proteins. This process involves E1 ubiquitin-activating, E2 ubiquitin conjugating and E3 ubiquitin-ligating enzymes (Box 7). Protein-ubiquitylation was at first associated with protein degradation. Now, it becomes



apparent that ubiquitylation of proteins is involved in various cellular pathways such as the DDR. For example, Histone H2B is ubiquitylated by the Rad6-Bre1 ubiquitin E2-conjugating E3-ligating complex, which is a prerequisite for methylation of H3K79 by Dot1. These two modifications affect cell survival in response to IR and the G1/S checkpoint in the presence DNA damage [48, 50]. In mammalian cells, ubiquitylation has recently been found to be an important component of the DSB response. The two ubiquitin ligases RNF8 and RNF168 are responsible for histone H2AX and H2A polyubiquitylation and thereby affect the recruitment of the downstream repair and signaling factors such as BRCA1 through its associated partner RAP80 that binds ubiquitin. The adaptor 53BP1 is also recruited via the RNF8 and RNF168 ubiquitylation cascade yet in an unclear mechanism [51].

### Post-translational modifications at the interface between checkpoint signaling and repair

#### *Sumoylation*

Sumoylation is a cascade of reactions similar to ubiquitylation at the exception that it results to covalent binding of an ubiquitin-

like moiety called SUMO to protein-targets. At the difference with ubiquitylation, sumoylation is not implicated in protein degradation but rather in other processes such as nucleocytoplasmic trafficking [52] or gene expression regulation [53]. In the DDR, sumoylation was found to modify Rad52 and impact on two events. Firstly, it likely protects Rad52 from proteasomal degradation when cells accumulate DNA intermediates in the process of HR. Secondly, it may determine the type of HR pathway by promoting gene conversion to the detriment of break induced replication and single-strand annealing. Srs2 and Sgs1 are other targets of sumoylation. Sumoylated-Srs2 seems to prevent unscheduled HR at replication forks, while Sgs1 modification stimulates HR at telomere and as such promotes telomere maintenance. PCNA is also sumoylated by the E2/E3 complex Ubc9/Siz1. Sumo-modified PCNA promotes Srs2 recruitment to replication forks, which prevents HR by disrupting Rad51 filaments [40]. In mammalian cells, sumoylation was recently implicated in the DSB response. The two SUMO E3 ligases, PIAS1 and PIAS4 are recruited to DSB sites and may regulate subsequent recruitment of repair factors like BRCA1 and 53BP1 [51].

*Neddylation*

Neddylation is a process similar to ubiquitylation or sumoylation by which the ubiquitin-like Rub1 protein (NEDD8 in humans) is conjugated to target proteins. The cellular processes that involve neddylation remain largely unknown due to the limited number of neddylation substrates that have been identified, namely the cullin-RING ubiquitin ligases (CRL) [54]. In yeast, the 3 CRL Rtt101, Cdc53 and Cul3 are neddylated in vivo, however only Rtt101 has been implicated in the DDR [55]. Moreover, absence of Rub1 does not seem to affect Rtt101 activity [56, 57]. Thus far, there is no evidence for a role of neddylation in the yeast DDR. On the other hand, in human cells, p53 is neddylated under unchallenged conditions, which triggers its proteasomal degradation [58]. In addition, neddylated forms of p53 transiently appear after UV exposure, which strongly suggests that neddylation regulates p53 levels and activity in response to DNA damage [58].

**DNA damage response networks**

Over the past ten years, the development of technologies allows genome-wide measurements of cellular organization, processes and responses to stressors. These technologies turned out to be powerful tools to study complex cellular responses including DDR.

*Genome-wide analysis tools to study the DDR*

**Microarray studies** have been used to monitor the transcriptional changes after various stress conditions including DNA damage. These studies helped to classify genes in functional categories. For example, yeast cells exposed to various DNA damaging agents including IR and the alkylating agent MMS, were used to identify

a group of transcriptionally responsive genes which included DNA repair genes such as MAG1, NTG1, RAD7, RAD54, RAD51 and the RNR subunits [59, 60]. In addition, the combination of microarray data enabled the creation of large databases [61]. These databases have been used to characterize unknown genes or drugs and helped to define molecular targets of known drugs based on the following observations. First, mutants that affect the same cellular process are likely to display similar transcriptional profiles. Secondly, if a gene mutation induces a transcription profile that correlates with that of wild-type cells treated with a particular drug, it is likely that the protein encoded by this gene, is a target of that drug. For example, Hughes et al. found that functionally related genes had profiles that matched such as ribosomal or histone deacetylase genes. They also showed that wild-type cells treated with an inhibitor of the HMG-CoA reductase had a similar transcription profile as cells deleted for the gene coding one of isoenzyme of the HMG-CoA reductase [61]. In human studies, transcription profiling is used to characterize and classify tumor types. The ultimate goal is to use expression profiling to determine the disease state and the response of patients to a pharmaceutical treatment.

**Transcription profiling** also helped to identify transcription factors driving the response to DNA damaging agents. Work from Jelinsky et al. showed that genes transcriptionally regulated similar to MAG1, have a consensus regulatory element, which is almost identical to that of MAG1. They found that this regulatory element was identical to the proteasome associated control element (PACE) and that the genes containing this element as well as MAG1 were regulated by the transcription factor Rpn4 [62]. They proposed that regulation of DDR genes possessing this regulatory

element is linked to protein degradation.

**Genomic phenotyping** has been another useful tool to identify gene products that affect particular phenotypes such as sensitivity or resistance to DNA damaging compounds [63]. These studies were used to characterize the mechanism of action of DNA damaging compounds and classify unknown genes in functional categories. For example, Lee et al. exposed the whole yeast deletion library to 12 different DNA damaging compounds, among which some are used in cancer treatment. Surprisingly, they found more genes required for protection against DNA damaging agents than it was previously anticipated. Among them were genes without functional annotations or not related to the DDR. They also showed that while genes involved in DNA repair pathways such as NER, HR or PRR were typically required for protection against the different compounds, their relative importance was variable depending on the compound. PRR genes as well as the previously characterized PSO2 gene were particularly found to promote resistance to interstrand cross-linking agents [64]. Interestingly, genes encoding proteins known to physically interact were found to display similar responses to the different compounds. In human cells, genomic phenotyping (that identify gene products that affect particular phenotypes such as sensitivity or resistance to DNA damaging compounds) may be used in the clinic to understand the sensitivity of patients to chemotherapeutic agents.

**Genome-wide protein-protein interaction** and yeast two-hybrid studies have revealed the extent to which gene products are organized in complexes to perform cellular processes [65]. These data were used in combination with previously described genomic-phenotyping data

to identify protein sub-networks that may drive the cellular response to DNA damage. These sub-networks were found to contain proteins involved in various molecular processes including DDR, chromatin remodeling, RNA and protein metabolism. This interactome-genome phenotyping integration showed that the interplay between multiple and functionally unrelated cellular processes is necessary to cope with DNA damage [63].

**Genome-wide genetic interaction** technologies such as synthetic genetic array have also been used to functionally group genes. Pan and coworkers used a synthetic lethality screen to interrogate the functional interactions between cellular processes participating to DNA integrity [66]. In a synthetic lethality screen, query mutants are crossed to an array of mutants each carrying a single gene deletion, to generate a library of double mutants that are then scored for cellular growth defects such as cell death or reduced fitness. Based on the assumption that genes working in the same pathway tend to interact similarly with other genes, they were able to define functionally distinct groups of interacting genes or modules. They also found that these modules were interacting with each other and as such predicted new function for known modules. For example, the fact that the sister chromatid cohesion module CTF18/CTF8/DCC1 interacted with the DNA checkpoint module RAD9, led Pan and coworkers predict and confirm a role for the CTF18 module in the S-phase checkpoint. Based on their interaction profiles, they showed that new genes such as DIA2, HST3 or HST4 are involved in DNA replication. Finally, synthetic lethal interactions between modules led them to suggest that DNA oxidation and errors occurring during replication are likely to be the major source of spontaneous DNA damage [66].

7

### *The EMAP approach*

Collins et al. developed a technology called Epistatic Mini Array Profiling (EMAP), which allows the precise measurement of both negative (synthetic lethality) and positive interactions (synthetic fitness) between pairs of genes [67]. This approach is based on synthetic genetic array technology [68], which is a high-throughput technique that explores genetic interactions through the systematic construction of double mutant yeast strains. Briefly, query strains carrying a single gene deletion are mated against an array of different gene deletion strains resulting in heterozygous diploids. Following sporulation and a series of selection steps haploid double-gene deletion strains are obtained. Growth rates are determined by measuring colony sizes. Size measurements are then normalized and statistically analyzed to assign each double mutant a quantitative S score [69]. This score reports on the extent to which it grew better (positive S score or interaction) or worse (negative S score or interaction) than expected [69]. Positive interactions (i.e., epistasis) typically occur among genes involved in the same complex or pathway, while negative interactions (i.e., synthetic sickness or lethality) usually identify genes in compensatory pathways.

Collins and colleagues generated the first EMAP, which focused on chromatin metabolism [67]. This map exhibited a modular organization, which allowed the authors to predict with high confidence protein complexes and to dissect large protein complexes in functional sub-complexes. Importantly, focusing on epistatic (positive) relationships between genes, they characterized a whole new pathway involved in the DDR that is driven by the Rtt109-dependent H3K56 acetylation [67]. The next step using this technique is to ask whether genetic interactions change

under particular DNA damaging conditions. Recently, Bandyopadhyay et al. have developed a technology called differential epistatic mapping (dE-MAP), which allows to measure the genetic interaction changes in response to a perturbation such as DNA damage induction [70].

### *From pathway analysis to network*

Computational data analysis of transcription profiling and genetic or protein interaction studies not only identified new components of cellular pathways but also revealed extensive interconnections between them. The integration of these different datasets has led to the new notion of cellular networks in which cellular pathways are only components connected to each other and regulated at different levels. Integrating other data such as post-translation modifications (e.g. ubiquitylation or phosphorylation) are likely to give a more dynamic view of the cellular networks and predict their rewiring under stress conditions such as the presence of DNA damage. The next step to understand the cellular responses to genotoxic stresses is to collect transcription data including microRNAs, protein and genetic interaction data both gathered under the same DNA damaging conditions since most of these datasets have been collected under unchallenged conditions or vastly differing exposure conditions to stressors.

**In this thesis**

The number of factors engaged in the global responses to DNA damage and the multiple layers of regulation, make the coordination of various responsive pathways and underlying mechanisms a complex task for the cell. The aim of this thesis is to improve our understanding of the crosstalks between cellular processes that are necessary for the cells to respond to specific types of DNA damage. To reach this goal, we used a high-throughput genetic approach called EMAP. To assess the genetic interaction changes that are induced by specific types of DNA damage, we generated EMAPs under three different DNA damaging conditions. A recently developed algorithm that allows quantifying the genetic interaction changes in response to a perturbation helped us in the analysis of this new type of genetic data [71].

In **chapter 2**, we describe the set-up and the analysis of our genetic screen and show that it is an extremely powerful method to highlight associations between DNA damaging drugs and DNA repair pathways. Four different novel interactions defined in our genetic map that is presented in this chapter, are studied at the molecular level and presented in the following chapters.

In **chapter 3**, we describe a new role for Rtt109, the histone H3 acetyltransferase, in regulation of the mutagenic bypass of DNA lesions.

In **chapter 4**, we show that the neddylation machinery affects genomic stability and cell cycle control in response to the Top1-inhibitor camptothecin, most likely by regulating the steady state level of DDR factors including Nhp10 and Mms22.

**Chapter 5** describes the identification and the characterization of a new DDR factor, Irc21. We demonstrate that Irc21 influences genomic stability, DNA damage checkpoint and repair.

**Chapter 6** reports on the coordination between the Sae2 endonuclease and the Pph3-Psy2 phosphatase complex in regulation of the DNA damage checkpoint.

In **chapter 7**, we discuss the implication of our findings in future research and in possible therapeutic outcomes.

The functional analysis of genetic interactions found in our genetic screen confirms that our approach was successful in the investigation of the interconnection between factors and pathways to mediate an appropriate cellular response to various types of DNA damage. We unraveled new factors and connections between cellular pathways and show how they act in the DDR. While we functionally investigated only a piece of this genetic network, we hope that it will initiate further studies leading to a better understanding of the DDR in yeast and in higher eukaryotes

7



## REFERENCES

1. Lindahl, T., Instability and decay of the primary structure of DNA. *Nature*, 1993. 362(6422): p. 709-15.
2. Hoeijmakers, J.H., DNA damage, aging, and cancer. *N Engl J Med*, 2009. 361(15): p. 1475-85.
3. Bartek, J., J. Bartkova, and J. Lukas, DNA damage signalling guards against activated oncogenes and tumour progression. *Oncogene*, 2007. 26(56): p. 7773-9.
4. Ciccio, A. and S.J. Elledge, The DNA damage response: making it safe to play with knives. *Mol Cell*, 2010. 40(2): p. 179-204.
5. Moynahan, M.E. and M. Jasin, Mitotic homologous recombination maintains genomic stability and suppresses tumorigenesis. *Nat Rev Mol Cell Biol*, 2010. 11(3): p. 196-207.
6. Dobbs, T.A., J.A. Tainer, and S.P. Lees-Miller, A structural model for regulation of NHEJ by DNA-PKcs autophosphorylation. *DNA Repair (Amst)*, 2010. 9(12): p. 1307-14.
7. Paciotti, V., et al., The checkpoint protein Ddc2, functionally related to *S. pombe* Rad26, interacts with Mec1 and is regulated by Mec1-dependent phosphorylation in budding yeast. *Genes Dev*, 2000. 14(16): p. 2046-59.
8. Nakada, D., K. Matsumoto, and K. Sugimoto, ATM-related Tel1 associates with double-strand breaks through an Xrs2-dependent mechanism. *Genes Dev*, 2003. 17(16): p. 1957-62.
9. Melo, J.A., J. Cohen, and D.P. Toczyski, Two checkpoint complexes are independently recruited to sites of DNA damage in vivo. *Genes Dev*, 2001. 15(21): p. 2809-21.
10. Kondo, T., et al., Recruitment of Mec1 and Ddc1 checkpoint proteins to double-strand breaks through distinct mechanisms. *Science*, 2001. 294(5543): p. 867-70.
11. Majka, J. and P.M. Burgers, Yeast Rad17/Mec3/Ddc1: a sliding clamp for the DNA damage checkpoint. *Proc Natl Acad Sci U S A*, 2003. 100(5): p. 2249-54.
12. Majka, J., A. Niedziela-Majka, and P.M. Burgers, The checkpoint clamp activates Mec1 kinase during initiation of the DNA damage checkpoint. *Mol Cell*, 2006. 24(6): p. 891-901.
13. Mordes, D.A., E.A. Nam, and D. Cortez, Dpb11 activates the Mec1-Ddc2 complex. *Proc Natl Acad Sci U S A*, 2008. 105(48): p. 18730-4.
14. Blankley, R.T. and D. Lydall, A domain of Rad9 specifically required for activation of Chk1 in budding yeast. *J Cell Sci*, 2004. 117(Pt 4): p. 601-8.
15. Cohen-Fix, O. and D. Koshland, The anaphase inhibitor of *Saccharomyces cerevisiae* Pds1p is a target of the DNA damage checkpoint pathway. *Proc Natl Acad Sci U S A*, 1997. 94(26): p. 14361-6.
16. Sanchez, Y., et al., Control of the DNA damage checkpoint by chk1 and rad53 protein kinases through distinct mechanisms. *Science*, 1999. 286(5442): p. 1166-71.
17. Liang, F. and Y. Wang, DNA damage checkpoints inhibit mitotic exit by two different mechanisms. *Mol Cell Biol*, 2007. 27(14): p. 5067-78.
18. Sweeney, F.D., et al., *Saccharomyces cerevisiae* Rad9 acts as a Mec1 adaptor to allow Rad53 activation. *Curr Biol*, 2005. 15(15): p. 1364-75.
19. Osborn, A.J. and S.J. Elledge, Mrc1 is a replication fork component whose phosphorylation in response to DNA replication stress activates Rad53. *Genes Dev*, 2003. 17(14): p. 1755-67.
20. Alcasabas, A.A., et al., Mrc1 transduces signals of DNA replication stress to activate Rad53. *Nat Cell Biol*, 2001. 3(11): p. 958-65.
21. Bashkirov, V.I., et al., Direct kinase-to-kinase signaling mediated by the FHA phosphoprotein recognition domain of the Dun1 DNA damage checkpoint kinase. *Mol Cell Biol*, 2003. 23(4): p. 1441-52.
22. Zhao, X., E.G. Muller, and R. Rothstein, A suppressor of two essential

- checkpoint genes identifies a novel protein that negatively affects dNTP pools. *Mol Cell*, 1998. 2(3): p. 329-40.
23. Zhao, X. and R. Rothstein, The Dun1 checkpoint kinase phosphorylates and regulates the ribonucleotide reductase inhibitor Sml1. *Proc Natl Acad Sci U S A*, 2002. 99(6): p. 3746-51.
24. Agarwal, R., et al., Two distinct pathways for inhibiting pds1 ubiquitination in response to DNA damage. *J Biol Chem*, 2003. 278(45): p. 45027-33.
25. Lew, D.J. and D.J. Burke, The spindle assembly and spindle position checkpoints. *Annu Rev Genet*, 2003. 37: p. 251-82.
26. Clerici, M., et al., A Tel1/MRX-dependent checkpoint inhibits the metaphase-to-anaphase transition after UV irradiation in the absence of Mec1. *Mol Cell Biol*, 2004. 24(23): p. 10126-44.
27. Clemenson, C. and M.C. Marsolier-Kergoat, The spindle assembly checkpoint regulates the phosphorylation state of a subset of DNA checkpoint proteins in *Saccharomyces cerevisiae*. *Mol Cell Biol*, 2006. 26(24): p. 9149-61.
28. Keogh, M.C., et al., A phosphatase complex that dephosphorylates gammaH2AX regulates DNA damage checkpoint recovery. *Nature*, 2006. 439(7075): p. 497-501.
29. Leroy, C., et al., PP2C phosphatases Ptc2 and Ptc3 are required for DNA checkpoint inactivation after a double-strand break. *Mol Cell*, 2003. 11(3): p. 827-35.
30. O'Neill, B.M., et al., Pph3-Psy2 is a phosphatase complex required for Rad53 dephosphorylation and replication fork restart during recovery from DNA damage. *Proc Natl Acad Sci U S A*, 2007. 104(22): p. 9290-5.
31. Galgoczy, D.J. and D.P. Toczyski, Checkpoint adaptation precedes spontaneous and damage-induced genomic instability in yeast. *Mol Cell Biol*, 2001. 21(5): p. 1710-8.
32. Yoo, H.Y., et al., Adaptation of a DNA replication checkpoint response depends upon inactivation of Claspin by the Polo-like kinase. *Cell*, 2004. 117(5): p. 575-88.
33. de Laat, W.L., N.G. Jaspers, and J.H. Hoeijmakers, Molecular mechanism of nucleotide excision repair. *Genes Dev*, 1999. 13(7): p. 768-85.
34. Prakash, S. and L. Prakash, Nucleotide excision repair in yeast. *Mutat Res*, 2000. 451(1-2): p. 13-24.
35. Boiteux, S. and M. Guillet, Abasic sites in DNA: repair and biological consequences in *Saccharomyces cerevisiae*. *DNA Repair (Amst)*, 2004. 3(1): p. 1-12.
36. Hoeijmakers, J.H., Genome maintenance mechanisms for preventing cancer. *Nature*, 2001. 411(6835): p. 366-74.
37. Jiricny, J., The multifaceted mismatch-repair system. *Nat Rev Mol Cell Biol*, 2006. 7(5): p. 335-46.
38. Kadyrov, F.A., et al., A possible mechanism for exonuclease 1-independent eukaryotic mismatch repair. *Proc Natl Acad Sci U S A*, 2009. 106(21): p. 8495-500.
39. Harfe, B.D. and S. Jinks-Robertson, DNA mismatch repair and genetic instability. *Annu Rev Genet*, 2000. 34: p. 359-399.
40. Lee, K.Y. and K. Myung, PCNA modifications for regulation of post-replication repair pathways. *Mol Cells*, 2008. 26(1): p. 5-11.
41. Heyer, W.D., et al., Rad54: the Swiss Army knife of homologous recombination? *Nucleic Acids Res*, 2006. 34(15): p. 4115-25.
42. San Filippo, J., P. Sung, and H. Klein, Mechanism of eukaryotic homologous recombination. *Annu Rev Biochem*, 2008. 77: p. 229-57.
43. Daley, J.M., et al., Nonhomologous end joining in yeast. *Annu Rev Genet*, 2005. 39: p. 431-51.
44. Fernandez-Capetillo, O., et al., H2AX: the histone guardian of the genome. *DNA Repair (Amst)*, 2004. 3(8-9): p. 959-67.
45. Redon, C., et al., Yeast histone 2A serine 129 is essential for the efficient repair of checkpoint-blind DNA damage. *EMBO Rep*, 2003. 4(7): p. 678-84.
46. Downs, J.A., et al., Binding of chromatin-modifying activities to

phosphorylated histone H2A at DNA damage sites. *Mol Cell*, 2004. 16(6): p. 979-90.

47. van Attikum, H., O. Fritsch, and S.M. Gasser, Distinct roles for SWR1 and INO80 chromatin remodeling complexes at chromosomal double-strand breaks. *EMBO J*, 2007. 26(18): p. 4113-25.

48. Wysocki, R., et al., Role of Dot1-dependent histone H3 methylation in G1 and S phase DNA damage checkpoint functions of Rad9. *Mol Cell Biol*, 2005. 25(19): p. 8430-43.

49. Chen, C.C., et al., Acetylated lysine 56 on histone H3 drives chromatin assembly after repair and signals for the completion of repair. *Cell*, 2008. 134(2): p. 231-43.

50. Game, J.C., M.S. Williamson, and C. Baccari, X-ray survival characteristics and genetic analysis for nine *Saccharomyces cerevisiae* deletion mutants that show altered radiation sensitivity. *Genetics*, 2005. 169(1): p. 51-63.

51. Bekker-Jensen, S. and N. Mailand, The ubiquitin- and SUMO-dependent signaling response to DNA double-strand breaks. *FEBS Lett*, 2011. 585(18): p. 2914-9.

52. Stade, K., et al., A lack of SUMO conjugation affects cNLS-dependent nuclear protein import in yeast. *J Biol Chem*, 2002. 277(51): p. 49554-61.

53. Rosonina, E., S.M. Duncan, and J.L. Manley, SUMO functions in constitutive transcription and during activation of inducible genes in yeast. *Genes Dev*, 2010. 24(12): p. 1242-52.

54. Rabut, G. and M. Peter, Function and regulation of protein neddylation. 'Protein modifications: beyond the usual suspects' review series. *EMBO Rep*, 2008. 9(10): p. 969-76.

55. Luke, B., et al., The cullin Rtt101p promotes replication fork progression through damaged DNA and natural pause sites. *Curr Biol*, 2006. 16(8): p. 786-92.

56. Laplaza, J.M., et al., *Saccharomyces cerevisiae* ubiquitin-like protein Rub1 conjugates to cullin proteins Rtt101 and Cul3 in vivo. *Biochem J*, 2004. 377(Pt 2): p. 459-67.

57. Rabut, G., et al., The TFIID subunit Tfb3 regulates cullin neddylation. *Mol Cell*, 2011. 43(3): p. 488-95.

58. Xirodimas, D.P., et al., Mdm2-mediated NEDD8 conjugation of p53 inhibits its transcriptional activity. *Cell*, 2004. 118(1): p. 83-97.

59. Jelinsky, S.A. and L.D. Samson, Global response of *Saccharomyces cerevisiae* to an alkylating agent. *Proc Natl Acad Sci U S A*, 1999. 96(4): p. 1486-91.

60. Gasch, A.P., et al., Genomic expression responses to DNA-damaging agents and the regulatory role of the yeast ATR homolog Mec1p. *Mol Biol Cell*, 2001. 12(10): p. 2987-3003.

61. Hughes, T.R., et al., Functional discovery via a compendium of expression profiles. *Cell*, 2000. 102(1): p. 109-26.

62. Jelinsky, S.A., et al., Regulatory networks revealed by transcriptional profiling of damaged *Saccharomyces cerevisiae* cells: Rpn4 links base excision repair with proteasomes. *Mol Cell Biol*, 2000. 20(21): p. 8157-67.

63. Begley, T.J., et al., Damage recovery pathways in *Saccharomyces cerevisiae* revealed by genomic phenotyping and interactome mapping. *Mol Cancer Res*, 2002. 1(2): p. 103-12.

64. Lee, W., et al., Genome-wide requirements for resistance to functionally distinct DNA-damaging agents. *PLoS Genet*, 2005. 1(2): p. e24.

65. Gavin, A.C., et al., Proteome survey reveals modularity of the yeast cell machinery. *Nature*, 2006. 440(7084): p. 631-6.

66. Pan, X., et al., A DNA integrity network in the yeast *Saccharomyces cerevisiae*. *Cell*, 2006. 124(5): p. 1069-81.

67. Collins, S.R., et al., Functional dissection of protein complexes involved in yeast chromosome biology using a genetic interaction map. *Nature*, 2007. 446(7137): p. 806-10.

68. Tong, A.H. and C. Boone, Synthetic genetic array analysis in *Saccharomyces cerevisiae*. *Methods Mol Biol*, 2006. 313: p.

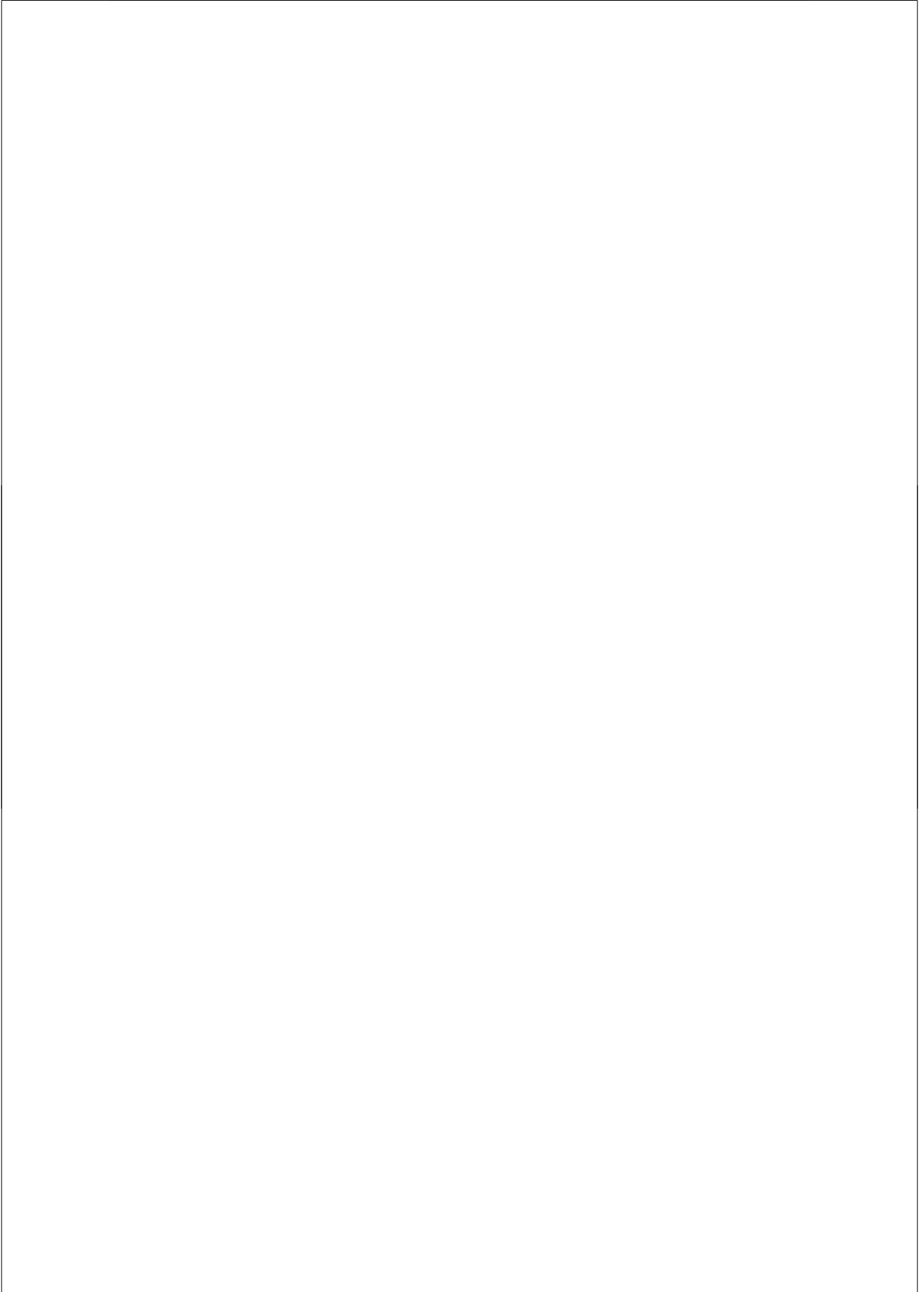
171-92.

69. Collins, S.R., et al., A strategy for extracting and analyzing large-scale quantitative epistatic interaction data. *Genome Biol*, 2006. 7(7): p. R63.

70. Baryshnikova, A., et al., Quantitative analysis of fitness and genetic interactions in yeast on a genome scale. *Nat Methods*, 2010. 7(12): p. 1017-24.

71. Bandyopadhyay, S., et al., Rewiring of genetic networks in response to DNA damage. *Science*, 2010. 330(6009): p. 1385-9.

7





## A MULTI-CONDITIONAL GENETIC INTERACTION MAP TO DISSECT DNA DAMAGE RESPONSE PATHWAYS

Aude Guénolé<sup>1,7</sup>, Rohith Srivas<sup>2,3,7</sup>, Kees Vreeken<sup>1</sup>, Ze Zhong Wang<sup>2</sup>,  
Shuyi Wang<sup>4,5</sup>, Nevan J. Krogan<sup>4,5,\*</sup>, Trey Ideker<sup>2,3,6,\*</sup>, Haico van  
Attikum<sup>1,\*</sup>

<sup>1</sup>Department of Toxicogenetics, Leiden University Medical Center, Einthovenweg 20, 2333 ZC, Leiden, The Netherlands, <sup>2</sup>Department of Bioengineering, University of California, San Diego, La Jolla, CA 92093 USA, <sup>3</sup>Department of Medicine, University of California, San Diego, La Jolla, CA 92093, USA, <sup>4</sup>Department of Cellular and Molecular Pharmacology, University of California, San Francisco, San Francisco, CA, 94158, USA, <sup>5</sup>California Institute for Quantitative Biosciences, University of California, San Francisco, San Francisco, CA, 94158, USA, <sup>6</sup>The Institute for Genomic Medicine, University of California, San Diego, La Jolla, CA 92093, USA, <sup>7</sup>These authors contributed equally to this work.

\*Correspondence: N.J.K. (krogan@cmp.ucsf.edu), T.I. (tideker@ucsd.edu),  
H.v.A. (h.van.attikum@lumc.nl)

### Partially published in:

- 1) Guénolé A, Srivas R, Vreeken K, Wang ZZ, Wang S, Krogan NJ, Ideker T, van Attikum H. *Dissection of DNA damage responses using multiconditional genetic interaction maps*. Mol Cell. 2013 Jan 24;49(2):346-58.
- 2) Ryan C, Greene D, Guénolé A, van Attikum H, Krogan NJ, Cunningham P, Cagney G. *Improved functional overview of protein complexes using inferred epistatic relationships*. BMC Syst Biol. 2011 May 23;5:80.
- 3) Hannum G, Srivas R, Guénolé A, van Attikum H, Krogan NJ, Karp RM, Ideker T. *Genome-wide association data reveal a global map of genetic interactions among protein complexes*. PLoS Genet. 2009 Dec;5(12):e1000782.

Chapter 2

2

**ABSTRACT**

To protect the genome, cells have evolved a diverse set of pathways designed to sense, signal and repair multiple types of DNA damage. To assess the degree of coordination and crosstalk among these pathways, we systematically mapped changes in the cell's genetic network across a panel of mechanistically distinct DNA-damaging agents, resulting in ~1,800,000 differential measurements. Each agent was associated with a distinct interaction pattern, which, unlike single mutant phenotypes or gene expression data, has high statistical power to pinpoint the specific signaling and repair mechanisms at work.



## INTRODUCTION

Failure of cells to respond to DNA damage is associated with genome instability and the onset of diseases such as premature aging and cancer [1]. To combat DNA damage, cells have evolved an intricate system, known as the DNA damage response (DDR), which senses DNA lesions and activates downstream pathways such as chromatin remodeling, cell cycle checkpoints and DNA repair [2]. Many studies have sought to use genome-scale technologies to better define and map the DDR, including systematic phenotyping of single mutants [3], RNAi screening [4] and gene expression profiling [5].

While these strategies have met with success in identifying new DDR genes, they have raised a number of questions with regard to how DDR pathways coordinate with one another. For instance, the initial view of DNA damage checkpoints was as a collection of pathways with the sole task of coordinating cell cycle progression with DNA repair [6]. However, recent studies have implicated checkpoints in other processes, including transcription regulation, telomere length maintenance, and apoptosis, suggesting that there is extensive crosstalk between such processes during the DDR [7, 8]. Increasing evidence suggests that much of this crosstalk is likely to be dependent on the nature of the DNA lesion. For example, the Bloom syndrome helicase (BLM; Sgs1 in budding yeast) functionally interacts with components of the S-phase replication checkpoint (e.g. Mrc1/Claspin) when replication forks stall, whereas it cooperates with factors of the DNA damage checkpoint (e.g. Rad17/hRAD9 of the 9-1-1 complex) after DNA double-stranded break (DSB) formation [9]. An important next step is therefore to understand how functional inter-connections between the various components of DDR pathways are formed and altered in response to various genotoxic

insults.

To address this issue, we turned to a recently-developed interaction mapping methodology called differential epistasis mapping or dE-MAP in the budding yeast *Saccharomyces cerevisiae* [10]. This approach is based on synthetic genetic array technology [11], which enables rapid measurement of genetic interactions, i.e., combinations of two or more mutations which lead to a dramatic departure in growth rate when compared to the product of the individual mutant growth rates [12]. Genetic interactions fall into one of two categories [13]: positive interactions (i.e., epistasis), which typically occur among genes involved in the same complex or pathway, and negative interactions (i.e., synthetic sickness or lethality) which identify genes in compensatory pathways. In the dE-MAP approach, synthetic genetic arrays are used to measure genetic interactions under standard conditions as well as under perturbations of interest and, by comparing the resulting networks, interactions that are altered in response to perturbation can be quantitatively assessed. These 'differential' genetic interactions reveal a unique view of cellular processes and their inter-connections under specific stress conditions [14].

Here, we apply our dE-MAP technique to systematically map the genetic modules and networks induced by distinct types of DNA damage, which we anticipate will be an important resource for the study of the DDR and its associated diseases.

## RESULTS & DISCUSSION

### Mapping differential genetic networks across distinct types of DNA damage

We constructed a dE-MAP in the budding yeast *S. cerevisiae* centered on the measurement of all possible interactions between a set of 55 query genes and a set of 2,022 array genes (Figure 1A). The 55 query genes were chosen to provide coverage of the pathways that define the DDR including representatives of the distinct DNA repair processes (Table S1). The array genes included all of the queries and, to explore crosstalk between DNA repair and other cellular functions, genes involved in cell cycle regulation, chromatin organization, replication, transcription and protein transport (Table S1). Double mutant strains were constructed for each query–array gene pairing (Methods) using synthetic gene array technology [11, 12]. Briefly, each query strain carrying a single gene deletion is mated against an array of strains (in this case 2,022 gene deletion strains) resulting in heterozygous diploids. The diploids are then transferred to

nitrogen-depleted media to induce meiosis and sporulation, after which they undergo a series of selection steps to obtain haploid double-gene deletion cells. Growth rates are determined by measuring colony sizes after 48 hours in both standard conditions (Untreated) as well as in the presence of three chemical agents that induce distinct types of DNA damage: the DNA alkylating agent methylmethane sulfonate (MMS), the topoisomerase I inhibitor camptothecin (CPT), and the DNA intercalating agent zeocin (ZEO). Colony size measurements are normalized and statically analyzed to assign each double mutant a quantitative genetic interaction score or S score [13]. This score reports on the extent to which the double mutant grew better (positive S Score) or worse (negative S Score) than the expected value, defined as the product of the individual single mutant fitnesses (or S score). In total, the genetic interaction map contained quantitative scores for 97,578 pairs of genes (Table S2). Several routine quality control measures were employed to ensure a high-quality dataset (Figure S1 and Supplementary Methods).

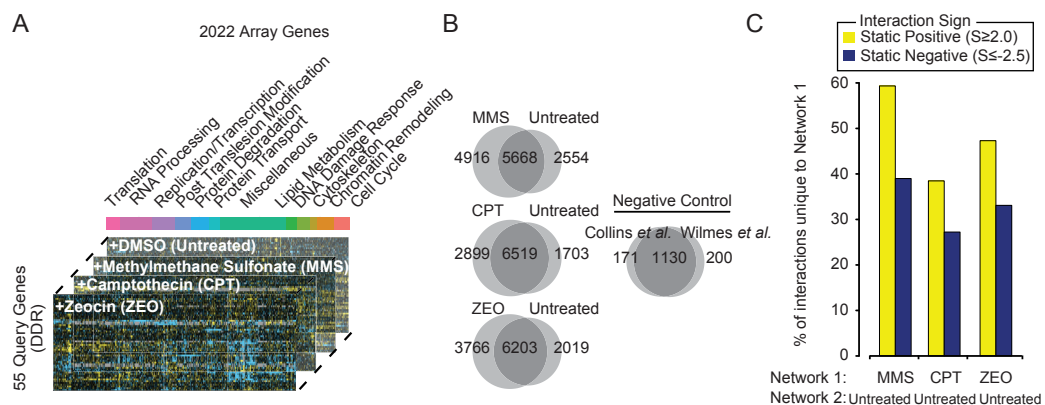


**Figure 1. Overview of the Multi-Conditional Static Network** (A) Experimental design of the differential genetic interaction screen. The stacked barplot illustrates the functional breakdown of array genes. A full list of the query and array genes is provided in Tables S1 and S2. (B) Overlap in significant static interactions ( $S \geq 2.0$ ,  $S \leq -2.5$ ) between treated and untreated conditions. The negative control represents the overlap between previously published networks measured in untreated conditions. (C) The percentage of positive and negative interactions that are unique to the treated network (Network 1) when compared to the untreated network (Network 2).

Using established scoring thresholds to highlight significant positive and negative interactions ( $S \geq 2.0$  or  $S \leq -2.5$ ) [13], we uncovered 8222 significant interactions in untreated conditions versus 10584, 9418, and 9969 significant interactions in MMS, CPT, and ZEO, respectively. A first comparison of these sets of interactions reveals numerous differences in genetic interactions between the treated and untreated conditions (Figure 1B). On average, 48% of positive interactions and 33% of negative interactions were unique to the treated networks, indicating the presence of DNA damage-induced epistasis and synthetic lethality (Figure 1C). To identify which of these differences were statistically significant, we used a previously published scoring methodology [10] to assess the difference in  $S$  score for each gene pair before versus after treatment. A  $p$ -value of significance was assigned by comparing this quantitative difference to a null distribution of differences derived from replicate genetic interaction screens from the same condition. We refer to this network as the ‘differential’ genetic network since

it is derived by examining the difference between two static networks (Figure 2A). At a  $p$ -value threshold of 0.002 (false discovery rate  $\approx 12.3\%$ ; Supplementary Methods), we identified 3150 significant differential interactions when comparing MMS to untreated conditions, versus 1120 and 1474 differential interactions when comparing CPT and ZEO to untreated conditions, respectively (Figure 2B).

Across all three differential networks, the number of differential positive interactions (interaction becomes more positive under DNA damage) was roughly equal to the number of differential negative interactions (interaction becomes more negative under DNA damage, Figure 2B). Finally, we found that characteristics of hubs (those genes with the greatest number of interactions) already described in static networks are conserved in differential networks. Indeed, genetic interaction hubs identified in static genetic networks have been associated with a number of important cellular properties [15-17]. For example, static genetic hubs identified in both  $S$ .

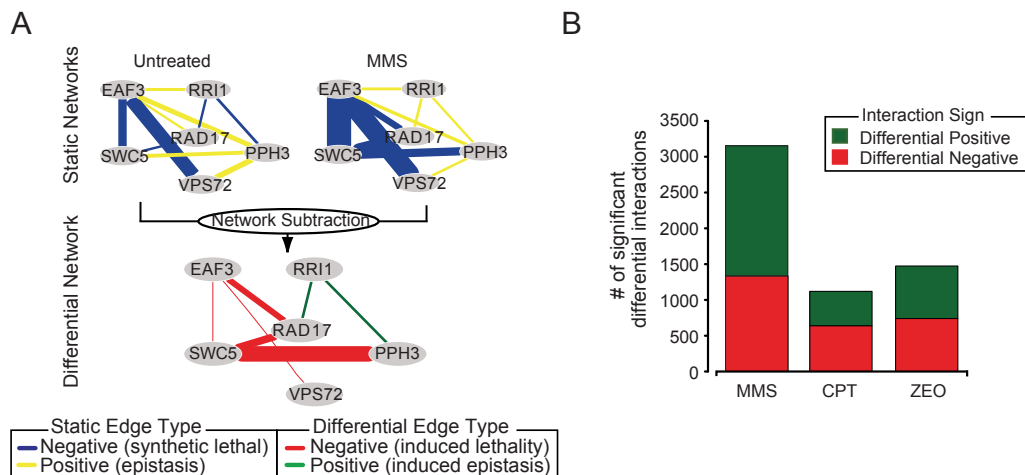


**Figure 2. Overview of the Multi-Conditional Differential Network** (A) Schematic overview of how differential genetic networks are derived by examining the difference between static treated and untreated genetic networks. The thickness of the edge scales with the magnitude of the genetic interaction. (B) Overview of the number of significant positive and negative differential interactions uncovered in each condition.

*cerevisiae* and *S. pombe* are more likely to exhibit a severe single mutant defect and display a much greater degree of pleiotropy [16, 17]. Analysis of the differential networks revealed that these features were also found amongst differential genetic interaction hubs. Genes with a higher number of differential interactions in response to MMS, CPT, or ZEO were significantly more likely to exhibit a single mutant sensitivity to that particular compound (Supplementary Figure S2A). Differential network hubs are also more likely to be essential for growth in response to numerous drugs and stresses indicating that they may be more pleiotropic (Supplementary Figure S2B) and help to

inter-connect various biological processes required for the DDR.

### Differential interactions effectively discriminate among different DNA damage responses

We next examined all networks, differential and static, for their ability to highlight genes that function in the DDR (Methods). All three differential networks had high enrichment for interactions with known DNA repair genes, while static networks had much less enrichment (MMS) or no enrichment (CPT, ZEO, Untreated) in this regard (Figure 3A). Instead, all four static networks showed the strongest enrichment for genes involved in

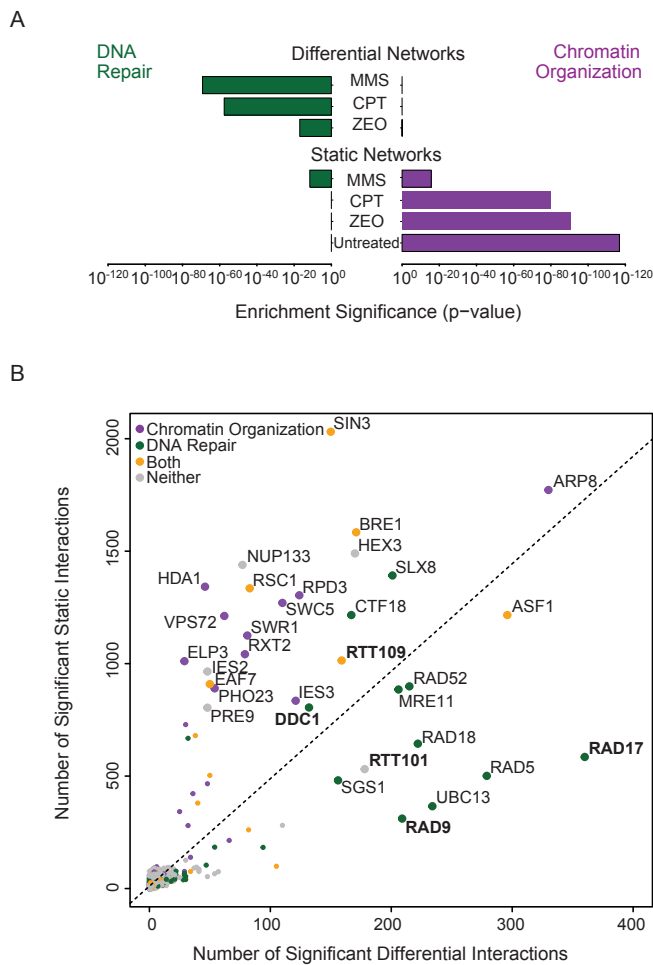


**Figure 3. Differential networks reveal specific pathways induced by different types of DNA damage** (A) The significance of enrichment for interactions with genes that function in either DNA repair (green bars) or chromatin organization (purple bars) is plotted for all networks. (B) The total number of significant static (y-axis) and differential (x-axis) interactions across all conditions for each gene considered in this study.

chromatin organization, as had been noted in the original report of the dE-MAP method [10]. Moreover, 15 of the top 20 differential interaction 'hubs' were annotated as a DNA repair gene, whereas the top interaction hubs in static networks were largely associated with chromatin organization (Figure 3B). Thus, in contrast to static interactions, differential interactions measured across a shift in conditions tend to highlight gene functions related to that condition.

Despite the strong enrichment for DNA repair genes across all differential

networks, we found that these networks were strikingly different from one another. Few differential interactions (584 interactions; 11%) were induced by more than one agent and only 45 interactions were induced by all agents (Figure 4A). In contrast, a control experiment indicated much better agreement between replicate differential networks generated in response to the same agent (Figure S3A). These findings were corroborated in an alternate analysis in which we hierarchically clustered all 55 query genes based on either their static (Figure S3B) or differential (Figure S3C) genetic interaction profiles (Supplementary

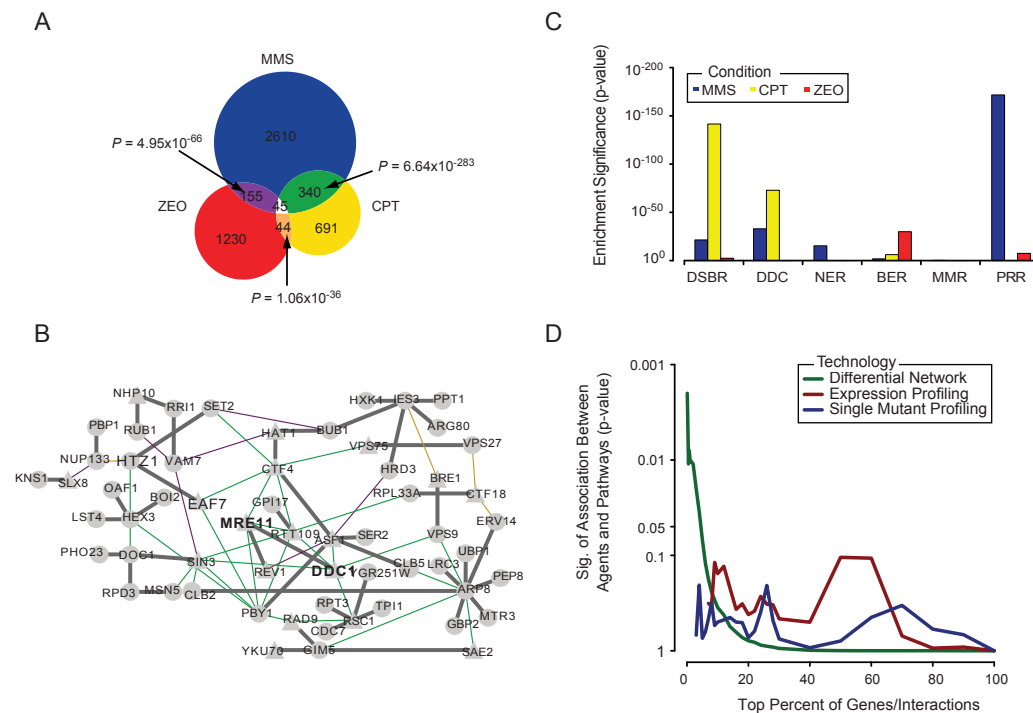


**Figure 4. Differential networks reveal specific pathways induced by different types of DNA damage** (A) The overlap in significant ( $P \leq 0.002$ ) differential interactions induced by each agent is shown. (B) Network of differential genetic interactions conserved in all three conditions (dark grey edges) or in two of three conditions (green edges = CPT & MMS; orange edges = CPT & ZEO; purple edges = ZEO & MMS). Triangular nodes represent genes known to be involved in DNA repair. (C) Enrichment of differential interactions containing genes involved in six major DNA repair pathways: DSB repair (DSBR), DNA damage checkpoint (DDC), nucleotide excision repair (NER), base excision repair (BER), mismatch repair (MMR) and post-replication repair (PRR). (D) The significance of association between agents and DNA repair pathways is computed using differential networks, single mutants, and differential gene expression across a range of thresholds.

Methods). Clustering using the differential metric, as opposed to the static interaction scores, lead to a clear separation between the different DNA damaging agents, underlining the stark differences amongst the genetic interactions induced by these three compounds. To determine whether these distinct interaction patterns were indicative of distinct DNA repair mechanisms, we examined the differential networks for enrichment of interactions with genes involved in six major DDR pathways (Figure 4B, Table S3, Methods). The CPT network was highly enriched for DSB repair ( $P = 10^{-143}$ ) and DNA damage checkpoint functions ( $P = 10^{-74}$ ), consistent with the known mechanism of action of CPT which stabilizes DNA topoisomerase 1-DNA complexes. During S-phase the replication machinery collides with these structures resulting in the production of DSB specifically during this phase of the cell cycle [18]. The MMS network displayed only a mild enrichment ( $P = 0.009$ ) for interactions with components of base excision repair (BER), an unexpected result given the mechanism of action of MMS which modifies guanine and adenine bases leading to base mispairing and replication fork blocks [19]. However, replication-blocking lesions can be bypassed by post-replication repair pathways (PRR) such as translesion synthesis (TLS) and DNA damage avoidance or, in case of fork collapse and subsequent chromosome breakage, are counteracted by DSB repair pathways [20]. All these pathways showed strong enrichment in the MMS network (Figure 4B). Finally, the ZEO network was found to enrich for interactions with genes involved in BER and PRR rather than for genes involved in DSB repair ( $P = 0.002$ ), suggesting that our ZEO treatment leads to the formation of abasic sites rather than DNA strand breakage, consistent with the mode of action of this intercalating agent at lower concentrations [21].

These functional enrichments suggest that the differential networks help decode the particular combination of DDR pathways underlying the response to each agent. To test this hypothesis explicitly, we measured the statistical association between the three agents and the six major DDR pathways as revealed by differential interactions (modified Pearson's Chi-Square Test, see Supplementary Methods). In contrast to functional enrichment, statistical association measures the extent to which interactions induced by each agent implicate a set of genes that discriminates among the six pathways (i.e., genes which associate with some DDR functions but not others). We found that differential interactions were indeed able to elicit a significant association between agents and pathways, especially for the top 5% of interactions (Figure 4C). Moreover, differential interactions performed very favorably at this task in comparison to single-mutant fitness [3] or differential mRNA-expression profiles [22, 23] gathered previously for either MMS, CPT, or bleomycin (a compound with similar properties to ZEO; see Supplementary Methods). Neither of these data types was able to significantly link DNA damaging agents to particular responses (Figure 4C). A likely explanation for the better performance of differential networks lies in the greater sample size afforded by this technology. Whereas single-mutant fitness and gene expression profiling are limited to measurements of individual genes (181 genes across the six DDR pathways), the differential networks cover interactions between DDR genes and over 30% of the yeast genome (39,973 interactions in total). Thus, while single mutant and gene expression profiling are adept at defining high-level biological functions (e.g., DNA repair), differential genetic interactions can begin to tease apart a very specific set of (partially overlapping) mechanisms.

2

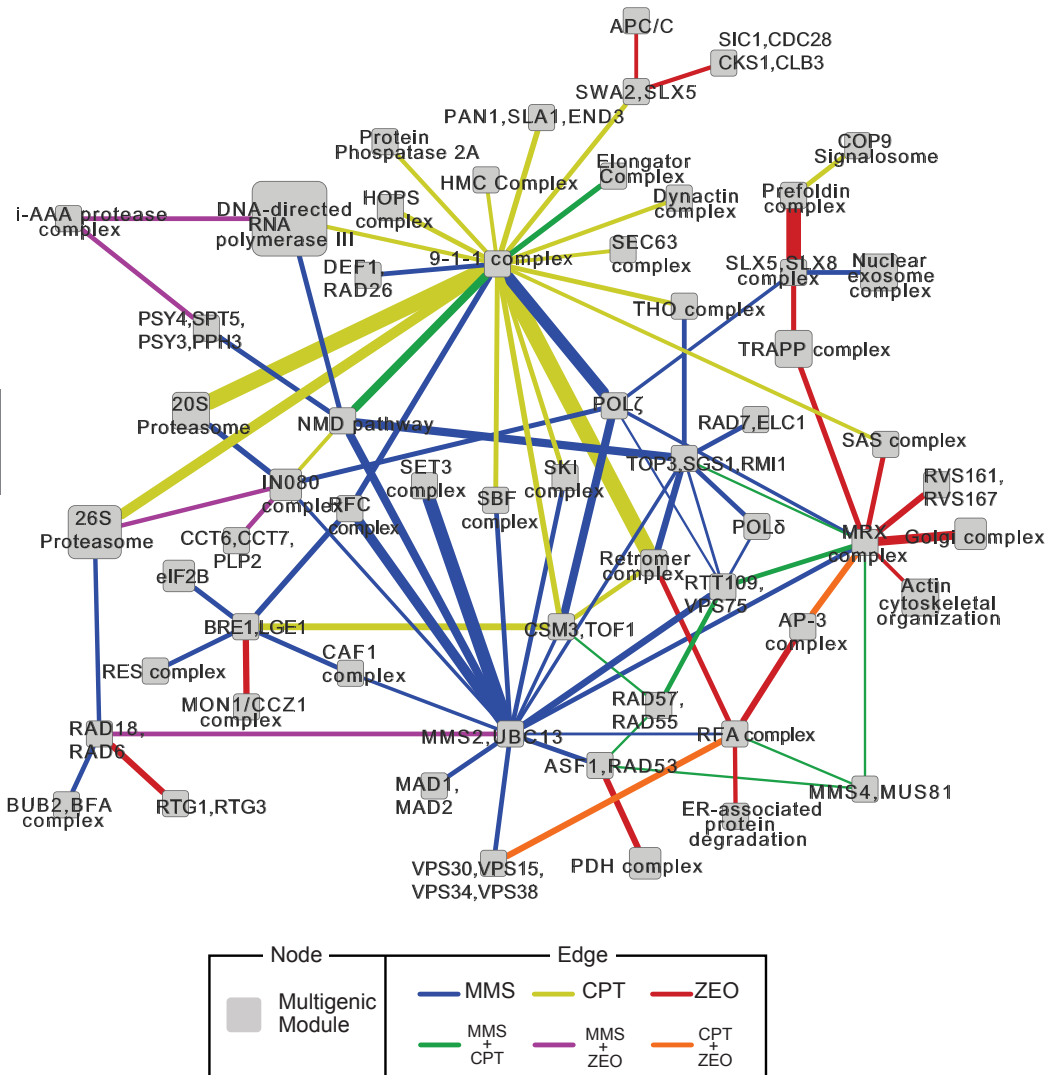


**Figure 5. A global map of DDR modules. A map of multi-protein modules connected by bundles of differential genetic interactions.** Node size scales with the number of proteins present in the module. Edge size scales with the significance of the enrichment for differential interactions spanning the two modules. For clarity only a portion of the entire map has been shown. The full list of module-module interactions is provided in Table S4.

**An integrated module network successfully and specifically maps drug induced-DNA damage responses**

An especially powerful approach for interpreting genetic interactions is in conjunction with knowledge of physical protein-protein interactions and protein complexes [24, 25]. Bandyopadhyay et al.

have previously demonstrated that, while static genetic interactions are enriched among components of the same physical complex, differential genetic interactions tend to occur between distinct but functionally-related complexes [10, 26, 27]. Based on this idea we used a recently-described integrative clustering algorithm

[28] to transform our differential genetic interaction data for all agents into a map of 179 modules and 452 module-module interactions (Figure 5 and Tables S4). Modules group genes with similar patterns of both genetic and physical interactions, many of which were found to coincide with known DNA repair complexes. Module-module interactions represent bundles of differential genetic interactions, which span across the genes in the two modules and point to DNA damage-induced cooperativity.

The low overlap we had observed among the genetic networks of the three agents (Figure 4A) was reproduced in the module map, as the vast majority (~90%) of module-module interactions were found to occur in response to a single agent. Indeed, each of the agents highlighted a different module as a central hub of interactions (Figure 5); these were the 9-1-1 DNA damage checkpoint complex (CPT), the Mms2/Ubc13 E2 ubiquitin conjugase complex (MMS) and the MRX double strand break repair complex (ZEO). Many of the interactions involving these hub modules recapitulate known drug-specific DDR mechanisms. For example, the 9-1-1 complex was found to genetically interact with the S-phase checkpoint complex Csm3/Tof1, which is consistent with recent work showing that both complexes are required for the response to CPT [29]. We also observed an MMS-dependent link between the INO80 chromatin remodeling complex and the Mms2/Ubc13 and Rad6/Rad18 ubiquitin E2 conjugase/E3 ligase complexes, which are involved in DNA damage tolerance. These observations are in line with recent work implicating a role for INO80 in this pathway that operates to overcome MMS-induced replication fork blocks [30]. In conclusion, our functional network was able to specifically discriminate the different drug-induced DNA damage responses not at a single gene

but at a pathway level.

## CONCLUSION

Here, we have measured ~100,000 differential interactions of DDR genes in response to three genotoxic agents with distinct modes of action. While the networks induced by each agent were largely divergent (Figure 4A), each was highly effective in pinpointing a set of pathways involved in specific types of DNA repair. To further aid in the discovery and mapping of these pathways, we integrated our multiconditional genetic network with protein interaction data to uncover a global map of gene modules and their inter-functional relationships (Figure 5). Here again, the module interactions induced by each agent were largely divergent, pointing to many agent-specific repair mechanisms.

Finally, this study illustrates that differential network analysis is a powerful approach for annotating gene function that is complementary to existing functional genomics technologies. Widespread availability of genome-wide knockout/RNAi libraries coupled with advances in sequencing technology has driven down both the cost and effort required to phenotype a large collection of gene knockouts or mutations or conduct differential mRNA expression profiling across dozens of conditions. However, the resolution of these technologies is ultimately limited to the total number of genes in a genome. In contrast, differential interaction mapping taps into a much larger (quadratic) space of gene-gene interactions, which we have shown enables the dissection of gene function in greater detail (Figure 2D). This power comes at a cost, as screening all gene pairs is presently arduous and expensive even in model organisms such as *S. cerevisiae*, requiring us to restrict coverage of the network map to a focused set of query genes. This tradeoff

2



in precision versus coverage is analogous to the two complementary strategies that have been employed in mapping disease-causing mutations: analysis of genotyped pedigrees, involving no more than two to three generations, provides a 'coarse' mapping to identify a large candidate region of the genome [31], after which 'fine mapping' techniques such as gene association studies, which leverage large unrelated populations, are used to pinpoint the location of the causal mutation more precisely [32]. Here, we have pursued a similar strategy by seeding our differential genetic interaction screen with genes, which have been previously annotated to high-level DDR processes. The resulting network highlights dynamic functional connections between numerous pathways and complexes at high resolution (Figure 5), suggesting a new paradigm for dissecting the mechanism of action of a family of related drugs or cellular responses.

2

## REFERENCES

1. Jackson, S.P., The DNA-damage response: new molecular insights and new approaches to cancer therapy. *Biochem Soc Trans*, 2009. 37(Pt 3): p. 483-94.
2. Ciccía, A. and S.J. Elledge, The DNA damage response: making it safe to play with knives. *Mol Cell*, 2010. 40(2): p. 179-204.
3. Hillenmeyer, M.E., et al., The chemical genomic portrait of yeast: uncovering a phenotype for all genes. *Science*, 2008. 320(5874): p. 362-5.
4. Paulsen, R.D., et al., A genome-wide siRNA screen reveals diverse cellular processes and pathways that mediate genome stability. *Mol Cell*, 2009. 35(2): p. 228-39.
5. Gasch, A.P., et al., Genomic expression programs in the response of yeast cells to environmental changes. *Mol Biol Cell*, 2000. 11(12): p. 4241-57.
6. Zhou, B.B. and S.J. Elledge, The DNA damage response: putting checkpoints in perspective. *Nature*, 2000. 408(6811): p. 433-9.
7. Longhese, M.P., DNA damage response at functional and dysfunctional telomeres. *Genes Dev*, 2008. 22(2): p. 125-40.
8. Norbury, C.J. and B. Zhivotovsky, DNA damage-induced apoptosis. *Oncogene*, 2004. 23(16): p. 2797-808.
9. Bjergbaek, L., et al., Mechanistically distinct roles for Sgs1p in checkpoint activation and replication fork maintenance. *EMBO J*, 2005. 24(2): p. 405-17.
10. Bandyopadhyay, S., et al., Rewiring of genetic networks in response to DNA damage. *Science*, 2010. 330(6009): p. 1385-9.
11. Tong, A.H. and C. Boone, Synthetic genetic array analysis in *Saccharomyces cerevisiae*. *Methods Mol Biol*, 2006. 313: p. 171-92.
12. Schuldiner, M., et al., Quantitative genetic analysis in *Saccharomyces cerevisiae* using epistatic miniarray profiles (E-MAPs) and its application to chromatin functions. *Methods*, 2006. 40(4): p. 344-52.
13. Collins, S.R., et al., A strategy for extracting and analyzing large-scale quantitative epistatic interaction data. *Genome Biol*, 2006. 7(7): p. R63.
14. Ideker, T. and N.J. Krogan, Differential network biology. *Mol Syst Biol*, 2012. 8: p. 565.
15. Tong, A.H., et al., Global mapping of the yeast genetic interaction network. *Science*, 2004. 303(5659): p. 808-13.
16. Costanzo, M., et al., The genetic landscape of a cell. *Science*, 2010. 327(5964): p. 425-31.
17. Ryan, C.J., et al., Hierarchical Modularity and the Evolution of Genetic Interactomes across Species. *Mol Cell*, 2012. 46(5): p. 691-704.
18. Ulukan, H. and P.W. Swaan, Camptothecins: a review of their chemotherapeutic potential. *Drugs*, 2002. 62(14): p. 2039-57.
19. Lundin, C., et al., Methyl methanesulfonate (MMS) produces heat-labile DNA damage but no detectable in vivo DNA double-strand breaks. *Nucleic Acids Res*, 2005. 33(12): p. 3799-811.
20. Kats, E.S., et al., The *Saccharomyces cerevisiae* Rad6 postreplication repair and Siz1/Srs2 homologous recombination-inhibiting pathways process DNA damage that arises in asf1 mutants. *Mol Cell Biol*, 2009. 29(19): p. 5226-37.
21. Wu, M., Z. Zhang, and W. Che, Suppression of a DNA base excision repair gene, hOGG1, increases bleomycin sensitivity of human lung cancer cell line. *Toxicol Appl Pharmacol*, 2008. 228(3): p. 395-402.
22. Travesa, A., et al., DNA replication stress differentially regulates G1/S genes via Rad53-dependent inactivation of Nrm1. *EMBO J*, 2012.
23. Caba, E., et al., Differentiating mechanisms of toxicity using global gene expression analysis in *Saccharomyces cerevisiae*. *Mutat Res*, 2005. 575(1-2): p. 34-46.
24. Kelley, R. and T. Ideker, Systematic

interpretation of genetic interactions using protein networks. *Nat Biotechnol*, 2005. 23(5): p. 561-6.

25. Zhang, L.V., et al., Motifs, themes and thematic maps of an integrated *Saccharomyces cerevisiae* interaction network. *J Biol*, 2005. 4(2): p. 6.

26. Bandyopadhyay, S., et al., Functional maps of protein complexes from quantitative genetic interaction data. *PLoS Comput Biol*, 2008. 4(4): p. e1000065.

27. Ulitsky, I., et al., From E-MAPs to module maps: dissecting quantitative genetic interactions using physical interactions. *Mol Syst Biol*, 2008. 4: p. 209.

28. Srivas, R., et al., Assembling global maps of cellular function through integrative analysis of physical and genetic networks. *Nat Protoc*, 2011. 6(9): p. 1308-23.

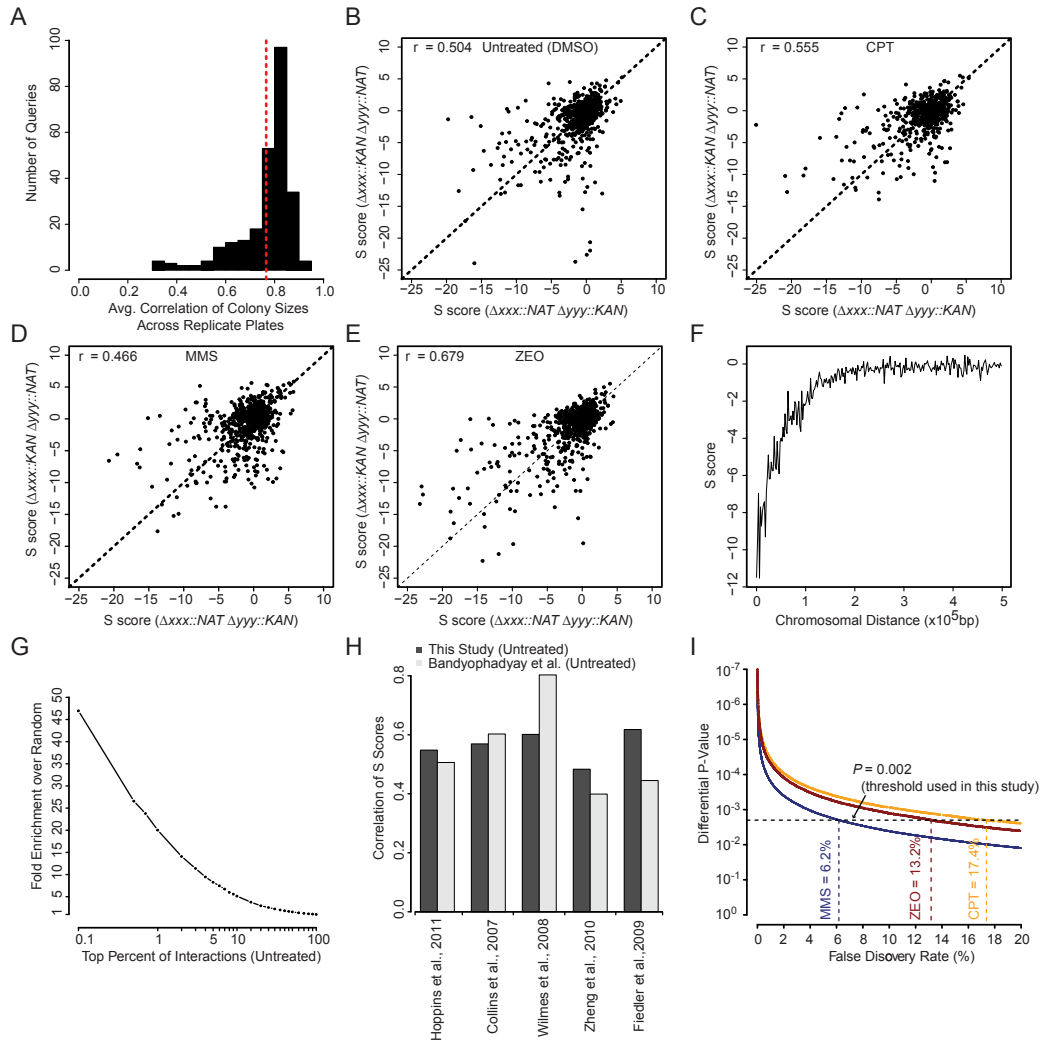
29. Redon, C., D.R. Pilch, and W.M. Bonner, Genetic analysis of *Saccharomyces cerevisiae* H2A serine 129 mutant suggests a functional relationship between H2A and the sister-chromatid cohesion partners Csm3-Tof1 for the repair of topoisomerase I-induced DNA damage. *Genetics*, 2006. 172(1): p. 67-76.

30. Kato, D., et al., Phosphorylation of human INO80 is involved in DNA damage tolerance. *Biochem Biophys Res Commun*, 2012. 417(1): p. 433-8.

31. Perez-Enciso, M., Fine mapping of complex trait genes combining pedigree and linkage disequilibrium information: a Bayesian unified framework. *Genetics*, 2003. 163(4): p. 1497-510.

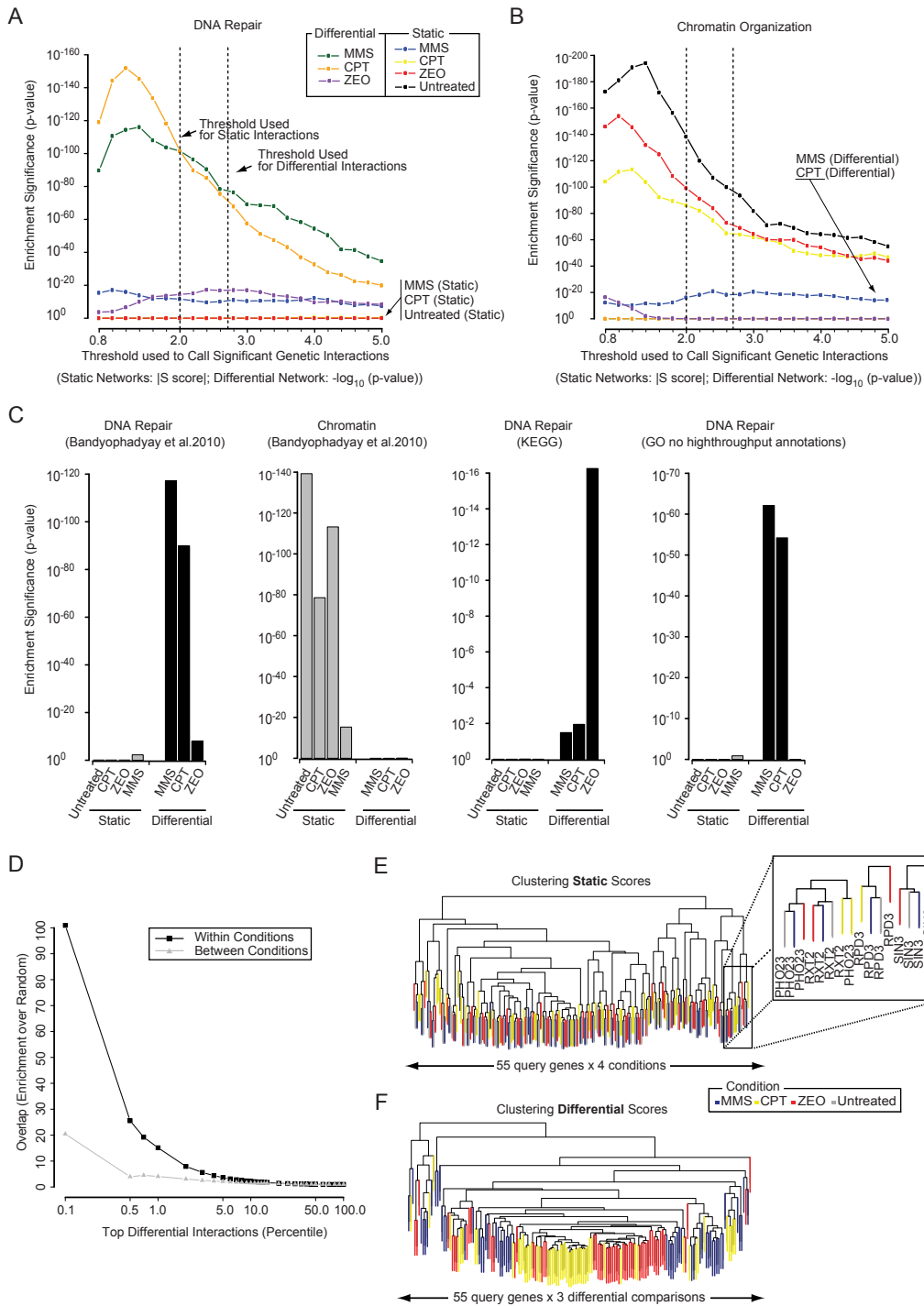
32. Hastbacka, J., et al., The diastrophic dysplasia gene encodes a novel sulfate transporter: positional cloning by fine-structure linkage disequilibrium mapping. *Cell*, 1994. 78(6): p. 1073-87.

**SUPPLEMENTAL DATA**



2

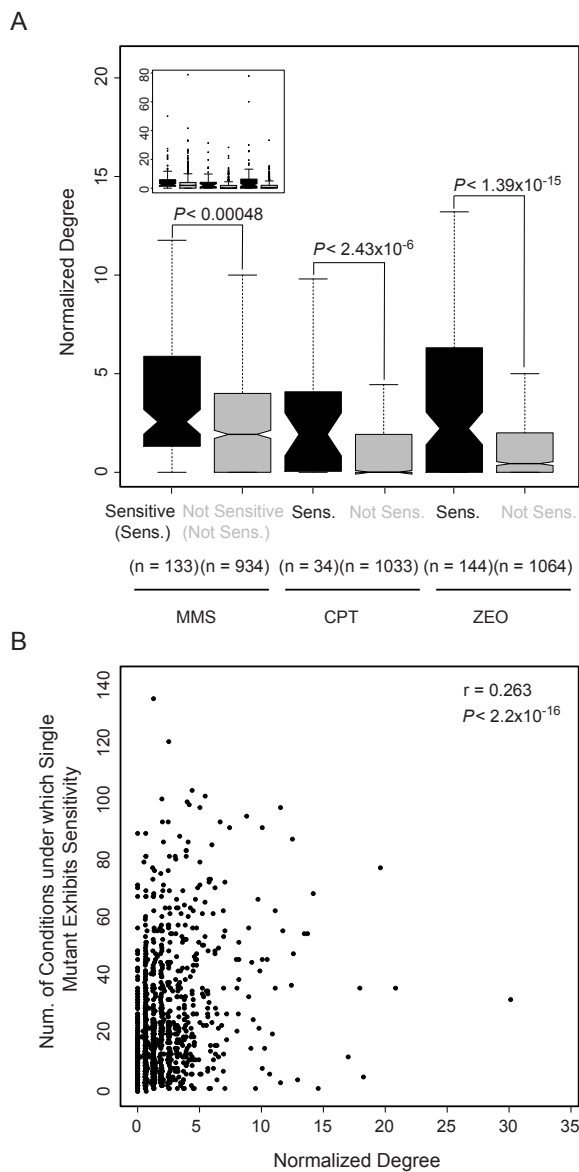
**Supplemental Figure S1. Quality of genetic interaction data** (A) Each query mutant was crossed against the set of array mutants six different times. This histogram displays the average correlation seen in colony size measurements between the six replicates for each query across all four conditions (Untreated, MMS, CPT, and ZEO). The dotted red-line indicates the average correlation seen across all queries and all conditions ( $r = 0.78$ ). (B-E) Correlation of genetic interaction scores derived from ‘marker swap’ experiments for (B) Untreated, (C) CPT, (D) MMS, and (E) ZEO. (F) Genetic interaction scores for pairs of genes in linkage. (G) The fold-enrichment for low-throughput genetic interactions from the Biogrid database (Stark et al., 2006) is shown. Fold-enrichment is defined as  $n/r$ , where  $n$  is the number of highest scoring static genetic interactions in untreated conditions ( $x$ -axis) found in the Biogrid database, while  $r$  is the number of overlapping interactions expected at random. (H) Correlation of S scores measured under untreated conditions from this study (dark grey) or a previously published dE-MAP (Bandyopadhyay et al., 2010) (light grey) versus five large genetic interaction screens. (I) The differential  $p$ -value ( $x$ -axis) is plotted versus the corresponding multiple hypothesis corrected false discovery rate (FDR) (corrected using the Benjamini-Hochberg procedure) for each condition.



**Supplemental Figure S2. Comparison of replicate differential genetic networks and robustness of functional enrichment results** (A) The overlap in replicate differential networks seen amongst the same condition (black line) or between two different conditions (grey line). Replicate networks were derived by splitting the six replicates obtained for each double mutant into two sets and scoring each set independently.

A multiconditional genetic map to dissect DNA damage responses

► **Supplemental Figure S2 (Suite).** Enrichment over random (y-axis) is defined as the ratio of overlapping interactions seen between replicate networks amongst the top percent of differential interactions (x-axis) to the number of overlapping interactions expected at random. (B) Dendrogram of each query gene in each of four conditions (Untreated, MMS, CPT, and ZEO) generated by hierarchically clustering their static genetic interaction patterns across 2022 array genes. The leaves of the dendrogram have been colored according to the condition. The insert shows an expanded view of one branch of the dendrogram. (C) As in B, except that the dendrogram is generated by hierarchically clustering the differential interaction profiles for each query gene in each of three pairwise differential comparisons (MMS vs. Untreated, CPT vs. Untreated, ZEO vs. untreated). Leaves of the dendrogram have been colored as in B. (D-E) The significance of enrichment for interactions with either (D) DNA repair or (E) chromatin organization genes is plotted for all static and differential genetic networks across a range of thresholds. For static networks the absolute value of the S score is used as a threshold. For differential networks the  $-\log_{10}$ (differential p-value) is used as a threshold. (F) Enrichment results using different databases to define DNA repair and chromatin organization gold-standard genes.



**Supplemental Figure S3. Differential genetic hubs display greater DNA damage sensitivity and tend to display pleiotropy**

(A) All genes considered in this screen are binned according to their single mutant sensitivity to MMS, CPT, or ZEO. The distribution of the normalized differential degree (# sig. interactions / # tested interactions) for the genes in each bin is summarized with a box-and-whisker plot. The inset shows the full range of the distribution of normalized degrees, while the main plot shows a zoomed-in portion. A p-value was calculated using the Mann-Whitney test. (B) The Hillenmeyer et al. study (Hillenmeyer et al., 2008) measured single-gene knockout sensitivities to over 400 different compounds. The normalized degree for each gene considered in this study is plotted against the number of drugs for which the gene knockout is sensitive.

2

## SUPPLEMENTAL TABLE

## Supplemental Table 1

Gene	ORF	Essential	Description
AHC1	YOR023C	No	Subunit of the Ada histone acetyltransferase complex
ARP8	YOR141C	No	Nuclear actin-related protein involved in chromatin remodeling
ASF1	YJL115W	No	Nucleosome assembly factor
BRE1	YDL074C	No	E3 ubiquitin ligase
CTF18	YMR078C	No	Subunit of a Ctf18 RFC-like complex
DCN1	YLR128W	No	Scaffold-type E3 ligase
DDC1	YPL194W	No	DNA damage checkpoint protein
DOT1	YDR440W	No	Nucleosomal histone H3-Lys79 methylase
EAF3	YPR023C	No	Esa1p-associated factor
EAF5	YEL018W	No	Esa1p-associated factor
EAF7	YNL136W	No	Subunit of the NuA4 histone acetyltransferase complex
ELP3	YPL086C	No	Subunit of Elongator complex
EXO1	YOR033C	No	5'-3' exonuclease and flap-endonuclease involved in recombination, double-strand break repair and DNA mismatch repair
HAT1	YPL001W	No	Catalytic subunit of the Hat1p-Hat2p histone acetyltransferase complex
HDA1	YNL021W	No	Putative catalytic subunit of the HDA1 histone deacetylase complex
HEX3	YDL013W	No	Protein containing a RING finger domain that interacts with Slx8p
HST3	YOR025W	No	Member of the Sir2 family of NAD(+)-dependent protein deacetylases
IES2	YNL215W	No	Protein that associates with the INO80 chromatin remodeling complex under low-salt conditions
IES3	YLR052W	No	Subunit of the INO80 chromatin remodeling complex
MRC1	YCL061C	No	S-phase checkpoint protein required for DNA replication
MRE11	YMR224C	No	Subunit of a complex with Rad50p and Xrs2p (MRX complex)
NHP10	YDL002C	No	Protein related to mammalian high mobility group proteins
NUP133	YKR082W	No	Subunit of the Nup84p subcomplex of the nuclear pore complex (NPC)
PHO23	YNL097C	No	Probable component of the Rpd3 histone deacetylase complex, involved
PPH3	YDR075W	No	Catalytic subunit of protein phosphatase PP4 complex
PRE9	YGR135W	No	Alpha 3 subunit of the 20S proteasome
PSY2	YNL201C	No	Subunit of protein phosphatase PP4 complex
RAD17	YOR368W	No	Checkpoint protein
RAD18	YCR066W	No	E3 ubiquitin ligase
RAD5	YLR032W	No	DNA helicase proposed to promote replication fork regression
RAD52	YML032C	No	Protein that stimulates strand exchange
RAD9	YDR217C	No	DNA damage-dependent checkpoint protein
RCO1	YMR075W	No	Essential subunit of the histone deacetylase Rpd3S complex
RPD3	YNL330C	No	Histone deacetylase
RRI1	YDL216C	No	Catalytic subunit of the COP9 signalosome (CSN) complex
RSC1	YGR056W	No	Component of the RSC chromatin remodeling complex
RTT101	YJL047C	No	Cullin subunit of a Roc1p-dependent E3 ubiquitin ligase complex
RTT109	YLL002W	No	Histone acetyltransferase
RUB1	YDR139C	No	Ubiquitin-like protein with similarity to mammalian NEDD8
RXT2	YBR095C	No	Subunit of the histone deacetylase Rpd3L complex
SAE2	YGL175C	No	Endonuclease involved in processing hairpin DNA structures
SET1	YHR119W	No	Histone methyltransferase, subunit of the COMPASS (Set1C) complex
SET2	YJL168C	No	Histone methyltransferase with a role in transcriptional elongation
SET3	YKR029C	No	Defining member of the SET3 histone deacetylase complex
SGS1	YMR190C	No	Nucleolar DNA helicase of the RecQ family
SIN3	YOL004W	No	Component of the Sin3p-Rpd3p histone deacetylase complex
SLX8	YER116C	No	Subunit of the Slx5-Slx8 SUMO-targeted ubiquitin ligase complex
SNF11	YDR073W	No	Subunit of the SWI/SNF chromatin remodeling complex
SWC5	YBR231C	No	Protein of unknown function
SWR1	YDR334W	No	Swi2/Snf2-related ATPase structural component of the SWR1 complex
TOF1	YNL273W	No	Subunit of a replication-pausing checkpoint complex
UBC13	YDR092W	No	E2 ubiquitin-conjugating enzyme
VPS72	YDR485C	No	Htz1p-binding component of the SWR1 complex
VPS75	YNL246W	No	NAP family histone chaperone
YKU70	YMR284W	No	Subunit of the telomeric Ku complex (Yku70p-Yku80p)

**Supplemental Table S1. Lists of query and array genes used in this study along with their function.** Refers to Figure 1. The list of array genes is not provided for the sake of space. The primary functional category was used to construct the barplot seen in Figure 1A

**Supplemental Table S2. List of all genetic interactions measured in this study.** For each gene pair, the static genetic interaction (S score) for all four conditions (Untreated, MMS, CPT, and ZEO), and differential p-value for each pairwise comparison (MMS versus Untreated, CPT versus Untreated, and ZEO versus Untreated) is provided. Refers to Figures 1 and 2. Differential p-values are presented as a signed  $-\log_{10}(\text{p-values})$ . The sign indicates the direction of the change in interaction with respect to the treatment. This table is not provided for the sake of space.

A multiconditional genetic map to dissect DNA damage responses

Supplemental Table 3

Gene	Main Functional Categories	DNA Repair sub-categories	Gene	Main Functional Categories	DNA Repair sub-categories
YEN1	DR	NA	TAF5	CO	NA
TTI2	CO	NA	EPL1	DR,CO	NA
YPL216W	CO	NA	SWC4	DR,CO	NA
TTI1	CO	NA	SWC3	CO	NA
TEL1	DR,CO	DSBR	PSF3	DR	DSBR
RAD9	DR	DDC,NER	RSC1	DR,CO	DSBR
DNL4	DR	DSBR	SWC5	CO	NA
RAD7	DR	NER	PSF2	DR	DSBR
RAD6	DR,CO	DDC,PRR,DSBR	RSC3	CO	NA
RAD5	DR	PRR,DSBR	RSC2	DR,CO	DSBR
HPA2	CO	NA	PSF1	DR	DSBR
MKT1	DR	NA	DNA2	DR	DSBR
LCD1	DR,CO	DDC	RSC4	CO	NA
HTB2	CO	NA	EAF1	DR,CO	NA
HTB1	DR,CO	PRR	DDR48	DR	NA
CSM3	DR	NA	RSC6	CO	NA
UTH1	CO	NA	RSC9	CO	NA
CHZ1	CO	NA	RSC8	DR,CO	DSBR
CSM2	DR	NA	EAF5	DR,CO	NA
ACS1	CO	NA	RTG2	CO	NA
ACS2	CO	NA	EAF3	DR,CO	NA
AHC1	CO	NA	YNG2	DR,CO	NA
ELC1	DR	NER	EAF7	DR,CO	NA
RAD1	DR	NER,DSBR,MMR	EAF6	DR,CO	NA
RAD2	DR	NER	CYC8	CO	NA
UME1	CO	NA	XRS2	DR	DSBR,BER
RAD3	DR	NER	RSC30	DR,CO	DSBR
RAD4	DR	NER	CDC45	DR	DSBR
ACT1	DR,CO	NA	TRF5	DR	NA
HTA2	DR,CO	NA	RTF1	CO	NA
HTA1	DR,CO	NA	NTG1	DR	BER
CTI6	CO	NA	NTG2	DR	BER
ASH1	CO	NA	GLC7	CO	DDC
SUS1	CO	NA	HSM3	DR	MMR
UME6	CO	NA	SAS2	CO	NA
RLF2	DR,CO	NA	SIT4	DR	NA
HFC2	CO	NA	SAS4	CO	NA
VPS71	CO	NA	SAS3	CO	NA
VPS75	DR,CO	DSBR	DEF1	DR	NER
VPS72	CO	NA	HIF1	CO	NA
LEO1	CO	NA	SDC1	CO	NA
SPP1	CO	NA	SAS5	CO	NA
RDH54	DR	DSBR	MET18	DR	NER
RNT1	CO	NA	DDC1	DR	DDC
SIR4	DR,CO	DSBR	SPT2	CO	NA
SIR3	DR,CO	DSBR	WSS1	DR	NA
FYV6	DR	DSBR	SPT5	DR,CO	NER
SIR2	DR,CO	DSBR	CTF4	DR	DSBR
SIR1	CO	NA	SPT6	CO	NA
GIS1	CO	NA	SPT3	CO	NA
IOC4	CO	NA	UNG1	DR	BER
IOC3	CO	NA	LIF1	DR	DSBR
SGS1	DR	DDC,DSBR	CHD1	CO	NA
CDC1	DR	NA	RCO1	CO	NA
ARD1	CO	NA	EXO1	DR	DSBR,MMR
APC5	CO	NA	IES1	CO	NA
IXR1	DR	NA	RPL40B	DR	NA
HUG1	DR	NA	IES3	CO	NA
SEN1	DR	NA	TFB4	DR	NER
SGV1	CO	NA	SMC5	DR	NA
FPR1	CO	NA	RXT3	CO	NA
FPR4	CO	NA	TFB5	DR	NER
CTF18	DR	DSBR	SMC6	DR	NA
YNK1	DR	NA	RXT2	CO	NA
RSP5	CO	NA	SNF12	CO	NA
FKH2	CO	NA	SMC1	DR	DSBR
FKH1	CO	NA	TFB1	DR	NER
SRS2	DR	DSBR	CSE4	CO	NA
ASF1	DR,CO	NA	HTL1	CO	NA
SNT1	CO	NA	NSE3	DR	NA
SWP82	CO	NA	SHU2	DR	NA
OGG1	DR	NER,BER	SHU1	DR	NA
SIN3	DR,CO	DSBR	NSE1	DR	PRR
SLD2	DR	DSBR	NSE4	DR	NA
SFH1	DR,CO	DSBR	NSE5	DR	NA
INO80	DR,CO	NA	YNG1	CO	NA
SWD3	CO	NA	SNF5	DR,CO	DSBR
SLD5	DR	DSBR	SNF6	DR,CO	NER
SWD2	CO	NA	TAF9	CO	NA
SWD1	CO	NA	SNF2	DR,CO	DSBR
SLD3	DR	DSBR	MRC1	DR	DDC
IMP2	DR	NA	TAF1	CO	NA
SOH1	DR	NA	SWC7	CO	NA
RPN4	DR	NA	TAF6	CO	NA
PMS1	DR	MMR	UBC7	CO	NA
CBF1	CO	NA	ISW2	CO	NA
MEC3	DR	DDC	ISW1	CO	NA
ARP9	CO	NA	SPT20	CO	NA
ARP7	CO	NA	TAH11	DR	DSBR
ARP8	CO	NA	PAA1	CO	NA
SAW1	DR	DSBR	MPH1	DR	NA
HHF1	CO	NA	CDC7	DR	DSBR
ARP5	CO	NA	CDC9	DR	NER,BER
ARP6	CO	NA	ELG1	DR	DSBR
MMS22	DR	DSBR	TSA1	NA	DDC
ARP4	DR,CO	NA	ABF1	DR,CO	NER
MMS21	DR	NA	DUN1	DR	DDC
MEC1	DR,CO	DDC	TAF10	CO	NA
ELF1	CO	NA	TAF12	CO	NA
BRE1	DR,CO	DDC,DSBR	IOC2	CO	NA





## Chapter 2

## Supplemental Table 3 (suite)

Gene	Main Functional Categories	DNA Repair sub-categories	Gene	Main Functional Categories	DNA Repair sub-categories
RTT109	DR,CO	DSBR	ESC2	DR	DDC,DSBR
MGT1	DR	NA	SSL1	DR	NER
PR12	DR	NA	SSL2	DR	NER
ULS1	CO	NA	HAT2	DR,CO	NA
HHO1	CO	NA	HAT1	DR,CO	NA
UBP8	CO	NA	SBS3	CO	NA
PHO4	CO	NA	MUS81	DR,CO	NA
DPB4	DR	NER,MMR	MSI1	DR,CO	NA
DPB3	DR	NER,MMR	MSH6	DR	MMR
DPB2	DR	NER,MMR	MSH3	DR	MMR
PTC2	NA	DDC	MSH2	DR	MMR
SCC4	DR	DSBR	MSH5	DR	MMR
PHO2	CO	NA	MSH4	DR	MMR
MLH2	DR	MMR	RPB9	DR	NER
MLH1	DR	MMR	RPB4	DR	NA
MLH3	DR	MMR	HPR1	DR	NER
SWI3	CO	NA	POB3	DR,CO	NA
SWI1	CO	NA	HHT1	DR,CO	NA
DIN7	DR	NA	DOT1	DR,CO	DDC,NER,PRR
ADA2	CO	NA	TDP1	DR	NA
PNG1	DR	NER	HHT2	DR,CO	NA
HNT3	DR	NA	ESA1	DR,CO	NA
HST4	CO	NA	THP1	DR	NER
MCD1	DR	DSBR	MSH1	DR	MMR
SLX1	DR	NA	BUJ6	CO	NA
BDF1	DR,CO	NA	HED1	DR	NA
RAD28	DR	NA	RAD59	DR	DSBR
RAD27	DR	DSBR,BER	RAD57	DR	DSBR
ORC2	CO	NA	RAD54	DR,CO	DSBR
RAD26	DR	NER	RAD55	DR	DSBR
SHG1	CO	NA	RAD52	DR,CO	PRR,DSBR
MRE11	DR	DSBR,BER	YKU80	DR,CO	DSBR
RAD10	DR	NER,DSBR,MMR	SLX8	DR	NA
CST9	DR	NA	BRE2	CO	NA
KRE29	DR	NA	TRA1	DR,CO	NA
HTZ1	CO	NA	BUR2	CO	NA
RAD18	DR	PRR	RSC58	CO	NA
PAF1	CO	NA	RTT102	CO	NA
NPL6	CO	NA	CDC28	DR	DSBR
SIF2	CO	NA	RTT106	CO	NA
RAD14	DR	NER	SUB2	DR	NER
RAD17	DR	DDC,DSBR	RTT107	DR	DSBR
RAD16	DR	NER	NEJ1	DR	DSBR
POL31	DR	NER,PRR,BER,MMR	JHD1	CO	NA
SGF73	CO	NA	JHD2	CO	NA
POL30	DR	NER,PRR,BER,MMR	TOF1	DR	NA
POL32	DR	NER,PRR,DSBR,BER,MMR	YAF9	DR,CO	NA
SPT16	DR,CO	NA	RFA3	DR	NER,DSBR
CPR1	CO	NA	RFA2	DR	NER,DSBR
SAC3	DR	NER	RFA1	DR	NER,DSBR
SNF11	CO	NA	MCK1	DR	DSBR
TFB2	DR	NER	PIF1	DR	NA
RPL40A	DR	NA	MMS4	DR	NA
PHR1	DR	NA	BMH1	NA	DDC
TFB3	DR	NER	BMH2	NA	DDC
NEW1	CO	NA	MAG1	DR	BER
PDS1	DR	NA	SET4	CO	NA
CTF8	DR	NA	SET3	CO	NA
PDS5	DR	DSBR	CTR9	CO	NA
STB2	CO	NA	SET2	CO	NA
NHP6B	DR,CO	NA	SET1	CO	NA
NHP6A	DR,CO	MMR	HMI1	DR	NA
MEI5	DR	DSBR	YKU70	DR,CO	DSBR
PUF4	CO	NA	ITC1	CO	NA
HIR2	CO	NA	NAP1	CO	NA
HIR1	CO	NA	SWR1	CO	NA
HIR3	CO	NA	HF11	CO	NA
PAN2	DR	PRR	PHO23	CO	NA
PAN3	DR	PRR	LGE1	CO	NA
ECO1	DR	DSBR	HDA3	CO	NA
RKR1	CO	NA	SAP30	CO	NA
HMO1	CO	NA	HDA2	CO	NA
RPD3	CO	NA	HDA1	CO	NA
RFC5	DR	MMR	SGF11	CO	NA
RFC3	DR	MMR	MLP1	DR,CO	NA
RFC4	DR	MMR	MCM7	DR	DSBR
YRA1	DR	NER	TPP1	DR	NA
RFC1	DR	MMR	GCN2	NA	DDC
HRR25	DR	NA	GCN5	CO	NA
RFC2	DR	MMR	THO2	DR	NER
POL3	DR	NER,PRR,BER,MMR	ELP3	CO	NA
POL4	DR	DSBR,BER	REV1	DR	PRR
POL1	DR	NA	MCM2	DR	DSBR
POL2	DR	NER,DSBR,MMR	LDB7	CO	NA
MPT5	CO	NA	MCM3	DR	DSBR
SCC2	DR	DSBR	MCM4	DR	DSBR
MGS1	DR	NA	MCM5	DR,CO	DSBR
APN2	DR	BER	MCM6	DR	DSBR
APN1	DR	BER	PSO2	DR	DSBR
UBC13	DR	PRR	REV7	DR	PRR
PIN4	NA	DDC	SGF29	CO	NA
CHK1	NA	DDC	REV3	DR	PRR
DOA1	DR	DSBR	NGG1	CO	NA
DEP1	CO	NA	PRP19	DR	NA
SPT10	DR,CO	NA	SAE2	DR	DSBR
SLX4	DR	DSBR	MCM10	DR	DSBR
SLX5	DR	NA	SAE3	DR	DSBR
MMS1	DR	NA	RVB1	DR,CO	NA
MMS2	DR	PRR	TOP2	CO	NA
RAD23	DR	NER	RAD24	DR	DDC,NER

**Supplemental Table 3 (suite)**

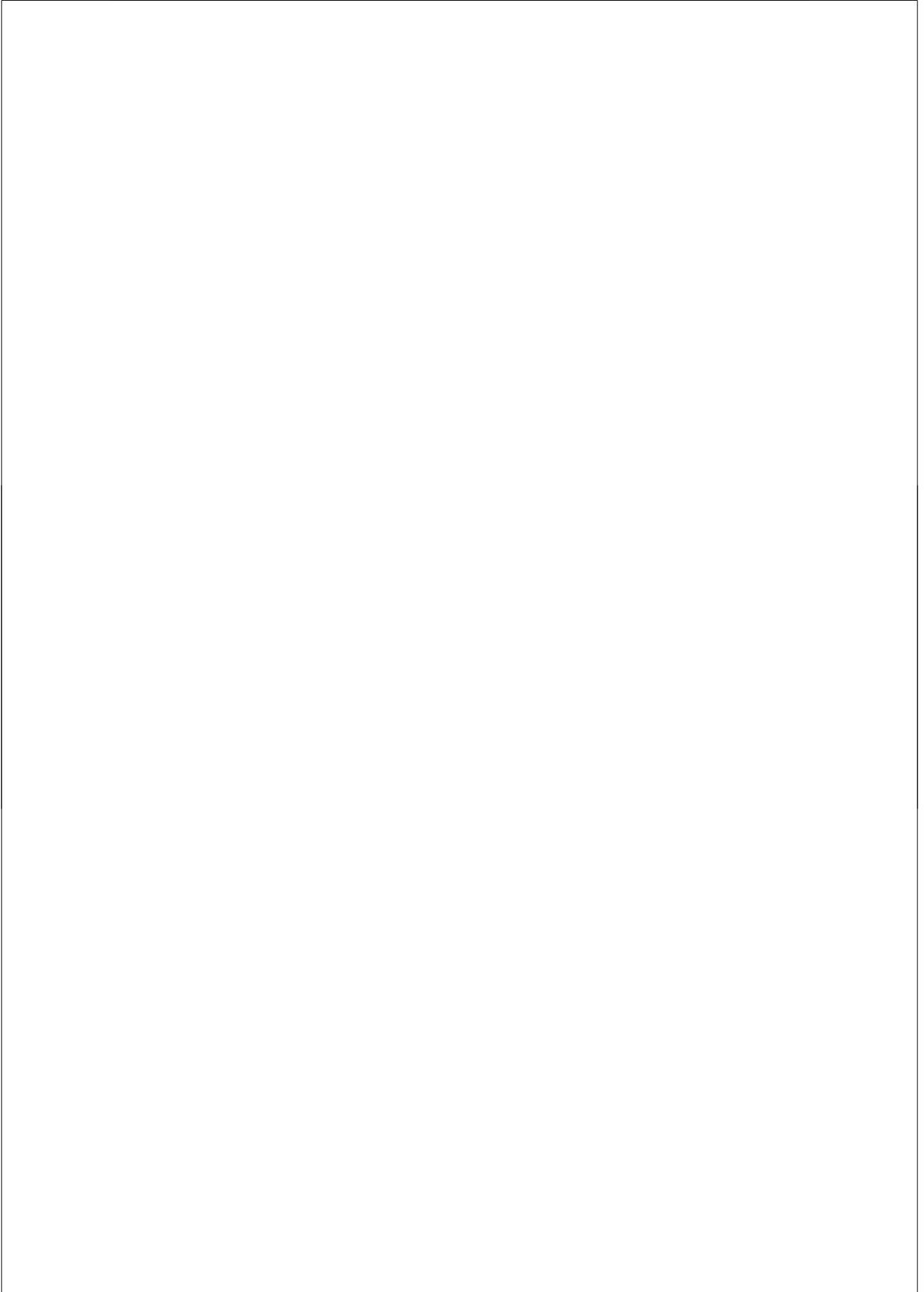
Gene	Main Functional Categories	DNA Repair sub-categories
HST3	CO	NA
FOB1	CO	NA
HST1	CO	NA
RPH1	DR,CO	NA
RAD53	DR	DDC
RAD50	DR	DSBR,BER
RAD51	DR	DSBR
HOS4	CO	NA
NTO1	CO	NA
HIM1	DR	NA
HOS2	CO	NA
HOS3	CO	NA
HOS1	CO	NA
TRM2	DR	DSBR
IWR1	CO	NA
DPB11	DR	DDC,NER,DSBR,MMR
NAT4	CO	NA
RAD30	DR	PRR
PAP2	DR	BER
RAD34	DR	NER
RAD33	DR	NER
RVB2	DR,CO	NA
HHF2	DR,CO	NA
SPT7	CO	NA
SPT8	CO	NA
SPT4	DR,CO	NER
CDC73	CO	NA
TAF14	CO	NA
RRD1	DR	NA
STH1	DR,CO	DSBR
NHP10	DR,CO	DSBR
TOP3	DR	NA
BDF2	DR	NA
TUP1	CO	NA
PSY3	DR	NA
TOP1	CO	NA
MGM101	DR	NA
CAC2	DR,CO	NA

**Supplemental Table S3. List of gold standard genes belonging to various DNA repair and chromatin organization pathways.** This list was downloaded from the Gene Ontology (GO) database on December 2010 (Ashburner et al., 2000). The main functional categories include: DNA Repair (DR) and Chromatin Organization (CO). The DNA repair sub-categories include: double-stranded break repair (DSBR), DNA damage checkpoint (DDC), nucleotide excision repair (NER), base excision repair (BER), mismatch repair (MMR), and post-replication repair (PRR)

A "NA" indicates no functional assignment. Refers to Figures 3 and 4.



**Supplemental Table S4. List of module-module interactions identified in this study.** For each module pair, the enrichment significance for the number of differential interactions spanning the two modules is provided for each condition. Refers to Figure 5. This table is not provided for the sake of space.





## RTT109 CHROMATIN MODIFIER REGULATES MUTAGENIC DNA DAMAGE BYPASS

Aude Guénolé<sup>1</sup>, Rohith Srivas<sup>2,3</sup>, Kees Vreeken<sup>1</sup>, Jaap Jansen<sup>1</sup>, Trey Ideker<sup>2,3,4</sup>, Haico van Attikum<sup>1</sup>

<sup>1</sup>Department of Toxicogenetics, Leiden University Medical Center, Einthovenweg 20, 2333 ZC, Leiden, The Netherlands, <sup>2</sup>Department of Bioengineering, University of California, San Diego, La Jolla, CA 92093 USA, <sup>3</sup>Department of Medicine, University of California, San Diego, La Jolla, CA 92093, USA, <sup>4</sup>The Institute for Genomic Medicine, University of California, San Diego, La Jolla, CA 92093, USA

*(Manuscript in preparation)*

Chapter 3

3

**ABSTRACT**

Mutations have been a driving force in the evolution of every organism. Although they can be beneficial, in most of the cases they lead to protein dysfunction, which in turn can impair important cellular pathways and cause diseases such as cancer. Mutations arise primarily from processing of DNA lesions that are induced by environmental threats or by endogenous cellular metabolism. Although cells have evolved mechanisms for the repair of DNA damage, they can also tolerate (unrepaired) DNA lesions that may pose blocks to replication forks. To date, template switching and translesion synthesis (TLS) are the best-characterized DNA damage tolerance pathways. The first process is error-free while the latter can be mutagenic. How DNA damage tolerance is regulated in the context of chromatin is largely unclear. Here, we report on a new role for the histone acetyltransferase Rtt109 in TLS. Our results suggest that Rtt109 affects DNA damage bypass mediated by different TLS polymerases.

**INTRODUCTION**

To cope with the deleterious effects of DNA damage, cells have evolved a variety of repair processes. However despite their efficacy, the replication machinery may encounter unrepaired DNA lesions that can block progression of replication forks. To prevent prolonged replication fork arrest and subsequent collapse of the complex molecular machinery that carries out DNA replication namely the replisome, cells possess error-free and error-prone mechanisms collectively referred to as DNA damage tolerance or post-replication repair (PRR) pathways. The coordination of these pathways during DNA replication is mediated by two ubiquitin-conjugating and ligating complexes Rad6-Rad18 and Rad5-Mms2-Ubc13. When replication forks are blocked by DNA lesions, PCNA is mono-ubiquitylated by the Rad6-Rad18 complex. Mono-ubiquitylation of PCNA promotes error-free and error-prone bypass through a mechanism called translesion synthesis (TLS), while its polyubiquitylation by the Mms2-Ubc13 complex favors the error-free bypass pathway of template switching. During TLS, the replicative polymerase Pol $\delta$  and specialized TLS polymerases such as Pol $\eta$  (Rad30), Rev1 and Pol $\zeta$  are able to incorporate nucleotides at the 3' of the lesion and as such allow the replication to restart downstream of the lesion [1]. Template switching is a mechanism that uses the sister chromatid as a template to bypass the lesion in a recombination-like event and likely involves key homologous recombination factors, including Rad52 [2]. Pol $\eta$ 's (encoded by RAD30) major function is to ensure error-free bypass of cyclobutane pyrimidine dimers (CPDs), which are lesions typically caused by ultraviolet (UV) light [3]. However, some reports also suggest that Pol $\eta$  is involved in mutagenic bypass events depending on the type of DNA lesion [4, 5]. On the other hand, Rev1 and the Pol $\zeta$  complex composed

of Rev7 and the catalytic subunit Rev3, are responsible for the vast majority of the mutagenic bypass events [6]. Biochemical and genetic evidence suggests that Rev1 stimulates Pol $\zeta$ -mediated extension from a mismatch or bypass of a lesion [7]. At last, in yeast, Pol3 and Pol32 (two subunits of the replicative polymerase Pol $\delta$ ) have also been implicated in damage-induced mutagenesis [8, 9]. Importantly, the two Pol $\delta$  subunits Pol31 and Pol32 were recently found in a stoichiometric four-subunit complex containing the Pol $\zeta$  subunits Rev3 and Rev7, providing a biochemical explanation for how Pol $\delta$  could affect DNA damage-induced mutagenesis [10].

In eukaryotic cells, DNA is wrapped around histone proteins resulting in densely packed chromatin, which limits the access of repair enzymes to DNA lesions. How chromatin is converted into a dynamic molecule that allows access and repair of DNA lesion has become a growing field of investigation. Histone modifications including phosphorylation, methylation, ubiquitylation and acetylation, as well as ATP-dependent chromatin remodeling (a process that changes nucleosome composition or positioning) affect the detection and repair of DNA damage. The role of histone modifiers and chromatin remodelers in the cellular response to DSB has been intensively investigated [11-13]. However, how they regulate DNA damage tolerance is largely unknown. The histone methyltransferase Dot1 and the chromatin remodeler Ino80 have been suggested to play a role in DNA damage tolerance, which indicates that chromatin modulation may be a critical step during this process [14, 15]. Here, we show that Rtt109, by promoting acetylation of histone H3 at lysine 56, affects the mutagenic bypass of UV- and MMS-induced DNA lesions through TLS, providing further insight into the mechanisms that regulate DNA damage tolerance in the context of chromatin.

## RESULTS

### *Epistatic interactions between RTT109 and the Polζ and Polδ complexes.*

We have made use of an advanced technology for analysis of epistasis between pairs of genes in yeast (EMAP), to investigate the changes in genetic interactions induced by three different DNA damaging compounds, namely methyl methanesulfonate (MMS), camptothecin (CPT) and zeocin (ZEO). To focus our study, we crossed 55 query DNA damage response (DDR) genes with an array of 2022 genes involved in the DDR, as well as in other cellular processes, such as cell cycle regulation, chromatin organization, replication, transcription, and protein transport (see chapter 1). We measured growth rates 48h after the obtained double mutant strains were exposed or not to the different DNA damaging agents. Finally, genetic interaction scores were obtained by normalization and statistical analysis of colony size (a measure of cell growth).

The resulting genetic interaction map revealed a strong MMS-induced response of the post-replication repair pathways comprising the Mms2-Ubc13 ubiquitin ligase known to channel bypass of replication fork-blocking lesions through the error-free template switching pathway (reviewed by [1]), suggesting that our genetic interaction map can highlight interactions relevant for DNA damage tolerance. To further interpret these drug-induced interactions, we combined our genetic networks with available protein-protein interaction data and generated a map that shows the rewiring of connections between functional modules in response to MMS, ZEO and CPT (Chapter 1, Figure 5). The module map not only shows that the Mms2-Ubc13 complex is a major hub in response to MMS, but also that the TLS polymerase Polζ engages multiple interactions under that

same condition (Figure 1A). In agreement with two previous studies reporting that mutants of the 9-1-1 checkpoint complex have decreased efficiency in TLS-induced mutagenesis, we found that the 9-1-1 complex and TLS polymerase Polζ interact in our network (Figure 1A) [16, 17]. Interestingly, the module map also highlighted MMS-dependent interactions involving the histone acetyltransferase Rtt109, including a positive interaction with POL32, one of the subunit of the replicative polymerase Polδ, consistent with work showing that Rtt109 affects replisome stability in response to replication fork-blocking lesions (Figure 1B) [18]. We also observed unanticipated epistatic relationships between RTT109 and the TLS polymerase genes REV1, REV3 and REV7; the latter two encoding for Polζ subunits (Figure 1B), were validated in spot dilution assays (Figure 1C). We also observed epistasis between the Rev1-Polζ complex and Rtt109 in response to DNA damage induced by UV light or camptothecin (CPT) (Figure 1C). Polζ-dependent TLS enables cells to replicate through DNA lesions, thereby preventing collapse of replication forks [19]. Moreover, Polζ, in conjunction with Polδ, is responsible for as much as 85% of the bypass events at abasic sites [20], mainly in an error-prone fashion [19]. Consequently, the epistatic links seen between Polζ, Polδ and Rtt109 suggest a role for the histone acetyltransferase in TLS.

To specifically study the role of Rtt109 in TLS, we employed UV light in concert with nucleotide excision repair (NER)-deficient rad14 strains (to prevent repair of DNA photolesions through NER) to favor lesion bypass by TLS. We also monitored their sensitivity to MMS-induced damage. Surprisingly and in contrast to the observed epistatic interaction between REV3 and RTT109 in NER-proficient



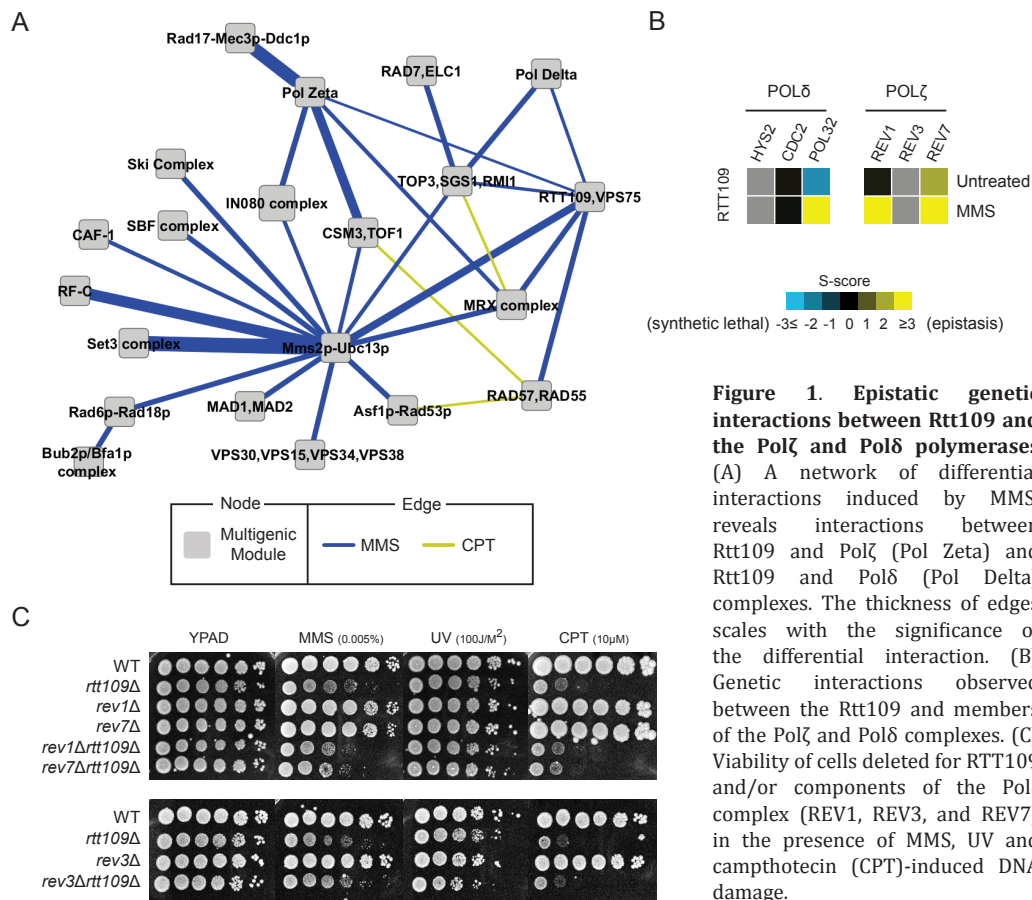


**Figure 1. Epistatic genetic interactions between Rtt109 and the Pol $\zeta$  and Pol $\delta$  polymerases** (A) A network of differential interactions induced by MMS, reveals interactions between Rtt109 and Pol $\zeta$  (Pol Zeta) and Rtt109 and Pol $\delta$  (Pol Delta) complexes. The thickness of edges scales with the significance of the differential interaction. (B) Genetic interactions observed between the Rtt109 and members of the Pol $\zeta$  and Pol $\delta$  complexes. (C) Viability of cells deleted for Rtt109 and/or components of the Pol $\zeta$  complex (REV1, REV3, and REV7) in the presence of MMS, UV and camptothecin (CPT)-induced DNA damage.

strains, it appeared that the NER deficient *rev3 $\Delta$ rtt109 $\Delta$*  strain was more sensitive to MMS than either single mutant (Figure 2A). This indicates that in the absence of NER Rtt109 and Rev3 play redundant roles in cell survival after MMS-induced DNA damage. To examine whether this phenotype depends on H3K56 acetylation by Rtt109, we assessed the MMS sensitivity of cells expressing a non-acetylatable histone H3 in which lysine 56 was replaced by an arginine (H3K56R). Similarly to the *rev3 $\Delta$ rtt109 $\Delta$*  strain, the *rev3 $\Delta$ H3K56R* strain was more sensitive to MMS than either single mutant strain (Figure 2B).

Next, to test the possible role of acetylation of H3K56 by Rtt109 in other

type of DNA damage that can be bypassed by TLS, the two strains defective for that process, *rtt109 $\Delta$*  and H3K56R, were assessed for their UV sensitivity. We also measured the UV sensitivity of cells deleted for ASF1, which encodes a H3/H4 histone chaperone that stimulates Rtt109's histone acetyltransferase activity by forming a heterodimeric complex with Rtt109 [21]. Again, the *rev3 $\Delta$ rtt109 $\Delta$* , the *rev3 $\Delta$ H3K56R* as well as the *rev3 $\Delta$ asf1 $\Delta$*  mutants were more sensitive to UV compared with either single mutant (Figure 2C-E). Altogether these results strongly suggest that Rtt109-dependent acetylation of H3K56 is a pathway that acts redundantly to Rev3 in mediating MMS and UV survival when NER activity is perturbed.

Rtt109 chromatin modifier regulates mutagenic dna damage bypass

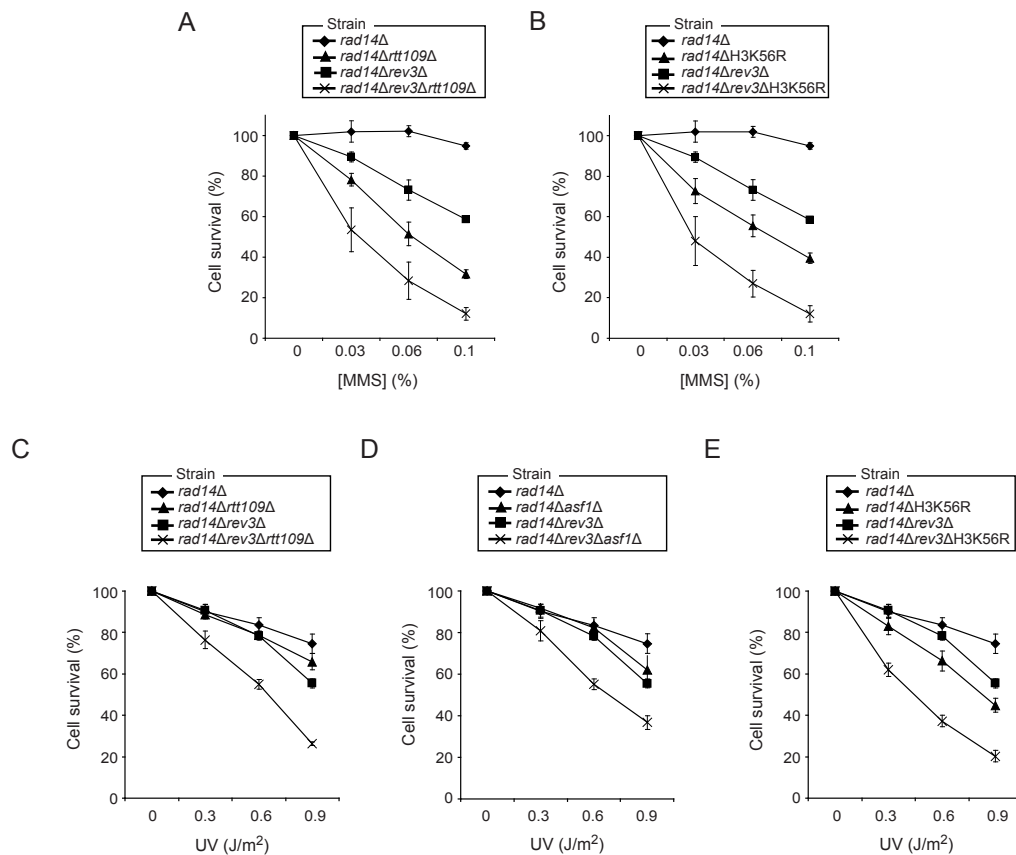


**Figure 2. Effect of Rtt109-mediated H3K56 acetylation on cell survival after MMS and UV exposure** (A) MMS survival was examined in wild-type (WT) *rev3Δ*, *rtt109Δ*, *rev3Δrtt109Δ* cells, and (B) in WT, *rev3Δ*, H3K56R non-acetylatable H3 mutant, *rev3ΔH3K56R*. (C) UV survival was examined in WT, *rev3Δ*, *rtt109Δ*, *rev3Δrtt109Δ* cells, (D) in WT, *rev3Δ*, *asf1Δ*, *rev3Δasf1Δ* cells and (E) in WT, *rev3Δ*, H3K56R, *rev3ΔH3K56R* cells. Cells were exposed for 20 minutes to the indicated doses of MMS before dilution and spreading on plates without or with canavanine (60mg/l). In the UV experiments, cells were first diluted and spread on plates before being exposed to the indicated UV doses. WT and all mutant strains were derived from a NER-deficient *rad14Δ* background. The data represent averages of three independent experiments and error bars represent the mean +/- standard deviations.

*Rtt109 is involved in MMS and UV-induced mutagenesis*

To investigate the possible role of Rtt109 in the mutagenic bypass of MMS and UV-induced damage, we utilized a CAN1 forward mutation assay, which reports any mutation that disrupts Can1 function resulting in a canavanine-resistance (*can1r*) phenotype. Cells with proficient TLS activity will accrue mutations at this locus at a much higher

rate enabling them to survive selection on media containing canavanine. As expected and in accordance with a role for Polζ in mutagenic bypass, *rev3Δ* cells (which were also deleted for RAD14 and therefore NER-deficient) were unable to form *can1r* colonies after transient exposure to MMS (Figure 3A). Interestingly, we found that MMS-exposed *rtt109Δ* cells were 2-fold less effective in accumulating *can1r* colonies compared to the NER deficient *rad14Δ*



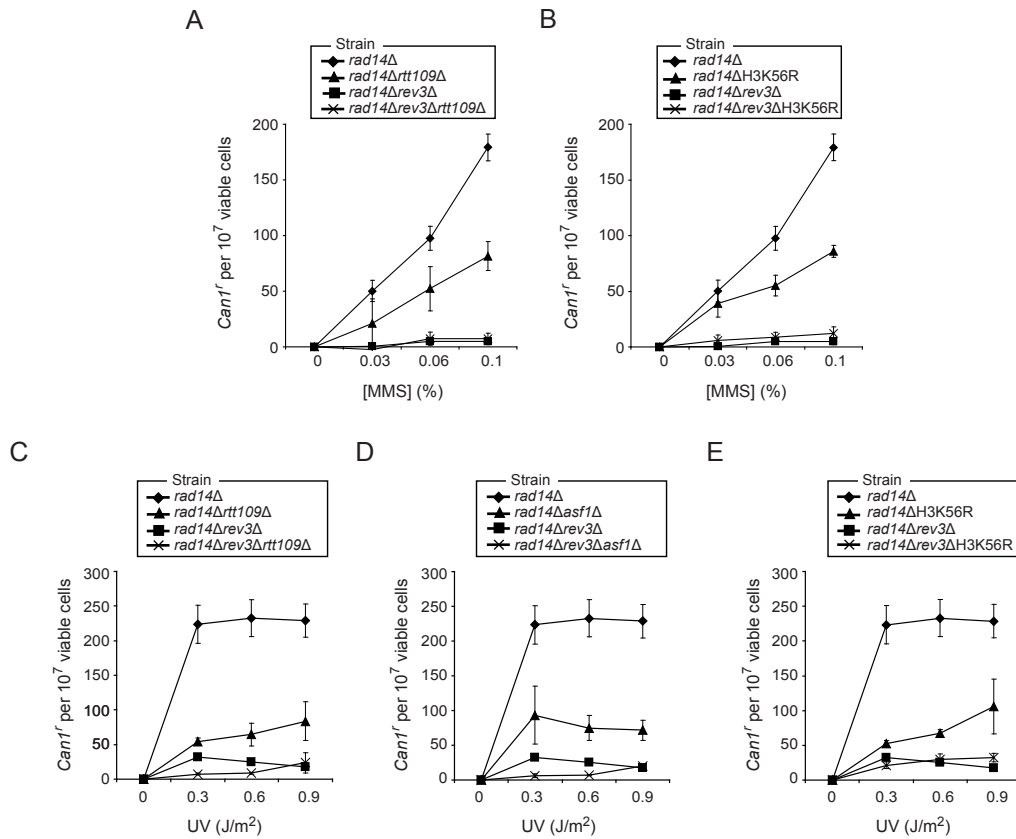


**Figure 3. H3K56 acetylation by Rtt109 affects the proficiency of UV-induced mutagenesis** (A) MMS-induced *can1r* mutation frequencies were examined in wild-type (WT), *rev3Δ*, *rtt109Δ*, *rev3Δrtt109Δ* cells and (B) in WT, *rev3Δ*, H3K56R (the non-acetylatable H3K56 mutant) and *rev3ΔH3K56R* mutant. (C) UV-induced *can1r* mutation frequencies were examined in wild-type (WT), *rev3Δ*, *rtt109Δ*, *rev3Δrtt109Δ* cells, (D) in WT, *rev3Δ*, *asf1Δ*, *rev3Δasf1Δ* cells and (E) in WT, *rev3Δ*, H3K56R, *rev3ΔH3K56R* cells. Cells were prepared as described in Figure 2. All strains are derived from a NER-deficient *rad14Δ* background. The data represent averages of three independent experiments and error bars represent the mean +/- standard deviations.

mutant (for reasons of clarity we will refer to this background as “wild-type” in the rest of this chapter) (Figure 3A). Similar to the *rtt109Δ* mutant, the H3K56R mutant showed a 2-fold decrease in *can1r* colonies formation after MMS treatment (Figure 3B). Altogether, these results imply that Rtt109 may promote mutagenic bypass of MMS-induced damage. It is important to note that the rates of spontaneous mutation were neither affected by deletion of RTT109 nor in cells expressing the H3K56

version of H3 (Figure S1).

Polζ is responsible for the bypass of multiple types of DNA damage of which UV lesions have been best studied [22, 23]. Thus, we turned our analysis to evaluate the role of Rtt109 in the bypass of UV-induced damages. By using the afore mentioned CAN1 forward mutation assay we tested wild-type, *rev3Δ* and *rtt109Δ* cells after exposure to various doses of UV.

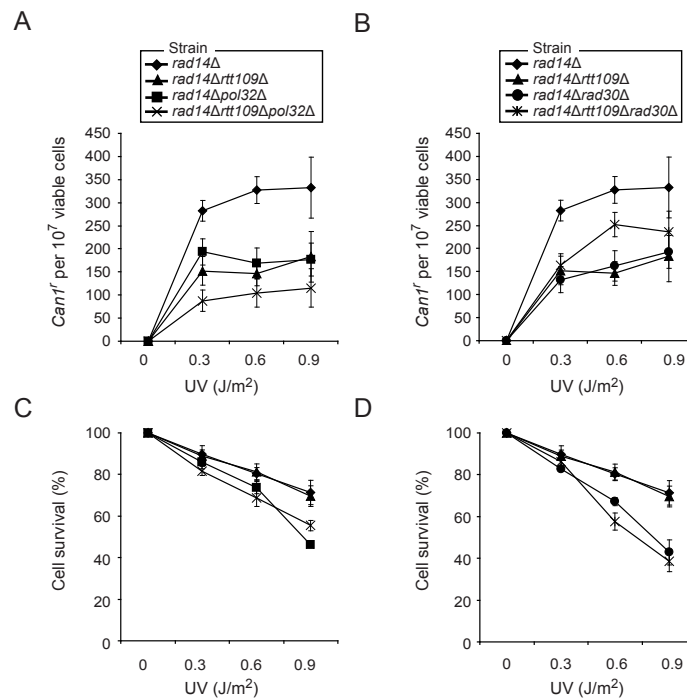


**Figure 4. Epistasis analysis of Rtt109, Pol $\delta$  and Pol $\eta$  in their proficiency of UV-induced mutagenesis** (A) UV-induced can1r mutation frequencies were examined in wild-type (WT), *pol32* $\Delta$ , *rtt109* $\Delta$ , *rtt109* $\Delta$ *pol32* $\Delta$  cells, (B) in WT, *rad30* $\Delta$ , *rtt109* $\Delta$ , *rtt109* $\Delta$ *rad30* $\Delta$  cells. (C) UV survival was examined in *pol32* $\Delta$ , *rtt109* $\Delta$ , *rtt109* $\Delta$ *pol32* $\Delta$  cells and (D) in WT, *rad30* $\Delta$ , *rtt109* $\Delta$ , *rtt109* $\Delta$ *rad30* $\Delta$  cells. Cells were diluted and plated on plates without or with canavanine (60mg/l) and exposed to the indicated UV doses. All strains are derived from a NER-deficient *rad14* $\Delta$  background. The data represent averages of three independent experiments and error bars represent the mean +/- standard deviations.

In agreement with previous work, we found that in the absence of REV3, cells almost abrogate UV damage-induced mutagenesis (Figure 3A; [17]). Strikingly, *rtt109* $\Delta$  strains displayed a nearly 5-fold decrease in the number of canr colonies compared to wild-type cells. To validate that this phenotype is a consequence of impaired Rtt109 activity, we measured the UV-induced mutagenesis rates in cells that were either deleted for ASF1 or expressed the H3K56R mutant allele of histone H3. These two mutants produced nearly the same number of canr colonies as the *rtt109* $\Delta$  strain did (Figure 3C-E). These results imply that Rtt109 is partially involved in the

Rev3-dependent mutagenic bypass of DNA lesions (accounting for at least 50 % of the MMS- and UV-induced mutation; Figures 3 and 4A-B).

*Rtt109 is epistatic with Pol $\eta$  but acts synergistically with Pol $\delta$  in UV-induced mutagenesis.*

We next asked to what extent Rtt109 and TLS polymerases cooperate to promote efficient lesion bypass. To this end, we monitored mutagenesis in Pol $\eta$ -deficient *rad30* $\Delta$  and Pol $\delta$ -deficient *pol32* $\Delta$  strains that were either proficient or deficient for Rtt109 (*rtt109* $\Delta$ *rad30* $\Delta$  and

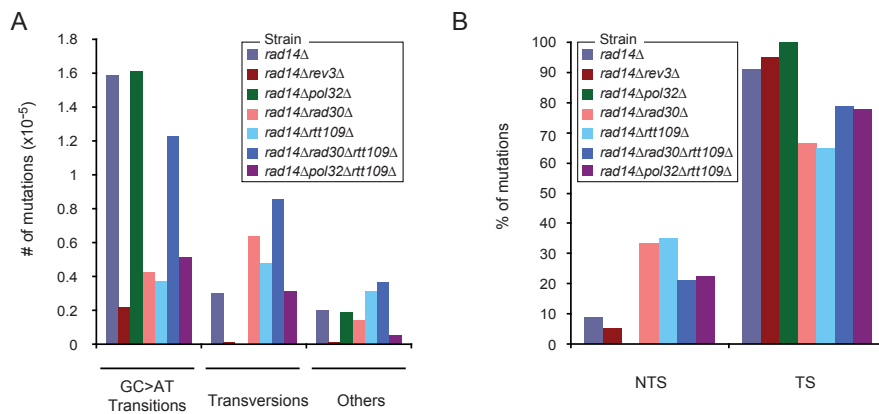


**Figure 5. Effect of Rtt109, Polζ, Polδ and Polη on UV-induced mutagenesis of CAN1** (A) UV-induced frequencies of GC to AT transitions, transversions and other mutations in WT, *rev3Δ*, *pol32Δ*, *rad30Δ*, *rtt109Δ*, *rtt109Δrad30Δ* and *rtt109Δpol32Δ* cells. (B) Strand distribution of the UV-induced mutations in WT, *rev3Δ*, *pol32Δ*, *rad30Δ*, *rtt109Δ*, *rtt109Δrad30Δ* and *rtt109Δpol32Δ*. The non-transcribed strand and the transcribed strand are noted NTS and TS, respectively. All strains are derived from a NER-deficient *rad14Δ* background.

3

*rtt109Δpol32Δ*). Consistent with a study from Giot et al., we found that *pol32Δ* cells display a 2-fold decrease in mutation rate when compared to wild-type (Figure 4A; [8]), an effect similarly to that observed in *rtt109Δ* cells. Surprisingly, *rtt109Δpol32Δ* mutants formed 1.7-fold less canr colonies than either single mutant (Figure 4A), whereas the UV sensitivity of this double mutant was comparable to that of the most sensitive single mutant (*pol32Δ*; Figure 4C). This suggests that Rtt109 and Pol32 work in two different UV-induced mutagenic pathways. On the other hand, the mutation rates in *rad30Δ* mutants were reduced as much as those observed in *rtt109Δ* cells (~2-fold decrease compared to wild-type; Figure 4B). Interestingly, this decrease was slightly alleviated by deletion of RTT109 in the *rad30Δ* mutant (Figure 4B), while the UV sensitivity of the *rtt109Δrad30Δ* double mutant was still comparable to that of the most sensitive single mutant (*rad30Δ*; Figure 4D). This suggests that Polη and Rtt109 cooperate during DNA damage bypass, but that loss of both these factors may alleviate

their (combined) suppressive effect on an error-prone, mutagenic pathway that likely involves Rev3.

*Rtt109* loss shows a pattern of mutations that lack the typical GC to AT transition induced by the bypass of UV lesions.

Understanding mechanisms of bypass by TLS have been profited from exploring the patterns of mutations induced by polymerases across UV lesions [22, 23]. Thus, we sought to further investigate the role of Rtt109 in TLS-mediated mutagenesis by comparing the UV-induced spectra of mutations of *rtt109Δ*, *rev3Δ*, *rad30Δ* and *pol32Δ* mutants under NER deficient conditions.

In agreement with previous reports, we observed that the prominent mutations induced after UV exposure were transitions and transversions [24]. Moreover, we found that GC to AT transitions represented 70 to 90% of all transitions [25]. These mutations are thought to arise from insertion of A's by Polη opposite cytosines that are

unstable in CPDs and rapidly deaminate into uracil [26, 27]. In accordance with this, we see a 4-fold decrease of this type of transition in *rad30Δ* cells. The remaining GC to AT transitions are likely caused by Polζ [25]. Loss of REV3 on the other hand nearly abolished mutagenesis and only a low level of GC to AT transitions possibly induced by Polη remained (Figure 5A). Interestingly, in *rtt109Δ* cells the frequency of GC to AT transitions was dramatically reduced, suggesting that Rtt109, like Rev3 and Rad30, promotes GC to AT transitions. Finally, in *pol32Δ* cells, the number of GC to AT transitions was similar to that of wild-type cells, indicating that Pol32 does not affect GC to AT transitions.

Together the data suggest that Rtt109 promotes UV-induced GC to AT transitions most likely depending on Rev3 and Rad30 activities. To test the latter, we examined these mutations in the *rtt109Δrad30Δ* double mutant. Surprisingly, the rate at which GC to AT transitions appeared was 3-fold increased when compared to either of the single mutants and nearly returned to wild-type levels (Figure 5A). In contrast, loss of Pol32 did not affect the transition rates observed in the *rtt109Δ* mutant in agreement with our previous notion that Pol32 does not promote GC to AT transitions. Collectively, these results suggest that the Rtt109-dependent GC to AT transitions are most likely generated by Rev3, but not Polη (Figure 5A).

The rate at which transversions occurred was much lower than that observed for transitions (wild-type; Figure 5A). Transversions were primarily induced by Rev3 and Pol32 activities as indicated by the lack of these mutations in *rev3Δ* and *pol32Δ* mutants (Figure 5A). Remarkably, elevated levels of transversions were observed in both *rad30Δ* and *rtt109Δ*

mutants when compared to wild-type (Figure 5A). These levels even further increased in the combined absence of Rad30 and Rtt109 (*rad30Δrtt109Δ* mutant; Figure 5A), which suggests that Rtt109 may co-operate with Rad30 to suppress transversion formation by Rev3 and Pol32. In line with this we found that loss of Pol32 in the *rtt109Δ* mutants partially reduced the transversion rates (Figure 5A).

UV light induces helix-distorting lesions that can perturb cellular processes including DNA replication and transcription. Fortunately, eukaryotic cells are equipped with a transcription-coupled NER (TC-NER) mechanism that efficiently clears DNA damage from the transcribed strand (TS) [28]. Here we used NER deficient *rad14Δ* strains which explains why UV-induced mutations were found primarily in the TS (90% in the TS, Figure 5B). When REV3 or POL32 was deleted in this background, mutations still accrued in the TS (95% and 100% respectively). Surprisingly, however, deletion of RTT109 or RAD30 decreased the levels of mutations in the TS, yet resulted in a bigger proportion of mutations in the non-transcribed strand (NTS) (35% versus 10% and 5% in wild-type and *rev3Δ* cells respectively, Figure 5B). These effects were partially reversed by the loss of Rad30 or Pol32. In conclusion, our work suggests that while Rtt109 may suppress the formation of transversions by Rev3 and Pol32, it may favor the formation of GC to AT transitions in the TS, which are most likely induced by Rad30 and Rev3. Thus, Rtt109 seems to operate at the crossroads of Rad30 and Rev3-dependent DNA damage bypass routes.

## DISCUSSION

In this study we found that acetylation of histone H3 on lysine K56 by Rtt109 plays a role in TLS-induced mutagenesis. Using

the CAN1 forward mutation assay, we first showed that Rtt109 loss in a NER deficient background reduces the frequency of MMS- and UV-induced mutations, which suggests that Rtt109 promotes DNA damage-induced mutagenesis (Figure 3A and 3C). Secondly, we found that *rtt109Δ* cells were inefficient at inducing the typical UV-signature of mutations i.e GC to AT transitions. It has recently been shown that while Rad30 is required, Polζ is essential for generating this GC to AT signature [25]. Accordingly, we found that Rtt109 may affect both the activities of Rad30 and Polζ. The mechanism by which the histone acetyltransferase Rtt109 promotes UV-induced GC to AT mutations is still unclear. Recently, a study by Hendriks et al. in mammalian cells proposed that transcription (particular under repair deficient conditions) enhances the formation of uracil by deamination of CPD-containing cytosines [29]. In yeast, a similar phenomenon referred to as transcription-associated mutagenesis or TAM was also described to be enhanced in presence of DNA damage [30, 31]. Interestingly, Rtt109 by acetylating H3K56 has been associated with transcriptional activation and RNA PolII elongation [32, 33]. More recently, H3K56ac by Rtt109 was found to facilitate transcription of heterochromatic regions [34]. This suggests that loss of Rtt109 perturbs transcription and thereby may reduce transcription-associated cytosine-deamination mediated by DNA damage and decrease the relative proportion of mutations induced by lesions in the TS. We also showed that MMS-induced mutagenesis, likely caused by the bypass of abasic sites, is impaired in *rtt109Δ* cells (Figure 3A). A report proposed that the stalling of RNA PolII at abasic sites caused by MMS treatment increased the mutation rate [35]. Thus, the role of Rtt109 in promoting transcription could similarly explain the MMS-induced mutagenesis

defect seen in *rtt109Δ* cells. However, neither the loss of Rtt109, nor that of Rad30 affects the transcription levels of CAN1 in unperturbed cells (Figure S2). Although this suggests that Rtt109 may not indirectly affect transcription-associated mutagenesis in this manner, it still needs to be examined whether Rtt109 loss affects transcription of CAN1 in UV- or MMS-exposed cells. Importantly, the frequency of GC to AT transitions observed in *rtt109Δrad30Δ* cells is nearly the same as in wild-type cells, which attests that together Polδ (or more precisely the two Pol31 and Pol32 subunits found in a complex with Polζ) and Polζ are able to replace Polη's role in the mutagenic bypass of CPDs. This could be due to the recovery of a wild-type level of transcription in the *rtt109Δrad30Δ* mutant. Or in the contrary, this could come from massive deamination of cytosines caused by persistent transcription stalling (that would enhance the rate of uracil to be replicated). These two options need to be further investigated. Another validation would be to show how reversion of CPDs by photoreactivation affects mutagenesis in *rtt109Δ* cells. At last, analyzing the epistasis between Rtt109 and the uracil-glycosylase Ung1 which is required for the repair of spontaneous deaminated-cytosines would give further insight into the contribution of Rtt109 in this mechanism.

Emerging evidence emphasizes the importance of histone modifications in controlling TLS in the context of chromatin. For instance, two recent studies show that loss of Dot1, the H3K79 methyltransferase, alleviates the sensitivity of the *rtt107Δ*, *rad52Δ*, *rad14Δ*, *apn1Δ* repair mutants to the DNA alkylating agent MMS [14, 36]. In both reports, the authors explain the alleviating phenotype by an increased TLS efficiency in *dot1Δ* and propose that H3K79 methylation by Dot1 downregulates TLS.

We could envisage that H3K56 acetylation by Rtt109 prevents the action of Dot1 thereby alleviating the Dot1 inhibiting effect on TLS. It becomes apparent that these histone modifications are important to ease the access to DNA in a chromatin context and to facilitate the recruitment of factors involved in DNA metabolism such as transcription and DNA replication that can impact on DNA integrity.

PCR products were then sequenced with primers oHA-1072, oHA-1073 (5'-GGCATATTCTGTACGCAG-3'), oHA-1159 (5'-GGAACAAGTTCATTATTGTG-3'). DNA sequencing was performed according to the standard Sanger sequencing method using the 96-capillary 3730XL system from Applied Biosystems. The sequences were analyzed with ContigExpress software (Vector NTI).

## MATERIAL & METHODS

### *Sensitivity assays on plates*

Overnight cultures were diluted 1:20, grown for 3 hours at 30 °C and diluted to  $1 \times 10^7$  cells/ml. Fivefold dilution series were spotted on plates containing 10  $\mu$ M CPT or 0.005% MMS or spotted on plates and then exposed to a UV dose of 100J/m<sup>2</sup>. Growth was scored after 3 days at 30 °C.

### *Mutagenesis assays*

Mutagenesis assays were performed as described previously (Johnson, 1998). Briefly, serial dilutions of cells were spread on YPAD to determine cell viability and on SC-Arg plates containing canavanine (60mg/l) to monitor the efficiency of can1r colony formation. In the MMS experiment, cells were exposed for 20 minutes to the indicated MMS concentrations and washed before they were diluted and plated.

### *Can<sup>r</sup> mutation spectra*

Can<sup>r</sup> mutation spectra were determined by PCR amplification and sequence analysis of the CAN1 gene of independent can<sup>r</sup> colonies generated during the mutagenesis experiments. Genomic DNA was isolated and the CAN1 gene was amplified by PCR using the forward primer oHA-1071 (5'-CTTCAGACTTCTTA ACTCC-3') and the reverse primer oHA-1072 (5'-GAGGGTGAGAATGCGAAAT-3'). Purified



## REFERENCES

1. Chang, D.J. and K.A. Cimprich, DNA damage tolerance: when it's OK to make mistakes. *Nat Chem Biol*, 2009. 5(2): p. 82-90.
2. Gangavarapu, V., S. Prakash, and L. Prakash, Requirement of RAD52 group genes for postreplication repair of UV-damaged DNA in *Saccharomyces cerevisiae*. *Mol Cell Biol*, 2007. 27(21): p. 7758-64.
3. Johnson, R.E., S. Prakash, and L. Prakash, Efficient bypass of a thymine-thymine dimer by yeast DNA polymerase, Pol $\epsilon$ . *Science*, 1999. 283(5404): p. 1001-4.
4. Zhang, H. and W. Siede, UV-induced T $\rightarrow$ C transition at a TT photoproduct site is dependent on *Saccharomyces cerevisiae* polymerase  $\epsilon$  in vivo. *Nucleic Acids Res*, 2002. 30(5): p. 1262-7.
5. Abdulovic, A.L. and S. Jinks-Robertson, The in vivo characterization of translesion synthesis across UV-induced lesions in *Saccharomyces cerevisiae*: insights into Pol  $\zeta$ - and Pol  $\epsilon$ -dependent frameshift mutagenesis. *Genetics*, 2006. 172(3): p. 1487-98.
6. Lawrence, C.W., Cellular functions of DNA polymerase  $\zeta$  and Rev1 protein. *Adv Protein Chem*, 2004. 69: p. 167-203.
7. Acharya, N., et al., Complex formation with Rev1 enhances the proficiency of *Saccharomyces cerevisiae* DNA polymerase  $\zeta$  for mismatch extension and for extension opposite from DNA lesions. *Mol Cell Biol*, 2006. 26(24): p. 9555-63.
8. Giot, L., et al., Involvement of the yeast DNA polymerase  $\delta$  in DNA repair in vivo. *Genetics*, 1997. 146(4): p. 1239-51.
9. Huang, M.E., et al., Pol32, a subunit of *Saccharomyces cerevisiae* DNA polymerase  $\delta$ , suppresses genomic deletions and is involved in the mutagenic bypass pathway. *Genetics*, 2002. 160(4): p. 1409-22.
10. Johnson, R.E., L. Prakash, and S. Prakash, Pol31 and Pol32 subunits of yeast DNA polymerase  $\delta$  are also essential subunits of DNA polymerase  $\zeta$ . *Proc Natl Acad Sci U S A*, 2012. 109(31): p. 12455-60.
11. Rogakou, E.P., et al., Megabase chromatin domains involved in DNA double-strand breaks in vivo. *J Cell Biol*, 1999. 146(5): p. 905-16.
12. Downs, J.A., et al., Binding of chromatin-modifying activities to phosphorylated histone H2A at DNA damage sites. *Mol Cell*, 2004. 16(6): p. 979-90.
13. van Attikum, H., O. Fritsch, and S.M. Gasser, Distinct roles for SWR1 and INO80 chromatin remodeling complexes at chromosomal double-strand breaks. *EMBO J*, 2007. 26(18): p. 4113-25.
14. Conde, F. and P.A. San-Segundo, Role of Dot1 in the response to alkylating DNA damage in *Saccharomyces cerevisiae*: regulation of DNA damage tolerance by the error-prone polymerases Pol $\zeta$ /Rev1. *Genetics*, 2008. 179(3): p. 1197-210.
15. Falbo, K.B., et al., Involvement of a chromatin remodeling complex in damage tolerance during DNA replication. *Nat Struct Mol Biol*, 2009. 16(11): p. 1167-72.
16. Pages, V., et al., Role of DNA damage-induced replication checkpoint in promoting lesion bypass by translesion synthesis in yeast. *Genes Dev*, 2009. 23(12): p. 1438-49.
17. Paulovich, A.G., C.D. Armour, and L.H. Hartwell, The *Saccharomyces cerevisiae* RAD9, RAD17, RAD24 and MEC3 genes are required for tolerating irreparable, ultraviolet-induced DNA damage. *Genetics*, 1998. 150(1): p. 75-93.
18. Han, J., et al., Acetylation of lysine 56 of histone H3 catalyzed by Rtt109 and regulated by ASF1 is required for replisome integrity. *J Biol Chem*, 2007. 282(39): p. 28587-96.
19. Prakash, S., R.E. Johnson, and L. Prakash, Eukaryotic translesion synthesis DNA polymerases: specificity of structure and function. *Annu Rev Biochem*, 2005. 74: p. 317-53.
20. Andersen, P.L., F. Xu, and W. Xiao, Eukaryotic DNA damage tolerance and translesion synthesis through covalent

- modifications of PCNA. *Cell Res*, 2008. 18(1): p. 162-73.
21. Tsubota, T., et al., Histone H3-K56 acetylation is catalyzed by histone chaperone-dependent complexes. *Mol Cell*, 2007. 25(5): p. 703-12.
22. Nelson, J.R., C.W. Lawrence, and D.C. Hinkle, Thymine-thymine dimer bypass by yeast DNA polymerase zeta. *Science*, 1996. 272(5268): p. 1646-9.
23. Gibbs, P.E., et al., The relative roles in vivo of *Saccharomyces cerevisiae* Pol eta, Pol zeta, Rev1 protein and Pol32 in the bypass and mutation induction of an abasic site, T-T (6-4) photoadduct and T-T cis-syn cyclobutane dimer. *Genetics*, 2005. 169(2): p. 575-82.
24. Kozmin, S.G., et al., Roles of *Saccharomyces cerevisiae* DNA polymerases Poleta and Polzeta in response to irradiation by simulated sunlight. *Nucleic Acids Res*, 2003. 31(15): p. 4541-52.
25. Haruta, N., Y. Kubota, and T. Hishida, Chronic low-dose ultraviolet-induced mutagenesis in nucleotide excision repair-deficient cells. *Nucleic Acids Res*, 2012. 40(17): p. 8406-15.
26. Barak, Y., O. Cohen-Fix, and Z. Livneh, Deamination of cytosine-containing pyrimidine photodimers in UV-irradiated DNA. Significance for UV light mutagenesis. *J Biol Chem*, 1995. 270(41): p. 24174-9.
27. Peng, W. and B.R. Shaw, Accelerated deamination of cytosine residues in UV-induced cyclobutane pyrimidine dimers leads to CC-->TT transitions. *Biochemistry*, 1996. 35(31): p. 10172-81.
28. Svejstrup, J.Q., Mechanisms of transcription-coupled DNA repair. *Nat Rev Mol Cell Biol*, 2002. 3(1): p. 21-9.
29. Hendriks, G., et al., Transcription-dependent cytosine deamination is a novel mechanism in ultraviolet light-induced mutagenesis. *Curr Biol*, 2010. 20(2): p. 170-5.
30. Datta, A. and S. Jinks-Robertson, Association of increased spontaneous mutation rates with high levels of transcription in yeast. *Science*, 1995. 268(5217): p. 1616-9.
31. Morey, N.J., C.N. Greene, and S. Jinks-Robertson, Genetic analysis of transcription-associated mutation in *Saccharomyces cerevisiae*. *Genetics*, 2000. 154(1): p. 109-20.
32. Williams, S.K., D. Truong, and J.K. Tyler, Acetylation in the globular core of histone H3 on lysine-56 promotes chromatin disassembly during transcriptional activation. *Proc Natl Acad Sci U S A*, 2008. 105(26): p. 9000-5.
33. Schneider, J., et al., Rtt109 is required for proper H3K56 acetylation: a chromatin mark associated with the elongating RNA polymerase II. *J Biol Chem*, 2006. 281(49): p. 37270-4.
34. Varv, S., et al., Acetylation of H3 K56 is required for RNA polymerase II transcript elongation through heterochromatin in yeast. *Mol Cell Biol*, 2010. 30(6): p. 1467-77.
35. Yu, S.L., et al., The stalling of transcription at abasic sites is highly mutagenic. *Mol Cell Biol*, 2003. 23(1): p. 382-8.
36. Levesque, N., et al., Loss of H3 K79 trimethylation leads to suppression of Rtt107-dependent DNA damage sensitivity through the translesion synthesis pathway. *J Biol Chem*, 2010. 285(45): p. 35113-22.

## SUPPLEMENTAL DATA

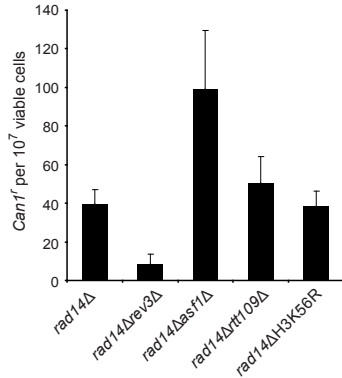


**Figure S1: The spontaneous mutations are not affected by Rtt109 deletion.** Spontaneous *can1r* mutation frequencies were examined in wild-type, *rev3Δ*, *asf1Δ*, *rtt109Δ* and H3K56-expressing cells. Cells were diluted and plated on plates without or with canavanine (60mg/l). All strains are derived from a NER-deficient *rad14Δ* background. The data represent averages of three independent experiments and error bars represent the mean +/- standard deviations.

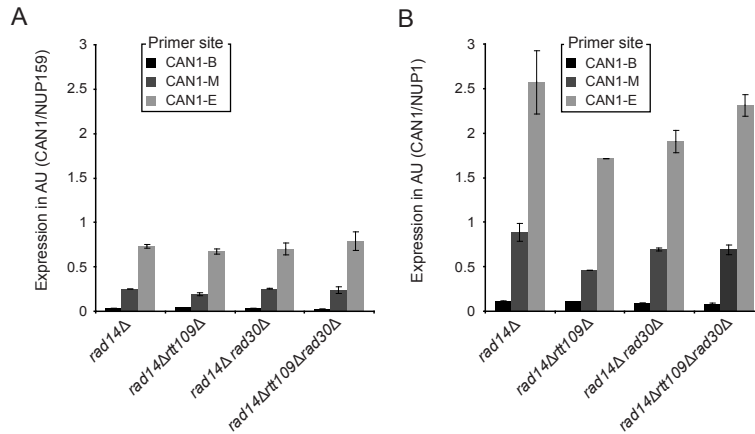


**Figure S2: The transcription level of the CAN1 gene is not affected by deletions of Rtt109 and Rad30 under unchallenged conditions** (A) Bar-plot showing the transcription levels of the beginning (CAN1-B), the middle of the gene (CAN1-M) and the end of the CAN1 gene (CAN1-E) in wild-type, *rtt109Δ*, *rad30Δ* and *rad30Δrtt109Δ* unchallenged cells. The transcription level analysis was done according to the procedure described in Taddei et al. (2006). The levels were normalized on the NUP159 gene. (B) as in (A) except that the transcription levels were normalized on the NUP1 gene. All strains are derived from a NER-deficient *rad14Δ* background. The data represent averages of two independent RT-PCR runs and error bars represent the mean +/- standard deviations.



## NEDDYLATION AFFECTS CELL CYCLE CONTROL AND GENOME INTEGRITY

Aude Guérolé<sup>1</sup>, Rohith Srivas<sup>2,3</sup>, Kees Vreeken<sup>1</sup>, Trey Ideker<sup>2,3,4</sup>, Haico van Attikum<sup>1\*</sup>

<sup>1</sup>Department of Toxicogenetics, Leiden University Medical Center, Einthovenweg 20, 2333 ZC, Leiden, The Netherlands, <sup>2</sup>Department of Bioengineering, University of California, San Diego, La Jolla, CA 92093 USA, <sup>3</sup>Department of Medicine, University of California, San Diego, La Jolla, CA 92093, USA, <sup>4</sup>The Institute for Genomic Medicine, University of California, San Diego, La Jolla, CA 92093, USA

\* H.v.A. (h.van.attikum@lumc.nl)

Partially published in:

Guérolé A, Srivas R, Vreeken K, Wang ZZ, Wang S, Krogan NJ, Ideker T, van Attikum H. *Dissection of DNA damage responses using multiconditional genetic interaction maps*. Mol Cell. 2013 Jan 24;49(2):346-58.

Chapter 4

4

**ABSTRACT**

Neddylaton is a process that similar to ubiquitylation results in covalent attachment of a small protein called Rub1 -homologue of human Nedd8- to targeted proteins. Importantly, this process is essential in the majority of eukaryotes with the exception of the budding yeast *Saccharomyces cerevisiae*. The dysregulation of neddylaton has been described in several cancers and neurodegenerative disorders. To date, only a limited number of Rub1/ NEDD8 targets have been identified. Thus, how neddylaton mechanistically affects cellular processes is largely unclear. Here, we found in yeast that components of the neddylaton machinery cooperate with DNA damage checkpoint proteins to promote genome stability and protect cells against DNA damage. We further showed that neddylaton facilitates G2/M progression in the presence of DNA damage induced by the topoisomerase-1 inhibitor camptothecin. Finally, we found that neddylaton regulates the steady state levels of DNA damage response factors such as Mms22 and Nhp10, providing an explanation for how this process controls cell cycle progression.

**INTRODUCTION**

Neddylation is a process by which the Rub1 protein (NEDD8 in humans) is conjugated to target proteins in a cascade of reactions that involves E1 activating, E2 conjugating (in *S. cerevisiae* only Ubc12) and E3 ligating enzymes in a manner analogous to ubiquitylation and SUMOylation [1]. Neddylation is an essential modification for cellular function in all eukaryotes, except in *S. cerevisiae*. Whereas ubiquitylation and SUMOylation have been shown to regulate a myriad of cellular processes, including DDR [2], those that involve neddylation remain largely unknown due to the limited number of neddylation substrates that have been identified [3]. The best-studied Rub1/Nedd8 targets are cullin-RING ubiquitin ligases (CRLs). The three yeast cullins Cdc53, Rtt101 and Cul3, as well as the eight mammalian cullins CUL1, CUL2, CUL3, CUL4A, CUL4B, CUL5, CUL7 and Parc are neddylated in vivo [4, 5]. Cullin neddylation results in conformational changes that help to anchor the E2 ubiquitin-conjugating enzyme to the E3 ligase complex. This new complex conformation is thought to facilitate ubiquitin transfer to CRL substrates and stimulate CRL ubiquitylation activity [6]. Importantly, multiple CRL targets are key components of processes that have been found to be misregulated in several types of cancer. The DNA replication licensing factor Cdt-1 is an edifying example. Mis-regulated CRL1<sup>Skp2</sup>/CRL4<sup>Cdt2</sup> results in Cdt-1 accumulation in several human tumors [7]. In addition, disruption of the adaptor protein Skp2 leads to high levels of cyclin E and cyclin-dependent kinase inhibitor p27, which gives rise to polyploid and polycentric cancer cells [8].

Recent work suggests that proteins other than cullins can also be modified through neddylation. Xirodimas and coworkers first reported that the tumor suppressor p53 is ubiquitylated by the E3

ubiquitin ligase Mdm2 and targeted for proteasomal degradation in unperturbed cells [9]. However, upon cellular stress, p53 is stabilized and induces a transcriptional program that results in cell growth inhibition and apoptosis [10]. More recently, Mdm2 was found to be neddylated and required for p53 neddylation [11]. In both cases, neddylation promotes degradation of the targeted protein. Additionally, neddylated-forms of p53 were detected transiently in cells treated with UV, which shows that neddylation is a process that can be triggered by DNA damage [11]. Thus, it becomes apparent that neddylation can also directly affect the level of proteins, including those that are key factors involved in cellular stress responses.

Here, we found that defects in neddylation and in the DNA damage checkpoint have synergistic effects on cell survival after induction of DNA damage and on genome stability maintenance. Additionally, we show that neddylation promotes G2/M transition in response to the topoisomerase 1-inhibitor camptothecin, which induces DNA damage during replication. Finally, we demonstrate that neddylation affects the levels of two DNA damage response factors, Mms22 and Nhp10. Collectively, our data suggest that neddylation plays a role in cell-cycle control by regulating the levels of particular DNA damage response factors.

## RESULTS & DISCUSSION

We performed a large-scale genetic interaction screen, called dE-MAP (for differential epistatic mapping), in the presence of three different DNA damaging compounds: the DNA alkylating agent methyl methanesulfonate (MMS), the topoisomerase-1 inhibitor camptothecin (CPT), and the radiomimetic antibiotic zeocin (ZEO). To identify which of the changes in genetic interactions between conditions were statistically significant, we used a previously published metric to assess the difference in genetic interaction

scores (S score) for each gene pair before versus after treatment [12]. We call this network 'differential' genetic network as it is derived from the difference between two static networks (Chapter 1, Figure 1). We then examined the genes which were highly responding to the drugs. The gene with the greatest overall number of interactions was RAD17, a component of the 9-1-1 checkpoint complex which is recruited to double-stranded break (DSB) sites to activate the Mec1-kinase signaling cascade, resulting in cell cycle arrest and repair [13]. Consistent with the role of Rad17 in the DSB

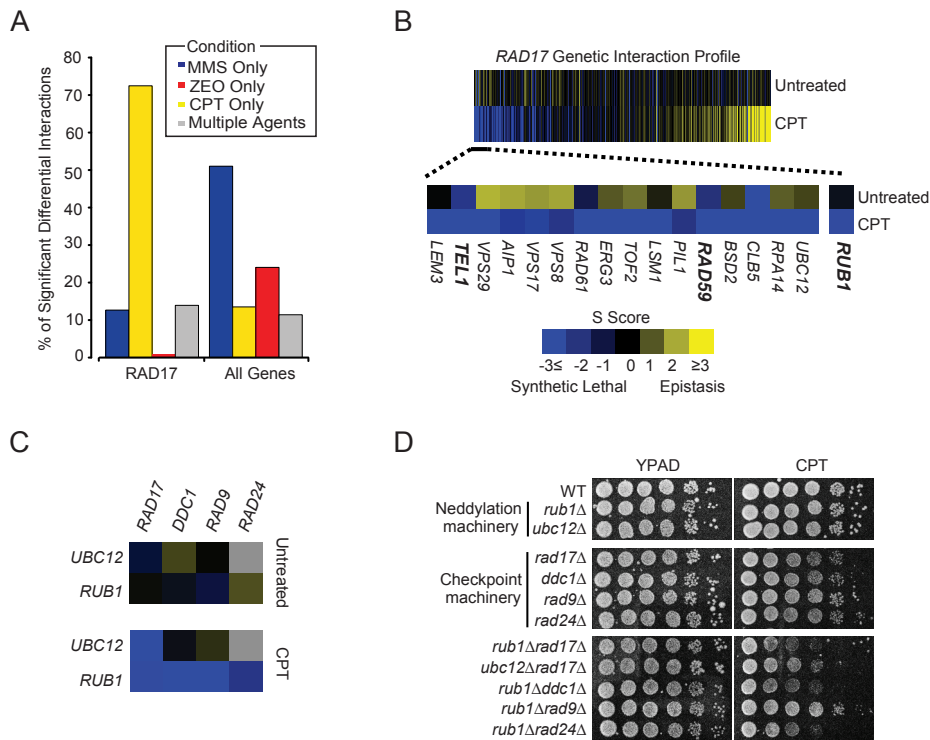


**Figure 1. Cells deficient for both neddylation and DNA damage checkpoints show reduced viability in the presence of CPT-induced DNA damage** (A) Percentage of RAD17's significant differential genetic interactions arising in response to MMS, CPT, ZEO, or multiple agents. As a control, the average percentage of significant differential interactions in each of these categories across all genes is shown. (B) Entire CPT-induced genetic interaction profile for RAD17 sorted (left to right) in order of most differential negative to most differential positive. A subset of the top differential negative interactions is also shown. (C) Genetic interactions between components of the neddylation machinery and the DNA damage checkpoint. (D) Viability of cells deficient for both neddylation and DNA damage checkpoints is strongly impaired in the presence of CPT. 10-fold serial dilutions of log-phase cells of the indicated genotypes were spotted onto YPAD and YPAD containing CPT (15  $\mu$ M) and incubated for 3 days at 30°C.



response [14], we found that the majority of its interactions were induced specifically in response to CPT (73%, Figure 1A). To gain further insight into potential CPT-induced pathways involving the checkpoint, we examined the entire CPT-induced genetic interaction profile of RAD17 (Figure 1B), which revealed strong negative interactions with prominent DSB repair genes (RAD59) and checkpoint regulators, such as TEL1. This is consistent with reports showing that Tel1 functions parallel to Rad17 to regulate checkpoint activation following DSBs [15]. Two additional genes, RUB1 and UBC12, which encode key components of the yeast neddylation machinery, displayed strong negative interactions with RAD17 (Figure 1B). In further support of a potential link between neddylation and checkpoint pathways, the CPT network revealed a number of additional negative interactions between RUB1/UBC12 and other checkpoint genes, including DDC1, RAD9 and RAD24 (Figure 1C). These interactions were also observed via spot dilution assays, confirming that cells defective for neddylation and DNA damage checkpoints are hypersensitive to CPT (Figure 1D).

To investigate a role for the neddylation machinery in DNA damage

checkpoint control, we assessed *rub1Δ* and *ubc12Δ* mutants for their progression through the cell cycle in the presence of CPT. After arrest in G1 and release into medium containing CPT, *rub1Δ* and *ubc12Δ* mutants had significant accumulation of cells in the G2 phase at 90 and 105 minutes, whereas wild-type cells efficiently progressed through G2 and M-phase into the next cell cycle (Figures 2A-B). As this delay was not observed in the absence of CPT (Figure 2C), we demonstrate for the first time that neddylation mutants display perturbations in cell cycle progression upon CPT treatment.

Since defects in cell cycle checkpoints have been shown to contribute to genome instability [16], we decided to measure the rate of gross chromosomal rearrangements (GCR) in the neddylation mutants. The assay utilized determines GCR rates by monitoring the loss of two counter-selectable markers, CAN1 and URA3, which are present on the left arm of the chromosome V (Figure 3A). The rate of GCR events in the *ubc12Δ* mutant was nearly 2.7-fold greater than in wild type, whereas the *rad17Δubc12Δ* double mutant showed, respectively, a 7- and 2-fold increase in GCR rates when compared to the *ubc12Δ* and *rad17Δ* mutants (Figure

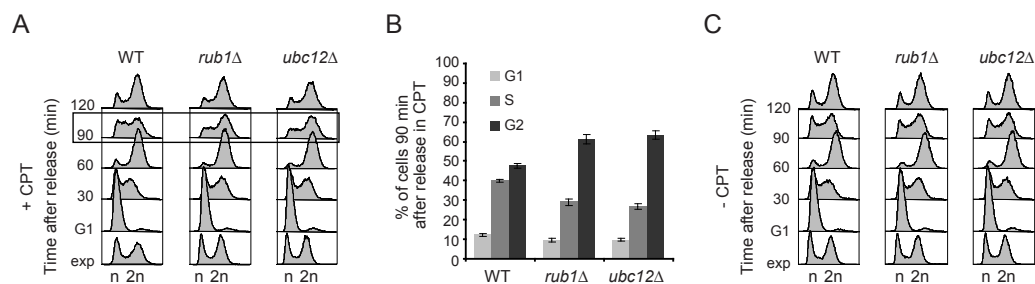


**Figure 2. Neddylation mutants show a delayed G2/M transition in the presence of CPT-induced lesions (A)** WT, *rub1Δ*, *ubc12Δ* cells were arrested in G1 with  $\alpha$ -factor and released in S-phase in YPAD plus 50  $\mu$ M CPT. (B) The percentage of cells in G1, S and G2 phases 90 minutes after release in CPT was determined. Data represent the mean  $\pm$  standard deviation from 3 independent experiments. (C) as in (A) except that cells were release in YPAD. Aliquots were taken at the indicated time for FACS analysis.

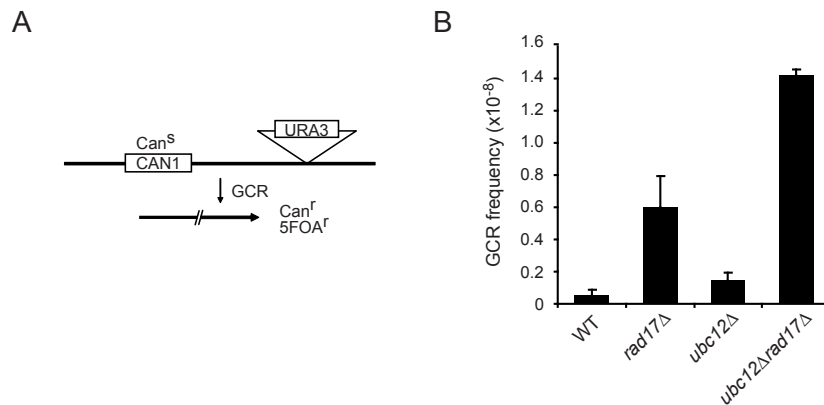


**Figure 3. Cells deficient for both neddylation and DNA checkpoints display increased Gross Chromosomal Rearrangements (GCR).** (A) Scheme of the working principle of the GCR assay developed by Chen and Kolodner, 1999. (B) Cells deficient for both neddylation and DNA damage checkpoints have increased rates of Gross Chromosomal Rearrangements (GCR). GCR frequencies were determined as previously described in the Experimental Procedures. The mean  $\pm$  standard deviation of three independent experiments is presented.

3B), suggesting that neddylation and checkpoint pathways are likely to cooperate in promoting genome stability.

We next asked whether the perturbations in cell cycle progression observed in the neddylation mutants were due to abnormal activation DNA damage checkpoints. It has been shown previously that CPT-induced DNA damage does not trigger activation of Rad53 [17]. It is not known whether Chk1 is also not activated under the same damaging condition. We found that wild-type cells neither showed

Rad53 nor Chk1 activation upon release from G1 into CPT ([17] and Figure 4A-B). We then monitored the presence of phosphorylated forms of Rad53 and Chk1 in *rub1Δ*. Surprisingly, also in *rub1Δ* mutants Rad53 and Chk1 were not activated upon DNA damage induced by CPT (Figure 4A-B), which suggests that the G2 delay seen in these mutants is not the consequence of DNA damage checkpoint activation.

The best-studied NEDD8/Rub1 targets are cullin proteins, which are

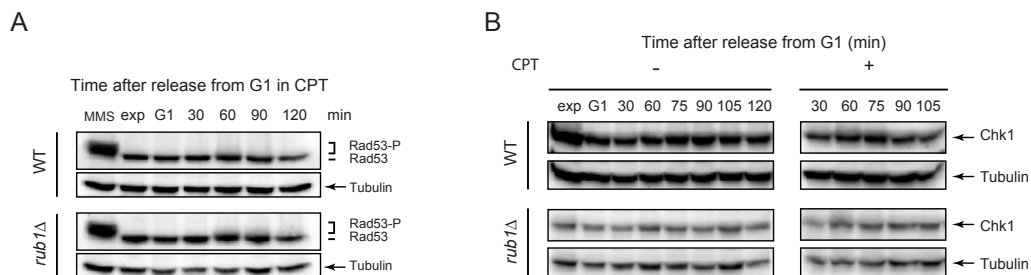


**Figure 4. Neddylation defects do not lead to DNA damage checkpoint activation.** Exponentially (exp) growing WT and *rub1Δ* cells were arrested in G1 with  $\alpha$ -factor and released in fresh medium containing CPT (50  $\mu$ M). MMS-treated exponentially growing cells served as a positive control. The phosphorylation status of (A) Rad53 and (B) Chk1 was monitored using Western blot analysis at the indicated time-points.

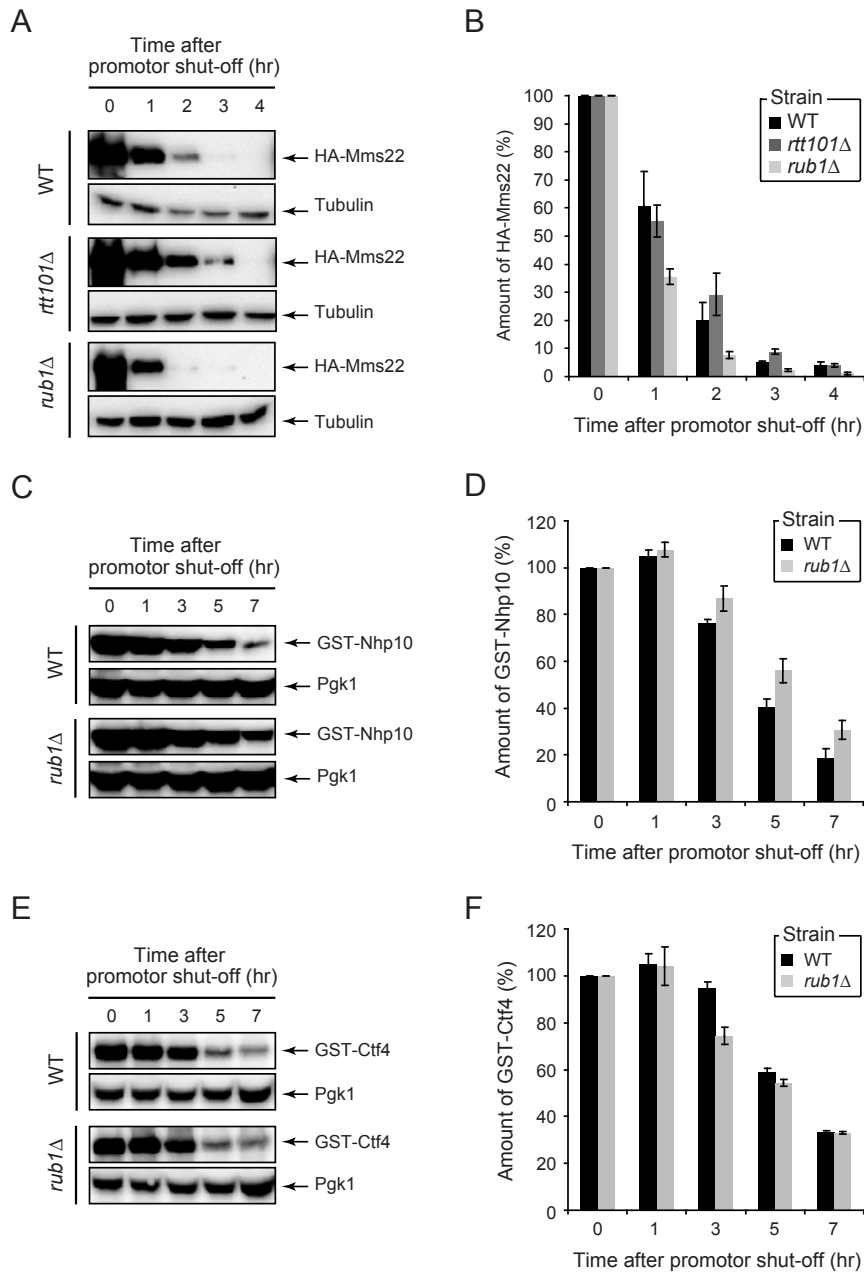


**Figure 5. Neddylation affects the turnover of the DNA damage response proteins Mms22 and Nhp10** (A) Expression of GAL1-HA-Mms22 was induced in WT, *rtt101*Δ and *rub1*Δ cells by growing the cells in 2% galactose for 3 hours. Cells were released in 2% glucose to shut-off expression of HA-Mms22, after which levels of HA-Mms22 were monitored by Western blot analysis. (B) Bar-plot showing the rate of HA-Mms22 protein degradation in WT, *rtt101*Δ and *rub1*Δ cells. The levels of HA-Mms22 protein were quantified and normalized to tubulin. The ratio at the start of shut-off was set to 100%. (C) as in (A) except that the expression of GAL1-GST-Nhp10 was monitored. (D) as in (B) except that the rate of GST-Nhp10 protein degradation is shown. The levels of GST-Nhp10 protein were quantified and normalized to Pgk1. In (E) as in (C) except that the expression of GAL1-GST-Ctf4 was monitored. (F) as in (D) except that the rate of GST-Ctf4 protein degradation is shown. The mean ± standard deviation of three to four independent experiments is presented.

scaffolds for the assembly of multi-subunit cullin-RING ubiquitin ligases (CRLs) [1, 4]. Interestingly, the yeast cullin Rtt101 has been shown to play a critical role in regulating the G2/M checkpoint by promoting proteasomal degradation of Mms22 [18]. Given the role of neddylation in CRL modification, we examined whether this process would affect the steady state levels of Mms22. We observed a faster degradation of Mms22 in a *rub1Δ* strain when compared to wild-type, suggesting that neddylation, in contrast to Rtt101-dependent ubiquitylation [18], promotes Mms22 stability (Figure 5A-B).

As another means of identifying potential DDR factors whose stability might be modulated by the neddylation machinery we examined the set of positive genetic interactions containing RUB1 in our CPT network, as previous work suggested that linear signal transduction pathways are often enriched for positive genetic interaction [19, 20]. The highest positive interaction exhibited by RUB1 in response to CPT was with NHP10 ( $P < 7.8 \times 10^{-8}$ ), a component of the INO80 chromatin remodeling complex with known roles in DNA repair and cell cycle control [21, 22]. In contrast to the faster turnover of Mms22, we found that Nhp10 degradation was slower in the *rub1Δ* strain compared to wild-type (Figure 5C-D). As a negative control, we selected the sister-chromatids cohesion factor, Ctf4, which displayed a very weak differential positive interaction with RUB1 in the CPT network, and found that the steady-state levels of this protein were not altered in a *rub1Δ* strain (Figure 5E-F). Taken together, these data implicate the neddylation machinery as a novel factor that regulates cell cycle progression in response to DNA damage and contributes to genome stability, most likely by regulating the steady state levels of DDR factors such as Mms22 and Nhp10.

While CRLs are the most well studied Rub1 substrates to-date, emerging evidence suggests that many other proteins may be modified by neddylation [3]. We infer from this that the stability of DDR factors such as Mms22 or Nhp10 may be regulated either by direct neddylation, or indirectly by the neddylation of E3 ubiquitin ligases or CRLs (Figure 6).

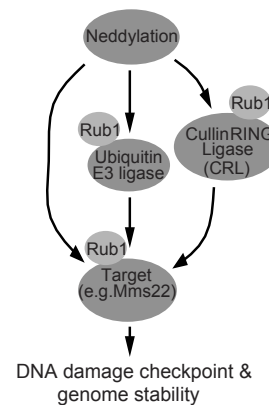


**Figure 6. Schematic illustrating mechanisms by which the neddylation machinery may regulate cell cycle progression and genome stability.** See text for details.

## CONCLUSION

Here we provide an intriguing connection between neddylation, control of the steady state levels of DDR factors, and cell cycle regulation. However, how regulation of Mms22 or Nhp10 by the neddylation pathway affects cell cycle progression is not clear. Nhp10 is a subunit of the chromatin remodeling INO80 complex, which has been found to associate with origins of replication [23, 24]. Vincent et al. showed that *nhp10Δ* mutants were less efficient in

replicating late regions of the genome after MMS, which means that under replication stress the presence of Nhp10 on DNA might be prolonged till late S beginning of G2 phase. As we observed that Rub1 promotes Nhp10 degradation, we envisage that neddylation is critical for the timely removal of Nhp10 from the DNA when replication stress has been overcome, allowing cells to progress through mitosis. Support for such a scenario also comes from work of Ben-Aroya et al., who showed that Mms22 is recruited to damaged chromatin but needs to be removed after repair in order to allow cells to enter mitosis [18]. However, to our surprise we found that instead of promoting degradation of Mms22, neddylation is required for its stabilization. Since neddylation has been mainly associated with protein degradation, it is tempting to propose that the regulation of Mms22 by Rub1 occurs in an indirect manner. The CRL Rtt101 has been proposed to target Mms22 for proteasomal degradation [18]. However, data suggest that Rub1 does not affect Rtt101 activity [25]. Thus, Rub1 may promote the degradation of another factor than Rtt101 that directly mediates Mms22 turnover. In line with this idea, the E3 ligase Mdm2 is targeted for degradation upon neddylation, which leads to the stabilization of its main target p53 [11].

Preliminary data suggest that Mms22 and Nhp10 may not be the only factors that are regulated by neddylation. Pds1 secures the attachment of sister-chromatids after DNA replication and becomes degraded by the anaphase-promoting complex (APC) to ensure separation of sister-chromatids before entry into mitosis. We hypothesized that Pds1 is another factor whose levels could be affected by neddylation. Indeed, we observed a slight delay in degradation of the anaphase inhibitor Pds1 in *rub1Δ* cells synchronized in G1 and released in CPT (data not shown). This suggests that

Rub1-mediated degradation of Pds1 may prevent prolonged cell cycle arrest in G2/M. In addition, we found that the Cdk1 inhibitor SIC1 displays a high positive interaction with RUB1 after CPT treatment. Sic1 inhibition of Cdk1 is necessary for cells to exit mitosis [26]. We could envisage that neddylated-Sic1 is degraded after CPT to prevent premature entry to mitosis. Thus, defects in neddylation would induce mitosis. However, we observed the opposite effect in *rub1Δ* cells, suggesting that the G2/M delay observed in CPT-treated *rub1Δ* cells is most likely the combined effect of changes in the steady state levels of several factors, which reveals a novel complex regulatory mechanism for cell cycle control in response to DNA damage.

It is important to note that such a mechanism could go unnoticed in unperturbed cells, yet becomes critical upon cellular stresses. In agreement with this, the MLN4924 inhibitor of the NEDD8 activating enzyme (NAE1) was found to sensitize cancer cells to ionizing radiation (IR) treatment [27]. Mechanistically, it was shown that CRL targets such as the cell cycle regulators p21, p27, Wee1 or Cdt1 are stabilized upon NAE1 inhibition and that IR treatment further enhances this stabilization effect. Knockdown of CDT1 or WEE1 in MLN4924 treated cells rescues the enhanced sensitivity to IR, suggesting that it is the accumulation of cell cycle regulators upon inhibition of neddylation that causes the hypersensitivity of cancer cells to IR.

Neddylation belongs to a group of processes that regulate protein stability such as sumoylation or ubiquitylation, which appear to interact with each other. The Mdm2 E3 ligase is able to both ubiquitylate and neddylate p53 [9, 11]. Moreover, the cullin Rtt101 was found to be ubiquitylated and neddylated on the same lysine K491 [25]. Finally, Xirodimas et al. showed that p53 is differently modified when cells

are exposed to UV. Both neddylated and ubiquitinated forms of p53 appear in unperturbed cells whereas only neddylated forms were present transiently 4hr after UV treatment. Collectively, the work strongly suggests that a tight regulation of these distinct protein modifications is important for the regulation of cellular processes, including those involved in stress responses. Future work will however be required to understand how these modifications are regulated and if they compete or cooperate with other posttranslational modifications such as those induced by sumoylation or phosphorylation.

## MATERIAL & METHODS

### *DNA damage sensitivity assays*

Overnight cultures were diluted 1:20, grown for 3 h at 30 °C and diluted to  $1 \times 10^7$  cells/ml. Fivefold dilution series were spotted on plates containing 15  $\mu$ M CPT and grown at 30 °C for 3 days.

### *Cell Cycle Profiling*

Exponentially growing cells were synchronized in G1 with  $\alpha$ -factor (7.5 $\mu$ M) and released in the presence or not of 50  $\mu$ M CPT. Samples were taken every 30 min for 2h. Cells were stained with propidium iodide. Flow cytometry analysis was performed on a BD™ LSRII instrument. BD FACSDiva™ software was used for data analysis.

### *GCR assay*

The gross chromosomal rearrangement assay was done according to a previously published protocol [28]. Briefly, cells were grown overnight in YPAD to a density of  $2-5 \times 10^9$  cells/ml. Cells were then spread on SC-Arg plates containing canavanine (60 $\mu$ g/ml) and 5-FOA (0.1%). A fraction of the cells was spread on YPAD to determine the plating efficiency. GCR rates were determined by scoring Can<sup>r</sup>-FOA<sup>r</sup> colonies

after loss of URA3 and CAN1 genes on chromosome 5 relatively to the total number of colonies scored on YPAD. Values reported are from three different experiments, which were each started using five independent colonies per strain.

### *Rad53 and Chk1 western blot analysis*

Exponentially growing cells were synchronized in G1 with  $\alpha$ -factor (7.5 $\mu$ M) and in the presence or not of 50  $\mu$ M CPT. Whole cell extracts were prepared for western blot analysis to examine Rad53 and Chk1 phosphorylation. Anti-Rad53 (Santa-Cruz, sc-6749), anti-HA (Santa Cruz, sc-7392) and anti-Tubulin (Sigma T6199; Clone DM1A) antibodies were used.

### *Mms22, Nhp10 and Ctf4 turnover*

Mms22, Nhp10 and Ctf4 turnover were examined as previously described [18] using cells expressing GAL1-HA-Mms22 [18], pGAL1-GST-NHP10 (Open Biosystems) or pGAL1-GST-NHP10 (Open Biosystems). Briefly, cells were grown to a density of  $5 \times 10^6$  cells/ml after which galactose was added to a final concentration of 2%. Cells were then grown for an additional 3h. Next, cells were washed and incubated in YPLGg + 2% glucose or SC-URA for the rest of the experiment to shut down the expression of HA-Mms22, GST-Nhp10 or GST-Ctf4. Samples were taken every hour for 7h after glucose addition after which whole cell extracts were prepared for western blot analysis to examine the HA-Mms22, GST-Nhp10 and GST-Ctf4 levels. Anti-HA (Santa Cruz Biotechnology, SC-7392), anti-Tubulin (Sigma T6199; Clone DM1A), anti-GST (Amersham) and anti-Pgk1 (Invitrogen) antibodies were used.

4

## REFERENCES

1. Liakopoulos, D., et al., A novel protein modification pathway related to the ubiquitin system. *EMBO J*, 1998. 17(8): p. 2208-14.
2. Bekker-Jensen, S. and N. Mailand, The ubiquitin- and SUMO-dependent signaling response to DNA double-strand breaks. *FEBS Lett*, 2011. 585(18): p. 2914-9.
3. Rabut, G. and M. Peter, Function and regulation of protein neddylation. 'Protein modifications: beyond the usual suspects' review series. *EMBO Rep*, 2008. 9(10): p. 969-76.
4. Laplaza, J.M., et al., *Saccharomyces cerevisiae* ubiquitin-like protein Rub1 conjugates to cullin proteins Rtt101 and Cul3 in vivo. *Biochem J*, 2004. 377(Pt 2): p. 459-67.
5. Jones, J., et al., A targeted proteomic analysis of the ubiquitin-like modifier nedd8 and associated proteins. *J Proteome Res*, 2008. 7(3): p. 1274-87.
6. Saha, A. and R.J. Deshaies, Multimodal activation of the ubiquitin ligase SCF by Nedd8 conjugation. *Mol Cell*, 2008. 32(1): p. 21-31.
7. Petropoulou, C., et al., Cdt1 and Geminin in cancer: markers or triggers of malignant transformation? *Front Biosci*, 2008. 13: p. 4485-94.
8. Nakayama, K., et al., Targeted disruption of Skp2 results in accumulation of cyclin E and p27(Kip1), polyploidy and centrosome overduplication. *EMBO J*, 2000. 19(9): p. 2069-81.
9. Xirodimas, D.P., C.W. Stephen, and D.P. Lane, Compartmentalization of p53 and Mdm2 is a major determinant for Mdm2-mediated degradation of p53. *Exp Cell Res*, 2001. 270(1): p. 66-77.
10. Lain, S., Protecting p53 from degradation. *Biochem Soc Trans*, 2003. 31(2): p. 482-5.
11. Xirodimas, D.P., et al., Mdm2-mediated NEDD8 conjugation of p53 inhibits its transcriptional activity. *Cell*, 2004. 118(1): p. 83-97.
12. Bandyopadhyay, S., et al., Rewiring of genetic networks in response to DNA damage. *Science*, 2010. 330(6009): p. 1385-9.
13. Zhou, B.B. and S.J. Elledge, The DNA damage response: putting checkpoints in perspective. *Nature*, 2000. 408(6811): p. 433-9.
14. Shinohara, M., et al., The mitotic DNA damage checkpoint proteins Rad17 and Rad24 are required for repair of double-strand breaks during meiosis in yeast. *Genetics*, 2003. 164(3): p. 855-65.
15. Usui, T., H. Ogawa, and J.H. Petrini, A DNA damage response pathway controlled by Tel1 and the Mre11 complex. *Mol Cell*, 2001. 7(6): p. 1255-66.
16. Jackson, S.P., The DNA-damage response: new molecular insights and new approaches to cancer therapy. *Biochem Soc Trans*, 2009. 37(Pt 3): p. 483-94.
17. Redon, C., et al., Yeast histone 2A serine 129 is essential for the efficient repair of checkpoint-blind DNA damage. *EMBO Rep*, 2003. 4(7): p. 678-84.
18. Ben-Aroya, S., et al., Proteasome nuclear activity affects chromosome stability by controlling the turnover of Mms22, a protein important for DNA repair. *PLoS Genet*, 2010. 6(2): p. e1000852.
19. Fiedler, D., et al., Functional organization of the *S. cerevisiae* phosphorylation network. *Cell*, 2009. 136(5): p. 952-63.
20. Sharifpoor, S., et al., Functional wiring of the yeast kinome revealed by global analysis of genetic network motifs. *Genome Res*, 2012. 22(4): p. 791-801.
21. van Attikum, H., et al., Recruitment of the INO80 complex by H2A phosphorylation links ATP-dependent chromatin remodeling with DNA double-strand break repair. *Cell*, 2004. 119(6): p. 777-88.
22. van Attikum, H., O. Fritsch, and S.M. Gasser, Distinct roles for SWR1 and INO80 chromatin remodeling complexes at chromosomal double-strand breaks. *EMBO J*, 2007. 26(18): p. 4113-25.
23. Vincent, J.A., T.J. Kwong, and T. Tsukiyama, ATP-dependent chromatin

remodeling shapes the DNA replication landscape. *Nat Struct Mol Biol*, 2008. 15(5): p. 477-84.

24. Shimada, K., et al., Ino80 chromatin remodeling complex promotes recovery of stalled replication forks. *Curr Biol*, 2008. 18(8): p. 566-75.

25. Rabut, G., et al., The TFIID subunit Tfb3 regulates cullin neddylation. *Mol Cell*, 2011. 43(3): p. 488-95.

26. Schwob, E., et al., The B-type cyclin kinase inhibitor p40SIC1 controls the G1 to S transition in *S. cerevisiae*. *Cell*, 1994. 79(2): p. 233-44.

27. Wei, D., et al., Radiosensitization of human pancreatic cancer cells by MLN4924, an investigational NEDD8-activating enzyme inhibitor. *Cancer Res*, 2012. 72(1): p. 282-93.

28. Chen, C. and R.D. Kolodner, Gross chromosomal rearrangements in *Saccharomyces cerevisiae* replication and recombination defective mutants. *Nat Genet*, 1999. 23(1): p. 81-5.





# 5

## IRC21 IS A GENERAL RESPONSE FACTOR IN CHECKPOINT CONTROL, REPAIR AND GENOME STABILITY

Aude Guérolé<sup>1</sup>, Rohith Srivas<sup>2,3</sup>, Kees Vreeken<sup>1</sup>, Trey Ideker<sup>2,3,4</sup>, Haico van Attikum<sup>1\*</sup>

<sup>1</sup>Department of Toxicogenetics, Leiden University Medical Center, Einthovenweg 20, 2333 ZC, Leiden, The Netherlands, <sup>2</sup>Department of Bioengineering, University of California, San Diego, La Jolla, CA 92093 USA, <sup>3</sup>Department of Medicine, University of California, San Diego, La Jolla, CA 92093, USA, <sup>4</sup>The Institute for Genomic Medicine, University of California, San Diego, La Jolla, CA 92093, USA

\* H.v.A. (h.van.attikum@lumc.nl)

Partially published in:

Guérolé A, Srivas R, Vreeken K, Wang ZZ, Wang S, Krogan NJ, Ideker T, van Attikum H. *Dissection of DNA damage responses using multiconditional genetic interaction maps*. Mol Cell. 2013 Jan 24;49(2):346-58.



Irc21, a novel factor in checkpoint control, repair and genome stability

### **ABSTRACT**

Due to multiple forms of genotoxic attacks, cells accumulate a large variety of DNA lesions. To protect their genome, cells use molecular pathways that signal and repair the lesions. Collectively, these pathways compose the DNA damage response. How these pathways are orchestrated and connected to enable an appropriate cellular response to the distinct type of DNA lesions that are encountered still remains to be discovered. We used a genome-wide genetic approach called EMap as a mean to dissect the responses to different types of DNA lesions induced either by the alkylating agent methyl methanesulfonate (MMS) or the topoisomerase-1 inhibitor camptothecin (CPT) and the DNA intercalating agent zeocin (ZEO). Although we observed clear drug-specific responses, the limited overlap between them was significant enough to define a common DNA damage response network. In that conserved space, we not only identified genetic interactions for known DNA damage response factors but also for several poorly characterized genes. Here, we describe that loss of one of these genes, called IRC21, alleviates several DNA damage response defects observed in DNA damage checkpoint deficient cells, including DNA damage sensitivity, impaired checkpoint activation and DNA repair, as well as genome instability. Thus, we identify Irc21 as a novel factor involved in regulating DNA damage responses and genome stability maintenance.

**INTRODUCTION**

Cells are under constant threat by endogenous and exogenous factors that induce multiple types of DNA damage. To protect against the deleterious effects that DNA damage can have on genome integrity, cells use a combination of pathways that signal and repair these lesions, collectively referred to as DNA damage responses (DDR). These responses to DNA damage typically involve a detection step that initiates signaling cascades that in turn coordinate several processes including cell cycle progression and DNA repair. However, how the pathways and factors involved in the DDR are orchestrated to allow cells to respond properly to different types of DNA lesions remained largely unclear.

In yeast, recent developments of high throughput genetic screens have enabled the dissection of pathways involved in cell organization. However, the genetic understanding of cellular functions has come mainly from static observations where cells were studied under a single standard condition [1, 2]. Recently, Bandyopadhyay et al. have developed a technology called differential epistatic mapping (dE-MAP), which allows to address the dynamic aspect of the cellular response to a perturbation [3]. In order to understand the genetic interaction changes that occur upon induction of different types of DNA damage, we previously generated d-EMAPs after exposure of cells to three different DNA genotoxic drugs: the alkylating agent methyl methanesulfonate (MMS), the topoisomerase-1 inhibitor camptothecin (CPT) and the DNA intercalating agent zeocin (ZEO). The genetic networks induced by each drug were very specific, which suggests that a unique set of DNA damage response pathways is triggered depending on the type of DNA damage that is induced. However, we also found a significant number of genetic changes that were

induced by at least two of the genotoxic compounds. We called this overlap between the genetic networks the common DDR network. Indeed, in that common space, the response involves the same genes irrespective of the type of DNA damage induced. Importantly, the common network not only included several known DDR factors, but also revealed unanticipated and poorly characterized genes such as IRC21.

Irc21 was previously identified in a genome-wide study in which mutants were screened for their ability to form spontaneous Rad52 foci. In that screen, deletion of IRC21 led to an increase in spontaneous Rad52 foci, thus the gene was called Increased Recombination Center 21, IRC21 [4]. In another genome-wide screen, *irc21Δ* mutants were found to be resistant to cisplatin and carboplatin [5]. Although this work may implicate a role for Irc21 in the DDR, a precise understanding of its function this response is lacking. Here, we demonstrate that Irc21 is an important novel DDR factor that affects cell cycle regulation, DNA damage repair and genome stability maintenance.

## RESULTS & DISCUSSION

We used a recently-developed technology to analyze epistasis between pairs of genes in yeast (EMAP) and investigate the genetic changes induced by three different DNA damaging compounds: methyl methanesulfonate (MMS), camptothecin (CPT) and zeocin (ZEO). To center our study, we employed 55 query genes, all involved in different aspects of the DDR. The queries were crossed against an array of 2022 genes, implicated in the DDR as well as in processes, such as cell cycle regulation, chromatin organization, replication, transcription, and protein transport. The mated strains passed through several selection steps, which resulted in a collection of haploid double mutant strains. All these mutants were left untreated or exposed to MMS, CPT or ZEO and their growth rates were measured 48h later. Eventually, genetic interaction scores were obtained by normalization and statistical analysis of the measured colony sizes (Chapter 1).

To precisely highlight the interactions that changed in response to DNA damage, we made use of a metric previously developed to measure the difference between the genetic score in untreated versus treated conditions [3]. The resulting score is called a differential interaction score. The analysis of our differential genetic networks showed that while the interactions induced by the three agents were largely divergent, it did implicate a “common” network of 584 interactions that were altered in response to at least two agents (Figure 1A). Many known DNA repair factors were highly connected within this network including DSB repair factors (RAD52, SAE2, MRE11, RAD59), post replication repair (PRR) genes (RAD18), and chromatin remodelers (SWR1) which have well-documented roles in the DDR [6, 7]. In particular, our analysis highlighted the damage checkpoint gene RAD17 as a hub not only of the CPT network (see above), but

also of conserved interactions across agents (Figure 1A, top inset). These included a differential positive interaction with IRC21, an as yet uncharacterized gene, in response to both CPT (differential  $P = 4.7 \times 10^{-7}$ ) and MMS ( $P = 8.3 \times 10^{-7}$ ), but not ZEO ( $P = 0.53$ ). We confirmed that Irc21 is expressed *in vivo* in yeast (Figure 1B), and that deletion of IRC21 in a *rad17Δ* mutant suppresses its sensitivity to CPT and MMS (Figure 1C). Importantly, this suppressive effect was also observed in other checkpoint mutants, including *ddc1Δ* (another mutant of the Rad17-Ddc1-Mec3 (9-1-1) complex) and *rad9Δ* (Figure 1D). Analysis of the Irc21 protein sequence revealed the presence of a cytochrome b5-like domain (Figure 1E), which is usually found in proteins that are involved in cytochrome P450-dependent metabolic processes [8]. To rule out that the suppression was due to Irc21 affecting drug metabolism via its cytochrome b5 domain, we exposed cells to ultraviolet light (UV) and ionizing radiation (IR) and were able to re-produce the suppressive phenotype in both cases (Figure 1F). Ectopic expression of Irc21 in the *rad17Δirc21Δ* mutant restored the sensitivity to DNA damaging agents to that observed for the *rad17Δ* mutant (Figure 1B and F). These results suggest that Irc21 affects cell survival in response to genotoxic insult by modulating the DNA damage checkpoint rather than by affecting drug metabolism.

To further explore this possibility, we profiled *rad17Δ*, *irc21Δ* and *rad17Δirc21Δ* mutants for their cell cycle progression in the presence of MMS. While the wild-type and *irc21Δ* strains displayed slow S-phase progression and accumulated in G2 two hours after release from G1, the checkpoint-deficient *rad17Δ* strain rapidly progressed through S-phase and accumulated in G2 within an hour (Figures 2A-B). Remarkably, deletion of IRC21 in the *rad17Δ* strain partially suppressed the checkpoint deficiency as we noted, from 60 to 120

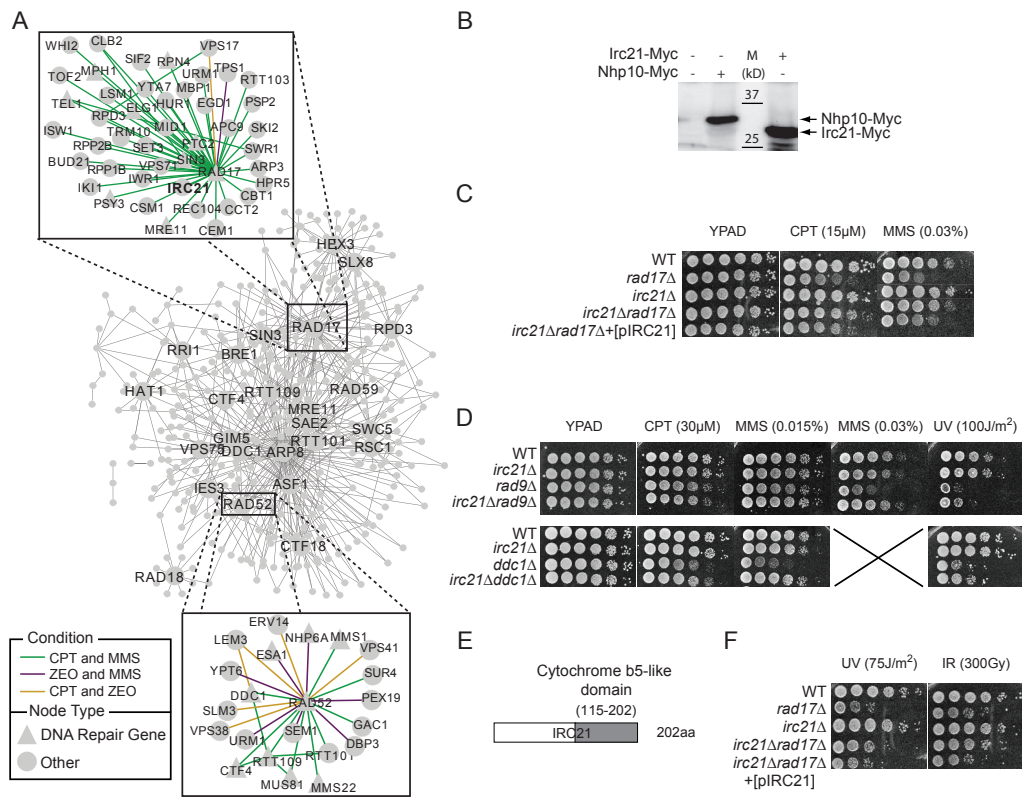


**Figure 1. Irc21 loss alleviates the sensitivity of *rad17Δ* cells to DNA damage** (A) Network of all 584 differential genetic interactions induced by at least two agents. The top 25 hubs in this network have been labeled. The sub-networks of interactions involving RAD17 and RAD52 are also shown. (B) Western blot analysis of cells expressing Myc-tagged Irc21. Cells from non-tagged and Nhp10-Myc expressing strains were used as negative and positive controls, respectively. (C) Effect of IRC21 deletion on the viability of *rad17Δ* cells. 10-fold serial dilutions of log-phase cells of the indicated genotypes were either spotted onto YPAD plates containing MMS or CPT. (D) as in C, except that *rad9Δ* and *ddc1Δ* cells were used and that cells were also spotted on YPAD and exposed to UV. (E) Schematic of the Irc21 protein showing a putative cytochrome b5-like domain in its C-terminus. (F) as in (C) except cells were exposed to UV and IR.

minutes after release in MMS, an increased fraction of cells remaining in S-phase (20.7% versus 10.7% at two hours after release; Figure 2B). Moreover, we observed that the *rad17Δ* mutant failed to activate the central checkpoint kinase Rad53, denoted by the absence of phosphorylated forms of Rad53 (Figure 2C). However the *rad17Δirc21Δ* double mutant displayed a moderate restoration of this phenotype with Rad53 becoming slightly phosphorylated already 60 minutes after release from G1 arrest in MMS-containing media (Figure 2C).

Checkpoint proteins detect DNA lesions, arrest the cell cycle and trigger DNA repair [6, 9]. Given that Irc21 modulates the DNA damage checkpoint, we examined whether it also functions in DNA damage repair. Rad52 is a key repair protein in yeast that is not only involved in the response to stalled or collapsed replication forks in S-phase, but also facilitates the repair of DSBs and single-stranded gaps [4]. It has been shown to accumulate into DNA damage-induced subnuclear foci that are thought to represent active repair centers

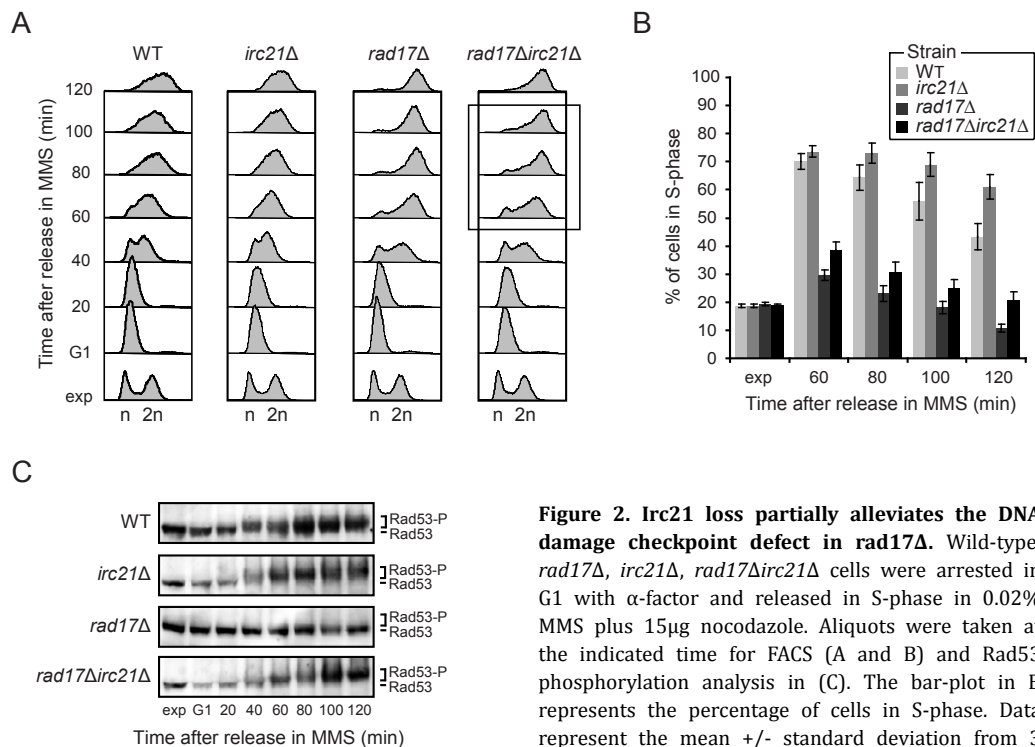


**Figure 2. Irc21 loss partially alleviates the DNA damage checkpoint defect in *rad17Δ*.** Wild-type, *rad17Δ*, *irc21Δ*, *rad17Δirc21Δ* cells were arrested in G1 with  $\alpha$ -factor and released in S-phase in 0.02% MMS plus 15 $\mu$ g nocodazole. Aliquots were taken at the indicated time for FACS (A and B) and Rad53 phosphorylation analysis in (C). The bar-plot in B represents the percentage of cells in S-phase. Data represent the mean  $\pm$  standard deviation from 3 independent experiments.

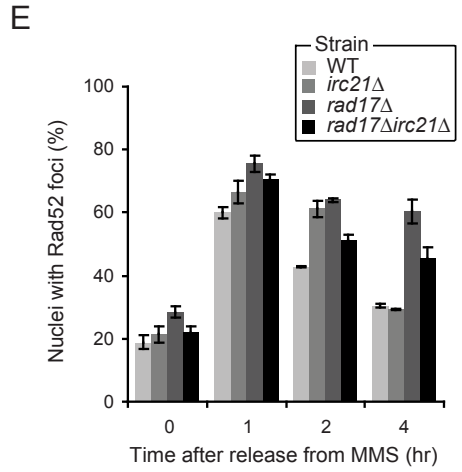
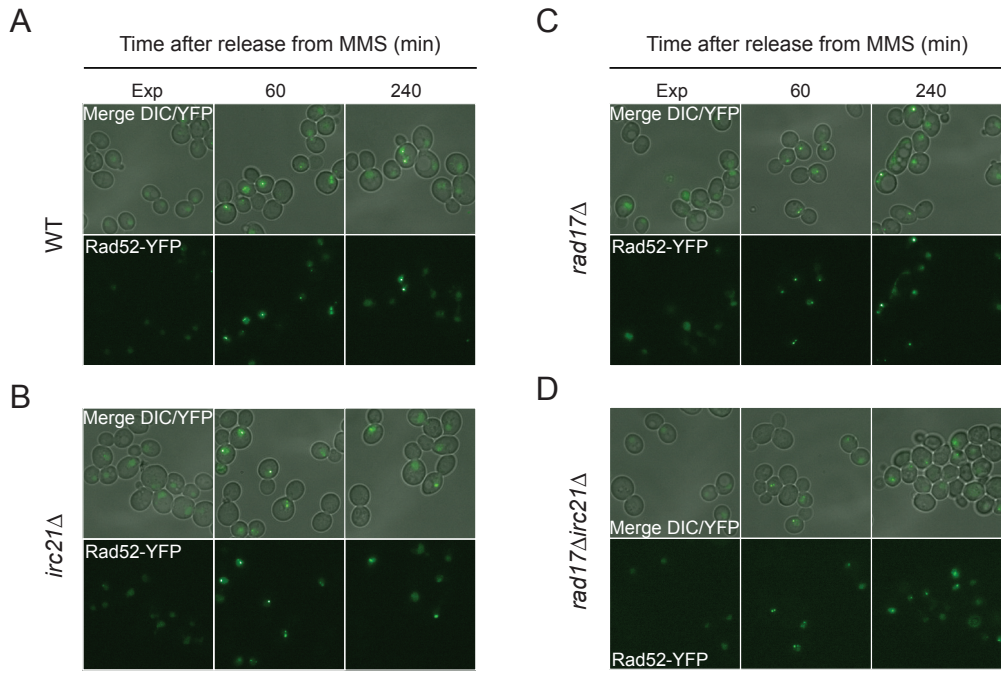
[10]. We used this phenotype to investigate the capacity of wild-type, *rad17Δ*, *irc21Δ* and *rad17Δirc21Δ* strains to repair DNA damage. To this end, we monitored the accumulation of Rad52 foci following exposure to MMS and found that the rate of assembly of Rad52 foci was similar in all strains as they all reached a maximum number of Rad52 foci one hour after exposure to MMS (Figure 3A-E). Interestingly, *irc21Δ* mutant have an early repair delay attested by a larger number of cells that contain Rad52 foci (60%) compared to wild-type cells (40%) two hours after release from MMS (Figure 3E). However, while Rad52 foci gradually disappeared by 2–4 hours in wild-type and *irc21Δ* cells, persistent foci were observed in the *rad17Δ* mutant, indicating abrogation of repair (Figure 3A-C and E). Surprisingly, deletion of IRC21 alleviated the repair defect seen in the *rad17Δ* strain, as indicated by the enhanced dissolution of Rad52 foci in

the *rad17Δirc21Δ* strain compared to that in the *rad17Δ* strain (4 hour time point, Figure 3A-E).

Finally we found that, whereas *irc21Δ* cells showed no alterations in genomic stability, *rad17Δ* cells displayed a 8.2-fold increase in GCR events compared to wild-type (Figure 4A-B). However, *rad17Δirc21Δ* cells only showed a 4.5-fold increase, suggesting that deletion of IRC21 partially rescues the deleterious impact of Rad17 loss on GCR (Figure 4B). Together, these results suggest that Irc21 not only modulates DNA damage checkpoint, but also promotes efficient repair of DNA damage and contributes to genome stability.

In contrast to previous high-throughput localization studies, which reported Irc21 localization in the cytoplasm [11], we found that Irc21-GFP localizes in

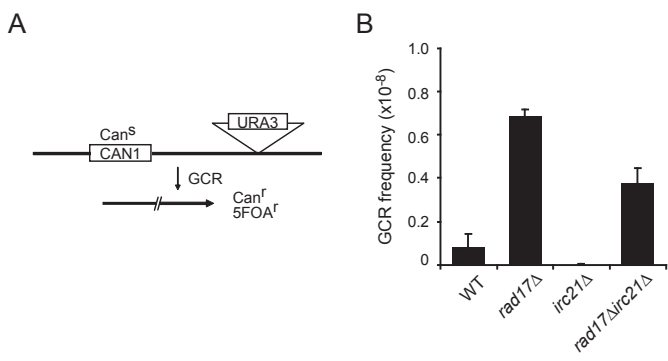




**Figure 3. Irc21 loss alleviates the repair defect of *rad17*Δ cells** (A) Wild-type (WT), (B) *irc21*Δ, (C) *rad17*Δ and (D) *rad17*Δ*irc21*Δ cells expressing Rad52-YFP were exposed for 1h to 0.02% MMS and then released in fresh YPAD. (E) Quantitative analysis of Rad52-YFP foci in cells from A-D. Images were taken at the indicated time points and scored for Rad52-YFP foci. At least 100 nuclei were analyzed per strain and per time point. Data represent the mean ± 1 s.d. from three independent experiments.

5

**Figure 4: Irc21 loss alleviates genome instability in *rad17*Δ cells.** (A) Scheme of the working principle of the GCR assay developed by Chen and Kolodner, 1999. (B) Effect of IRC21 deletion on GCR frequencies in *rad17*Δ cells. The mean GCR frequency ± standard deviation of three independent experiments is presented.



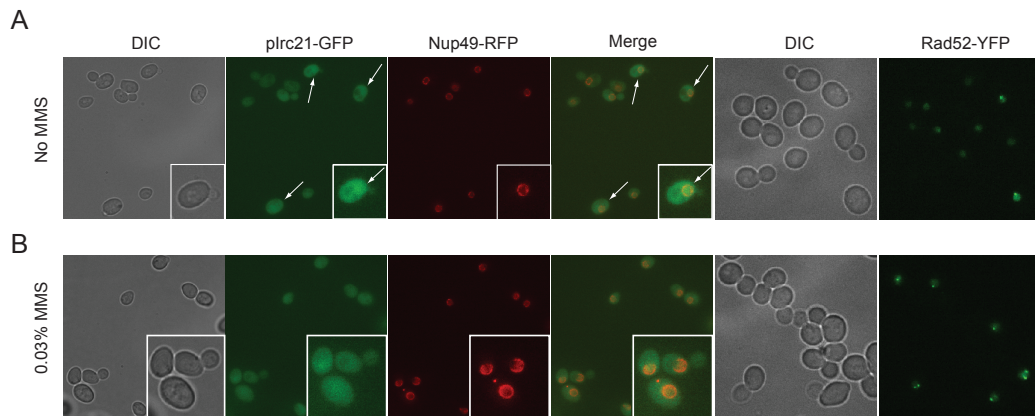


**Figure 5. Irc21 localizes in the nucleus and the cytoplasm but not in MMS induced foci (A and B)** Exponentially growing *irc21Δ* cells expressing Irc21-GFP and Nup49-RFP were grown in YPAD (A) or in YPAD containing 0.03% MMS for 1 hour (B), and then examined for Irc21 localization. Wild-type cells expressing Rad52-YFP were treated similarly and examined for Rad52 focus formation. (C) Ectopic expression of Irc21-GFP in *rad17Δirc21Δ* renders cells as sensitive to UV as *rad17Δ* cells, demonstrating the functionality of GFP-tagged Irc21. 10-fold serial dilutions of log-phase cells of the indicated genotypes were spotted onto YPAD plates, exposed to UV and incubated for 3 days at 30°C.

both the cytoplasm and nucleus (Figure 5A). We examined the functionality of the Irc21-GFP construct by drop-test analysis (Figure 5C). Irc21-GFP expressing *rad17Δirc21Δ* cells were as UV sensitive as *rad17Δ* cells, suggesting that the Irc21-GFP construct is functional (Figure 5C). We noticed that Irc21-GFP did not accumulate into MMS-induced sub-nuclear foci as observed for Rad52-YFP (Figure 5B), suggesting that it may not operate directly at DNA lesions.

Interestingly, we observed that *irc21Δ* strains are hypersensitive to MMS when combined with the TOR inhibitor rapamycin (Figure 6A), a compound that can lead to increased and decreased abundance of proteins (via the autophagy pathway) including factors involved in the DDR [12, 13]. This may suggest that Irc21 affects the DDR by regulating the steady state levels of distinct DDR proteins. Work

from Robert and colleagues demonstrated that the stability of the HR protein Sae2 following double-stranded breaks is dependent on the autophagy machinery [14]. To check whether the autophagy-dependent degradation of Sae2 is mediated by Irc21, we monitored the stability of Sae2 [14]. In agreement with this published work, we found that Sae2 was degraded much quicker after induction of a single DSB when cells are exposed to rapamycin (Figure 6B). However, this rapid degradation was neither dependent on Irc21 nor on Rad17 (Figure 6B). Earlier in the current work, we examined the role of Irc21 in response to MMS, which alkylates DNA bases and can lead to replication fork stalling (and not per se DSBs). We therefore examined the effect of MMS on the autophagy-dependent degradation of Sae2. We found that following exposure to MMS Sae2 was also degraded much more rapidly in rapamycin-treated

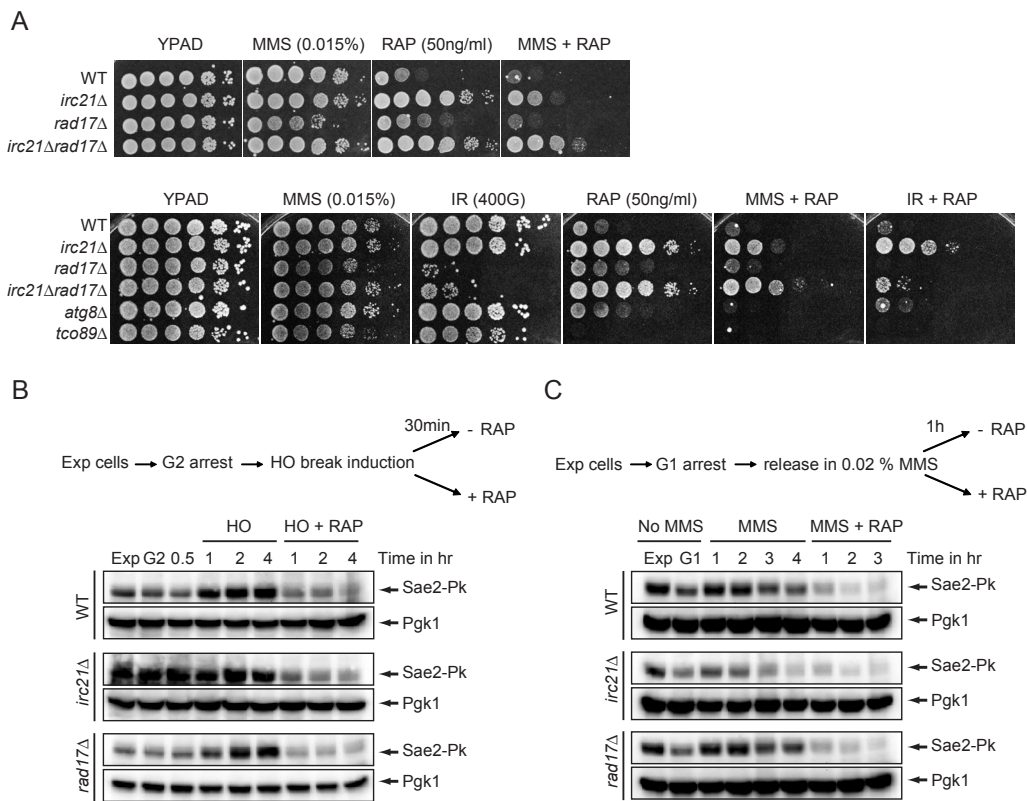


**Figure 6. Irc21 does not mediate the autophagy-dependent degradation of Sae2 following DNA damage (A)** *irc21Δ* cells are hypersensitive to MMS when combined with the TOR inhibitor rapamycin (RAP). 10-fold serial dilutions of log-phase cells of the indicated genotypes were either spotted onto YPAD plates containing MMS, RAP or both and incubated for 3 days at 30°C. (B) Exponentially (exp) growing WT, *irc21Δ* and *rad17Δ* cells were arrested in G2 with nocodazole after which a single double-stranded break was induced at MAT by the HO endonuclease as described previously [14]. Cells were then exposed to rapamycin (+RAP) or not (-RAP), after which the levels of Sae2-Pk and Pgk1 were monitored by Western blot analysis at the indicated time points. (C) As in B, except that exponentially growing cells were arrested in G1 using  $\alpha$ -factor, released into fresh medium containing 0.02% MMS, and then left untreated or exposed to rapamycin.

wild-type cells (Figure 6C). A similar rate of degradation was seen in rapamycin-treated *irc21Δ* cells, suggesting that this autophagy-dependent degradation of Sae2 in response to MMS-induced DNA damage, like that after DSB induction, was not dependent on Irc21 (Figure 6C). Interestingly, Sae2 levels were decreased in *irc21Δ* cells that were only exposed to MMS. A similar decrease in Sae2 levels was observed in wild-type cells exposed to MMS and rapamycin, which suggests that IRC21 deletion mimics the

effect of rapamycin on Sae2 levels (Figure 6C). Whether the effect on Irc21 on the steady state levels of Sae2 or other DNA repair factors affects the DDR needs further investigation.

## CONCLUSION

Here, we describe the discovery of Irc21 as a new factor that regulates the DRR. However the precise role of Irc21 in this response remain to be determined. Irc21 contains a cytochrome b5 domain. Cytochrome b5

Irc21, a novel factor in checkpoint control, repair and genome stability

proteins have been shown to positively regulate reactions catalyzed by cytochrome P450 proteins. P450 proteins inactivate multiple hormones and xenobiotic compounds and play key roles in lipid metabolism (reviewed in [15]). Thus, one possible role for Irc21 may be to metabolize drugs or regulate their uptake. Here, we found that deletion of IRC21 alleviates *rad17Δ* cells sensitivity to various source of DNA damage (Figure 1C-D and F). We noticed that the survival of *rad17Δirc21Δ* cells was more efficient after MMS and CPT than after IR and UV treatment, which suggest that the possible effect of Irc21 in drug metabolism may partially affect cell viability. In line with this idea, it was also shown that *irc21Δ* cells are resistant to carboplatin and cisplatin [5]. However, the improved survival of *rad17Δirc21Δ* cells after IR and UV confirmed a role for Irc21 in the cellular response to DNA damage that is independent of its putative drug metabolism activity. Moreover, upon MMS treatment, *irc21Δ* cells accumulate as many repair foci as wild-type cells, suggesting that the load of damage induced by MMS and so the MMS uptake is the same in the two strains (Figure 3A-B and E).

We found that *irc21Δ* cells are resistant to rapamycin (Figure 6A). Rapamycin treatment inhibits the target of rapamycin (TOR) signaling pathway, which causes severe changes in the transcription profile of many genes and stimulates autophagy, thereby affecting the steady state levels of certain proteins. We showed that both deletion of IRC21 and rapamycin treatment lead to a decrease in Sae2 levels after MMS exposure (Figure 6B-C). Interestingly, we found that Rad52-foci disappearance was delayed in *irc21Δ* cells (Figure 3E), indicating that DNA repair occurs at a slower rate that may be potentially caused by a partial loss of Sae2. Whether Irc21 affects Sae2 levels by affecting its transcription or degradation is

not clear. Consistent with previous work, we found that rapamycin, which stimulates autophagy by inhibiting TOR provokes Sae2 degradation [14]. However, we showed that this autophagy-mediated degradation of Sae2 was not dependent on Irc21, suggesting that Irc21 does not regulate protein levels via the autophagy machinery (Figure 6C). Beside, the fact that IRC21 deletion mimics rapamycin treatment may imply that Irc21, like rapamycin, is a negative regulator of the TOR pathway. Since TOR inhibition induces transcriptional changes, we could envisage that Irc21 affects the transcription pattern of SAE2 and probably multiple other genes by inhibiting TOR signaling.

Interestingly, we found that IRC21 has a similar differential genetic interaction profile to that of RRD1 on MMS. RRD1 deletion also confers resistance to rapamycin. Rrd1 is a peptidyl propyl isomerase that has been implicated in transcriptional changes in response to rapamycin and other transcriptional stress-inducing compounds [16]. It was proposed that Rrd1 promotes RNA polymerase II isomerisation in response to rapamycin, resulting in RNA pol II dissociation from chromatin [17]. Thus it may be that Irc21 like Rrd1 is involved in transcription regulation upon cellular stress. A number of recent studies in yeast and mammals have suggested that rapamycin treatment of cells and the subsequent inactivation of mTOR plays a role in up-regulating the level of numerous factors involved in DNA repair [12, 18]. Thus, the role of Irc21 in the DDR may be that it controls the mTOR-dependent up or down- transcriptional regulation of DNA repair factors.

## MATERIAL & METHODS

### *Cell survival assays*

Overnight cultures were diluted 1:20, grown for 3 h at 30 °C and diluted to  $1 \times 10^7$  cells/ml. 10-fold dilution series were spotted on

plates containing CPT or MMS or spotted on YPAD and exposed to IR or UV after which they were grown at 30 °C for 3 days.

#### *Cell Cycle Profiling*

Exponentially growing cells were synchronized in G1 with  $\alpha$ -factor (7.5 $\mu$ M) and released in 0.02% MMS. Samples were taken every 20 min for 2h. Cells were stained with propidium iodide. Flow cytometry analysis was performed on a BD™ LSRII instrument. BD FACSDiva™ software was used for data analysis.

#### *Checkpoint assay*

Exponentially growing cells were synchronized in G1 with  $\alpha$ -factor (7.5 $\mu$ M) and released in 0.02% MMS. Whole cell extracts were prepared for western blot analysis to examine Rad53 phosphorylation using anti-Rad53 (Santa-Cruz, sc-6749) antibody.

## 5

#### *Analysis of Rad52 foci*

Cells containing a Rad52-YFP expression vector were grown to mid-log phase, exposed to MMS for 1 hour, washed and concentrated in 1% low melting agar (Cambrex). Images were captured using a Leica AF6000 LX microscope at 100-fold magnification using a HCX PL FLUOTAR 100x 1.3 oil objective lens.

#### *GCR assay*

The Gross Chromosomal Rearrangement (GCR) assay was done according to a previously published protocol [19]. Briefly, cells were grown overnight in YPAD to a density of 2-5x10<sup>9</sup> cells/ml. Cells were then spread on SC-Arg plates containing canavanine (60 $\mu$ g/ml) and 5-FOA (0.1%). A fraction of the cells was spread on YPAD to determine the plating efficiency. GCR rates were determined by scoring Can<sup>r</sup>-FOA<sup>r</sup> colonies after loss of URA3 and CAN1 genes on chromosome 5 relative to the total number of colonies scored on YPAD.

Values reported are from three different experiments, which were each started using five independent colonies per strain.

#### *Western blot analysis of Sae2*

Exponentially growing cells were arrested in G2 with nocodazole after which a single double-stranded break was induced at MAT by the HO endonuclease as described previously [14]. In the MMS experiment, exponentially growing cells were arrested in G1  $\alpha$ -factor (7.5 $\mu$ M) and released into fresh medium containing 0.02% MMS. Cells were then exposed to rapamycin (+200ng/ml RAP) or not (-RAP), after which the levels of Sae2-Pk and Pkg1 were monitored by Western blot analysis using anti V5-TAG (Invitrogen) and anti-Pkg1 (Abcam 22C5) antibodies.

Irc21, a novel factor in checkpoint control, repair and genome stability

## REFERENCES

1. Collins, S.R., et al., Functional dissection of protein complexes involved in yeast chromosome biology using a genetic interaction map. *Nature*, 2007. 446(7137): p. 806-10.
2. Schuldiner, M., et al., Exploration of the function and organization of the yeast early secretory pathway through an epistatic miniarray profile. *Cell*, 2005. 123(3): p. 507-19.
3. Bandyopadhyay, S., et al., Rewiring of genetic networks in response to DNA damage. *Science*, 2010. 330(6009): p. 1385-9.
4. Alvaro, D., M. Lisby, and R. Rothstein, Genome-wide analysis of Rad52 foci reveals diverse mechanisms impacting recombination. *PLoS Genet*, 2007. 3(12): p. e228.
5. Lee, W., et al., Genome-wide requirements for resistance to functionally distinct DNA-damaging agents. *PLoS Genet*, 2005. 1(2): p. e24.
6. Harrison, J.C. and J.E. Haber, Surviving the breakup: the DNA damage checkpoint. *Annu Rev Genet*, 2006. 40: p. 209-35.
7. van Attikum, H., O. Fritsch, and S.M. Gasser, Distinct roles for SWR1 and INO80 chromatin remodeling complexes at chromosomal double-strand breaks. *EMBO J*, 2007. 26(18): p. 4113-25.
8. Zhang, H., E. Myshkin, and L. Waskell, Role of cytochrome b5 in catalysis by cytochrome P450 2B4. *Biochem Biophys Res Commun*, 2005. 338(1): p. 499-506.
9. Jackson, S.P., The DNA-damage response: new molecular insights and new approaches to cancer therapy. *Biochem Soc Trans*, 2009. 37(Pt 3): p. 483-94.
10. Lisby, M., R. Rothstein, and U.H. Mortensen, Rad52 forms DNA repair and recombination centers during S phase. *Proc Natl Acad Sci U S A*, 2001. 98(15): p. 8276-82.
11. Huh, W.K., et al., Global analysis of protein localization in budding yeast. *Nature*, 2003. 425(6959): p. 686-91.
12. Fournier, M.L., et al., Delayed correlation of mRNA and protein expression in rapamycin-treated cells and a role for Ggc1 in cellular sensitivity to rapamycin. *Mol Cell Proteomics*, 2010. 9(2): p. 271-84.
13. Dyavaiah, M., et al., Autophagy-dependent regulation of the DNA damage response protein ribonucleotide reductase 1. *Mol Cancer Res*, 2011. 9(4): p. 462-75.
14. Robert, T., et al., HDACs link the DNA damage response, processing of double-strand breaks and autophagy. *Nature*, 2011. 471(7336): p. 74-9.
15. Nebert, D.W. and D.W. Russell, Clinical importance of the cytochromes P450. *Lancet*, 2002. 360(9340): p. 1155-62.
16. Poschmann, J., et al., The peptidyl prolyl isomerase Rrd1 regulates the elongation of RNA polymerase II during transcriptional stresses. *PLoS One*, 2011. 6(8): p. e23159.
17. Jouvét, N., et al., Rrd1 isomerizes RNA polymerase II in response to rapamycin. *BMC Mol Biol*, 2010. 11: p. 92.
18. Bandhakavi, S., et al., Quantitative nuclear proteomics identifies mTOR regulation of DNA damage response. *Mol Cell Proteomics*, 2010. 9(2): p. 403-14.
19. Chen, C. and R.D. Kolodner, Gross chromosomal rearrangements in *Saccharomyces cerevisiae* replication and recombination defective mutants. *Nat Genet*, 1999. 23(1): p. 81-5.



# 6

## SAE2 AND PPH3 COOPERATE TO PROMOTE DNA REPAIR AND CHECKPOINT RECOVERY

Aude Guénolé<sup>1</sup>, Rohith Srivas<sup>2,3</sup>, Kees Vreeken<sup>1</sup>, Trey Ideker<sup>2,3,4</sup>, Haico van Attikum<sup>1\*</sup>

<sup>1</sup>Department of Toxicogenetics, Leiden University Medical Center, Einthovenweg 20, 2333 ZC, Leiden, The Netherlands, <sup>2</sup>Department of Bioengineering, University of California, San Diego, La Jolla, CA 92093 USA, <sup>3</sup>Department of Medicine, University of California, San Diego, La Jolla, CA 92093, USA, <sup>4</sup>The Institute for Genomic Medicine, University of California, San Diego, La Jolla, CA 92093, USA

\* H.v.A. (h.van.attikum@lumc.nl)

Partially published in:

Guénolé A, Srivas R, Vreeken K, Wang ZZ, Wang S, Krogan NJ, Ideker T, van Attikum H. *Dissection of DNA damage responses using multiconditional genetic interaction maps*. Mol Cell. 2013 Jan 24;49(2):346-58.





**ABSTRACT**

The DNA in our cells is constantly exposed to genotoxic stresses from endogenous and exogenous sources that induce a large variety of lesions. Defects in the repair of these lesions can cause mutations or chromosome rearrangements that affect genome stability and can lead to premature aging, neurological disorders or diseases such as cancer. Molecular mechanisms have evolved to signal and repair these lesions, collectively referred to as the DNA damages response (DDR). In a genetic screen performed to investigate the interactions between DDR factors under various DNA damaging conditions, we found that the DNA repair gene, SAE2, negatively interacts with a protein phosphatase encoding gene, PPH3. Here, we attempted to understand how this DNA repair factor and protein phosphatase interact to coordinate the signaling and repair of DNA damage. We found that cells deficient for SAE2 and PPH3 display severe checkpoint defects in response to DNA damage. Moreover, the repair of DNA damage induced by the alkylating agent MMS was impaired in these cells, whereas that of nuclease-induced DNA double stranded breaks remained unaffected when compared to that in the repair-deficient *sae2Δ* cells. We propose that the co-operation between Sae2 and Pph3 is important for efficient DNA repair and checkpoint activation in response to replication fork-associated damage induced by MMS, but is dispensable for DSB repair.

## INTRODUCTION

DNA double-stranded breaks (DSB) belong to the most deleterious type of DNA lesions. They can arise naturally during normal cellular processes such as DNA replication, or V(D)J recombination. However, DSB can also be induced exogenously by exposure of cells to agents such as ionizing radiation. If left unrepaired or repaired inaccurately, these lesions can lead to chromosome rearrangements or chromosome loss, which are hallmarks of diseases such as cancer.

To protect the genome, cells have evolved checkpoint pathways that signal the presence of DNA lesions and coordinate DNA repair and cell cycle progression. This orchestration is regulated by cascades of phosphorylation events that are initiated by the two key checkpoint kinases, Mec1 and Tel1 (ATR and ATM in mammals). The immediate consequence of Mec1/Tel1 activation is the apparition of stretches of phosphorylated histone H2A ( $\gamma$ H2AX) surrounding the DSB, that are thought to facilitate recruitment of repair factors such as chromatin remodeling complexes [1, 2]. The repair of DSBs involves either of two conserved mechanisms: non-homologous end joining (NHEJ) or homologous recombination (HR). During NHEJ the broken ends are religated in either an error-prone or error-free manner (reviewed in [3]). HR, on the other hand, uses homologous sequences, often present on sister chromatids, to copy the information required to seal the break in an error-free manner (reviewed in [4]).

A key step during HR is the 5'-3' degradation of the broken ends, generating 3' single-strand overhangs (ssDNA) that are rapidly coated with replication protein A (RPA). End-resection is initiated through the activities of the Sae2 and Mre11 nucleases, the latter of which is a member of the Mre11/Rad50/Xrs2 complex (MRX) (reviewed in [5]). MRX binds the ends and once activated by Sae2 proceeds with a clipping step that

results in the formation of short 3' single-strand DNA overhang ready to be further processed by the exonuclease Exo1 or the helicase Sgs1 and its associated nuclease Dna2 [6]. In the subsequent step of HR, RPA is replaced by Rad51 protein on the ssDNA overhangs, leading to formation of Rad51 nucleoprotein filaments. This filament catalyzes the search for homologous sequences and promotes strand invasion and heteroduplex formation. DNA synthesis occurs to copy the undamaged homologous template sequence and seal the break (see introduction, Box 6).

The end-resection step is not only important for the initiation of DSB repair by HR, but also triggers DNA damage checkpoint activation. If repair fails, continuous formation of ssDNA coated with RPA leads to accumulation of Mec1 at the site of damage [7]. The signal is then amplified and transmitted to the downstream effector kinases Rad53, Chk1 and Dun1, which activate cell cycle regulators such as Pds1, Cdc5, or Cdc20 to slow down or stop the cell cycle and inhibit mitotic exit until repair has been completed [8, 9]. Once repair is completed, de-activation of the checkpoint is necessary to allow cells to re-enter the cell cycle. Recently, it was found that the phosphatase Pph3/Psy2 contributes to this process by de-phosphorylating  $\gamma$ H2AX and Rad53 [10, 11]. However, how checkpoint de-activation is coordinated with DSB repair is still a poorly understood issue.

In a screen performed to map changes in genetic interactions that occur upon various genotoxic insults, we found SAE2 as one of the genes that displayed the greatest number of interactions. Interestingly, PPH3 was found among SAE2's interacting genes, suggesting a novel functional link between these factors. Here, we show that Sae2 and Pph3 co-operate to regulate checkpoints and DNA repair in response to replication-associated damage induced by MMS.

## RESULTS

As a mean to characterize interactions between DDR factors, we performed a genetic screen developed to measure the genetic interactions between pairs of genes [12]. 55 Query strains carrying deletions in different DDR genes were crossed to an array of 2022 strains that carry mutations in genes encoding factors involved in for instance cell cycle regulation, transcription, DNA replication and chromatin remodeling. To specifically explore the rewiring of genetic interactions under genotoxic conditions, we exposed the collection of double mutants to three distinct DNA damage agents: the DNA alkylating agent methyl methanesulfonate (MMS), the topoisomerase-1 inhibitor camptothecin (CPT) and the DNA intercalating antibiotic zeocin (ZEO), which induce different types of DNA lesion (Chapter 1). Strikingly the genetic interaction patterns induced by each drug were very specific (Chapter 1, figure 4A), suggesting that each drug induces a unique response to DNA damage (Chapter 1, figure 4C).

Genes with the most interactions in a genetic network are called hubs. One of them was SAE2, which encodes for the yeast homolog of the human endonuclease CtIP, known for its role in the processing of DSBs into 3' single-stranded tails [6]. Consistent with this role, we noted that the majority of SAE2's interactions (~60%) were induced specifically in response to the DSB-inducing agent CPT (Figure 1A). Moreover, SAE2 was found to interact positively with many known repair factors, including SGS1, TOP1, YKU70, and YKU80 (Figure 1B). Surprisingly, we also observed differential negative interactions between SAE2 and genes encoding for components of the PP4 complex (PPH3 and PSY2) not only in response to CPT, but also to MMS (Figure 1C). The PP4 complex is required for de-phosphorylation of the major checkpoint

kinase Rad53 and the subsequent recovery from DNA damage-induced cell cycle arrest [11], suggesting that Sae2 may work in parallel with PP4 in checkpoint deactivation.

To further explore this hypothesis, we profiled both the *pph3Δ* and *sae2Δ* single mutants as well the *sae2Δpph3Δ* double mutant for passage through the cell cycle following arrest in G1 and transient exposure to MMS. While *pph3Δ* cells showed a slightly slower progression through S-phase and a delay in the G2/M transition, *sae2Δ* cells only displayed a slightly more pronounced delay in progression through G2/M-phase compared to wild-type (Figure 2A). The double mutant, however, displayed a markedly slower progression through S-phase and arrested during the G2/M-transition, indicating that cells lacking Sae2 and Pph3 fail to efficiently deactivate the checkpoint (Figure 2A, Figure 3D). This finding was further confirmed when we monitored the activation by phosphorylation of Rad53 kinase. Indeed hyper-phosphorylated forms of Rad53 persisted for as long as ~five hours in the *sae2Δpph3Δ* double mutant (Figure 2B) whereas either single mutant showed complete de-phosphorylation at two hours after release from MMS. Noticeably, the *sae2Δpph3Δ* mutant already showed activation of Rad53 in unchallenged conditions, indicating a constitutively (although moderately) active checkpoint in these cells (Figure 2B).

To test whether the checkpoint hyper-activation in *sae2Δpph3Δ* cells is due to a repair defect, we monitored the assembly of the Rad52 repair protein into DNA damage-induced subnuclear foci, which are thought to represent active repair centers [13] (Figure 3A-B; [14]). Importantly, all strains equally accumulated RAD52 foci (maximum number of Rad52 foci comparable one hour after treatment), which attested that they

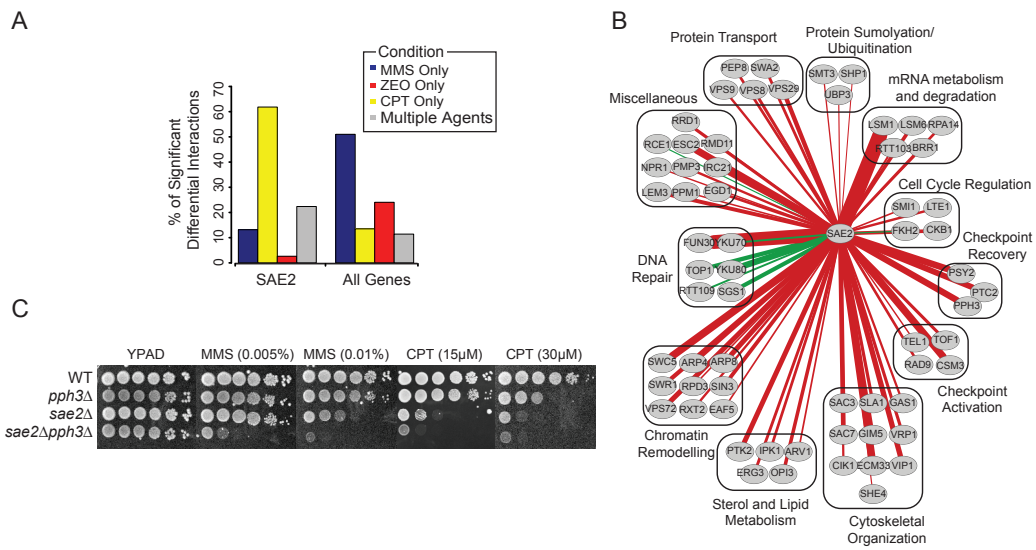


**Figure 1. Sae2 and Pph3 Negatively Interact in Presence of DNA Damage** (A) Percentage of SAE2's significant differential interactions in response to MMS, CPT, ZEO or multiple agents. As a control, the average percentage of significant differential interactions in each category across all genes is shown. (B) Network of all 64 significant positive (green edges) or negative (red edges) differential interactions with SAE2 in response to CPT. Thickness of the edge scales with significance of the interaction. (C) Viability of *sae2Δpph3Δ* cells is impaired in the presence of CPT and MMS-induced damages. 10-fold serial dilutions of WT, *sae2Δ*, *pph3Δ*, and *sae2Δpph3Δ* cells were grown on YPAD containing the indicated concentration of MMS or CPT.

6

were all similarly proficient in assembling the repair machinery (Figure 3C). However, four hours after exposure to MMS, both wild-type and single mutants were found to have largely completed repair (10% of

wild-type and *pph3Δ* cells and 20% of *sae2Δ* cells displaying Rad52 foci). In contrast, a large proportion (42%) of the *sae2Δpph3Δ* cells still displayed Rad52 foci, indicating a reduced repair capacity (Figure 3B-D).

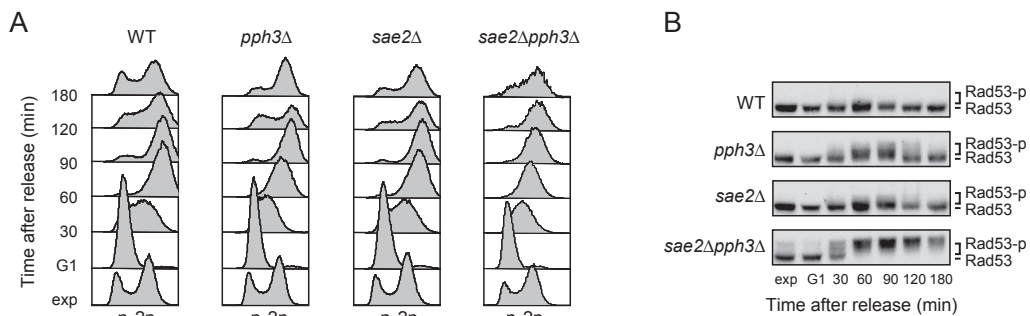


**Figure 2. *sae2Δpph3Δ* cells display abnormal checkpoint activation in the presence of MMS-induced lesions** (A) Exponentially (exp) growing wild-type (WT), *sae2Δ*, *pph3Δ*, *sae2Δpph3Δ* cells were arrested in G1 with  $\alpha$ -factor and treated 30 min with 0.02% MMS before release in fresh medium. Samples were taken at the indicated time points and analyzed by FACS as described in the Methods. (B) Western blot analysis of Rad53 phosphorylation in WT, *pph3Δ*, *sae2Δ*, *sae2Δpph3Δ* mutants following treatment described in (A).

To further confirm that the checkpoint hyper-activation seen in *sae2Δpph3Δ* cells may be due to a repair defect, we employed the YMV80 strain. In this strain, a single DSB, which is generated by a galactose-inducible HO endonuclease, is repaired by the single strand-annealing (SSA) (Figure 4A, [15]). We found that *sae2Δpph3Δ* cells were more sensitive to DSB induction by HO than either single mutant, which recapitulated the cell survival phenotype previously observed after MMS-induced damage (Figure 4B). Consistent with our previous observation (Figure 2B), we found that Rad53 already became (moderately) activated in *sae2Δpph3Δ* cells prior to DSB induction by

HO (Figure 4C). Interestingly, Rad53 was activated much faster in response to a single DSB in *sae2Δpph3Δ* cells compared to wild-type, *pph3Δ*, and *sae2Δ* cells (activation seen at one hour in *sae2Δpph3Δ*, compared to three hours in wild-type, *pph3Δ*, and *sae2Δ* cells). Moreover, Rad53 remained activated up to thirteen hours after break induction in the double mutant, while wild-type and single mutants had already fully recovered (Figure 4C). This checkpoint defect is further supported by the very slow S-phase progression and G2 arrest observed in *sae2Δpph3Δ* cells after HO break induction (Figure 4D). Thus, Sae2 and Pph3 cooperate to regulate a proper checkpoint response

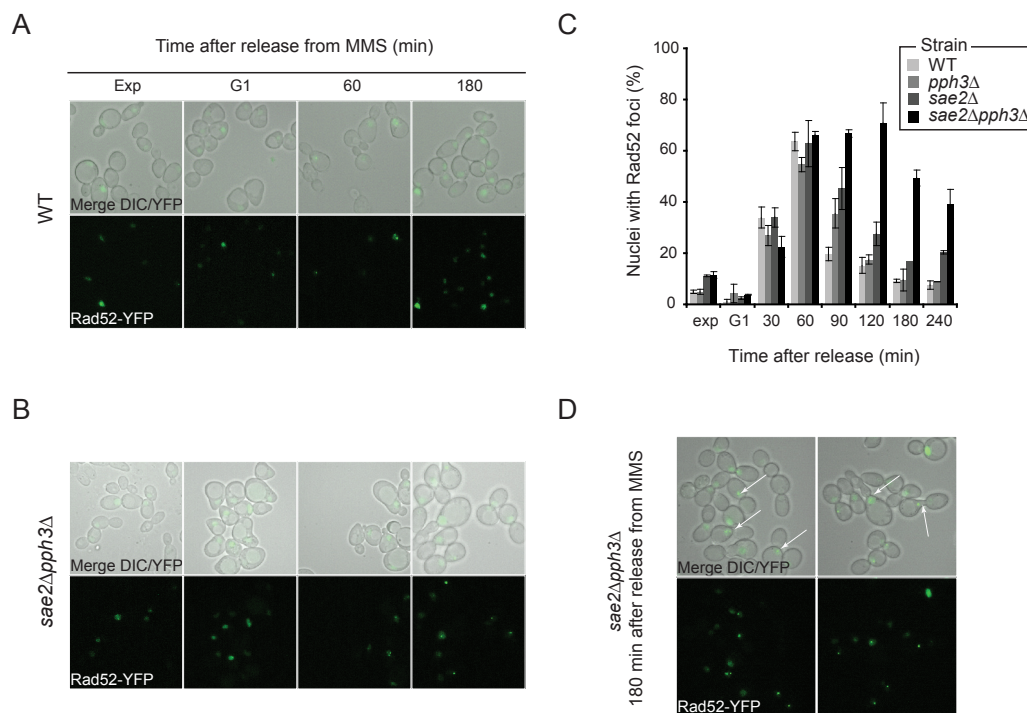


**Figure 3. Dissolution of Rad52-foci is impaired in the absence of Sae2 and Pph3** (A) Wild-type and (B) *sae2Δpph3Δ* cells expressing Rad52-YFP were arrested in G1 with  $\alpha$ -factor and treated 30 min with 0.02% MMS before release in fresh medium. (C) Quantitative analysis of Rad52-YFP foci in WT, *sae2Δ*, *pph3Δ*, *sae2Δpph3Δ* cells treated as in (A-B). Images were taken at the indicated time points and scored for Rad52-YFP foci. At least 100 nuclei were analyzed per strain and per time point. Data represent the mean  $\pm$  1 s.d. from three independent experiments. (D) *sae2Δpph3Δ* cells expressing Rad52-YFP were treated as in (B). Only the 180 minutes time point after release is shown to highlight cells with a 2 budded-cell shape and one undivided nucleus at the bud neck which still contains Rad52 foci.

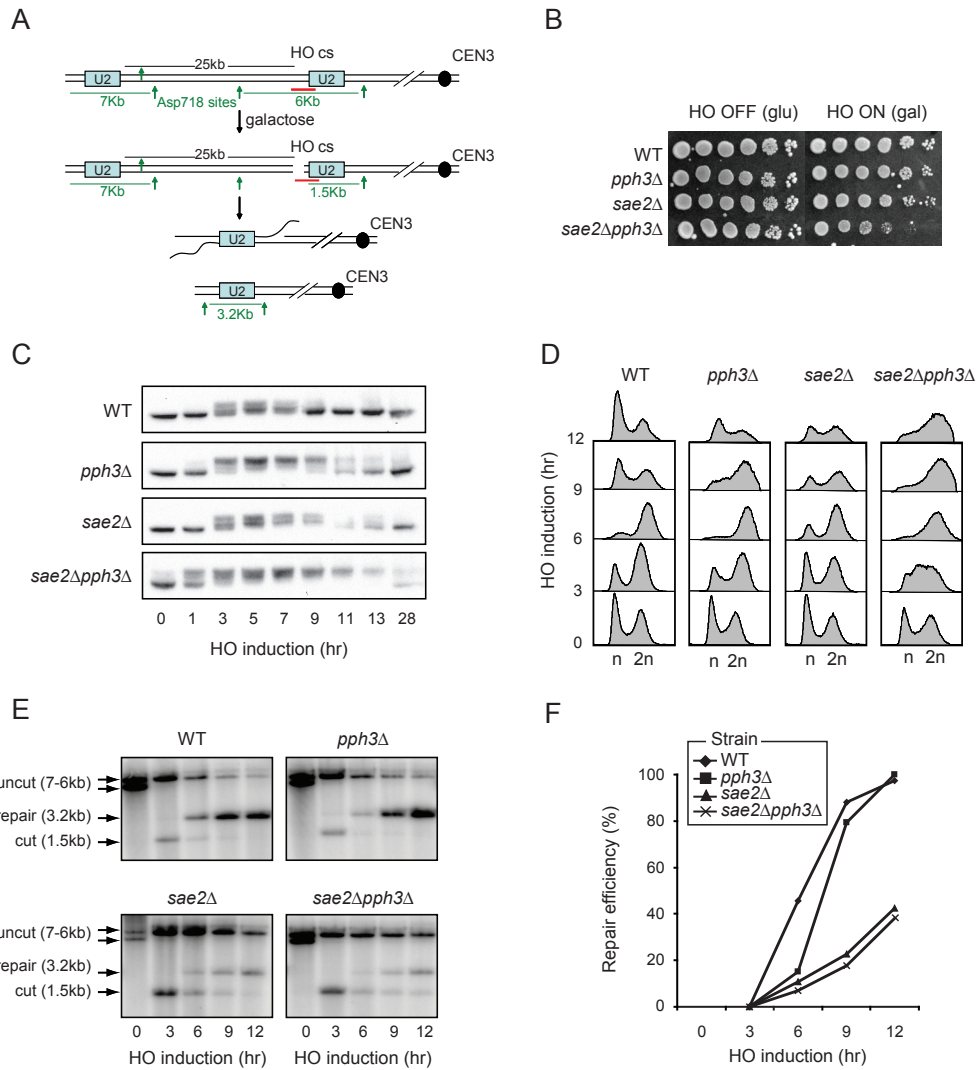


**Figure 4. *sae2Δpph3Δ* cells display abnormal checkpoint activation after an HO-induced DNA double strand break** (A) Schematic of the HO double strand break (DSB) induction system used to measure repair by single strand annealing (SSA) in the yHA-111 or YMV80 strain. A single DSB is induced by a galactose-inducible HO endonuclease. The DSB is repaired by SSA between the two LEU2 genes that flank the DSB site and that are separated by 25kb of intervening DNA sequences. The SSA repair product is detected by southern blot analysis using a 1.5kb probe covering the HO site and 5'end of the MAT proximal LEU2 gene. The probe recognizes 7kb and 6kb fragments before HO break induction, a 1.5kb cut product after HO induction and before extensive resection and a 3.5kb repair product after end-resection and successful SSA between the two LEU2 genes. (B) Viability of *sae2Δpph3Δ* cells is impaired in the presence of a single HO-induced DSB. 10-fold serial dilutions of log-phase cells of the indicated genotypes were spotted onto YPLG plates containing 2% glucose (HO-OFF) or 2% galactose (HO-ON) and incubated for 3 days at 30°C. (C) *sae2Δpph3Δ* cells show delayed S-phase progression and arrest during the G2/M transition in response to a single HO-induced DSB. The HO endonuclease was expressed by addition of 2% galactose to log-phase cultures of WT, *sae2Δ*, *pph3Δ*, *sae2Δpph3Δ* cells. Samples were taken for FACS analysis at the indicated time points. (D) Rad53 is hyper-phosphorylated in *sae2Δpph3Δ* cells. In the experiment described in (D), samples were taken at the indicated time points for western blot analysis of Rad53 phosphorylation. (E) Repair by single strand annealing (SSA) is similarly impaired in *sae2Δpph3Δ* as in *sae2Δ* cells. SSA repair product was detected in YMV80-derived strains by southern blot analysis at the indicated timepoints after HO induction. (F) The repair efficiency was determined (see Methods).

after MMS- and HO endonuclease-induced DNA damage.

We next assessed the formation of the SSA repair product by southern blot analysis (Figure 4E-F). While repair became detectable at six hours and was completed at twelve hours after HO induction in wild-type and *pph3Δ* cells, *sae2Δ* and *sae2Δpph3Δ* cells displayed a similar delay in repair (repair became detectable at 9h after HO induction and was not yet completed at 12h). This data suggests that the checkpoint hyper-activation observed in *sae2Δpph3Δ* cells may not be caused by defects in DSB repair. Moreover, it seems that the co-operative role of Sae2 and Pph3 in checkpoint regulation can be uncoupled from that in DNA repair (Figure 4E-F).

Finally, to investigate the difference in contribution of Sae2 and Pph3 to the repair of MMS- and HO endonuclease-induced DNA damage, we evaluated their effect on the processing of DNA lesions. To this end, we over-expressed the exonuclease Exo1 in *sae2Δ* and *sae2Δpph3Δ* cells and induced DNA damage by MMS or HO expression (Figure 5A-B). Exo1 plays an important role in promoting long-range resection of broken

DNA ends and its over-expression has been reported to rescue the end-resection and survival defects of *Sae2*-deficient cells [6, 16]. Accordingly, we found that over-expression of wild-type but not nuclease-dead Exo1 rescued the MMS sensitivity of *sae2Δ* cells to wild-type levels. However, only a partial rescue of this phenotype was seen in *sae2Δpph3Δ* cells (Figure 5A). On the other hand, overexpression of wild-type but not catalytic-dead Exo1 in *sae2Δpph3Δ* cells fully rescued their sensitivity to HO-induced DSBs (Figure 5B). Collectively, this suggests that the end-resection defect in *sae2Δpph3Δ* cells likely explains the sensitivity of these cells to HO-induced DSBs, whereas the MMS sensitivity of *sae2Δpph3Δ* could reflect defects in both end-resection and Rad53 de-phosphorylation. This also implies that the co-operative role of Sae2 and Pph3 is more important in response to replication-associated DNA lesions than to (nuclease-induced) DSBs.

## DISCUSSION

The functional analysis of the negative interaction between SAE2 and PPH3 revealed that cells lacking Sae2 and Pph3 have three characteristic DNA damage

6

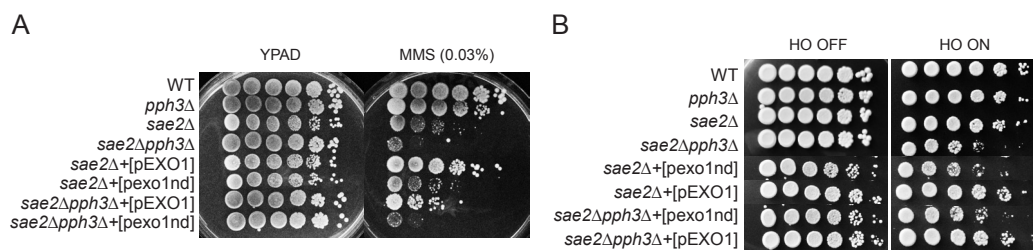


**Figure 5. Restoration of end-resection partially rescues the sensitivity of *sae2Δpph3Δ* cells to DNA damage** (A) Impaired viability of *sae2Δpph3Δ* cells is not fully rescued by Exo1 over-expression in the presence of MMS-induced damages. 10-fold serial dilutions of WT, *sae2Δ*, *pph3Δ* and *sae2Δpph3Δ* cells were grown on YPAD containing the indicated concentration of MMS. In the last four lanes *sae2Δ* and *sae2Δpph3Δ* cells that over-express Exo1 or nuclease-dead Exo1 from pEXO1 and pExo1nd, respectively. (B) Impaired viability of *sae2Δpph3Δ* cells is not fully rescued by Exo1 over-expression in the presence of an HO double strand break. 10-fold serial dilutions of WT, *sae2Δ*, *pph3Δ*, and *sae2Δpph3Δ* cells were grown on YPLGg plates containing 2% glucose (HO-OFF) or 2% galactose (HO-ON). In the last four lanes *sae2Δ* and *sae2Δpph3Δ* cells over-express wild-type Exo1 or nuclease-dead Exo1 from pEXO1 and pExo1nd, respectively.



checkpoint defects. First, *sae2Δpph3Δ* cells do not inactivate their checkpoint after induction of DNA damage. After MMS exposure, we found that Rad52 foci dissolution was much slower in *sae2Δpph3Δ* cells than in either single mutant, implying that these cells are impaired in DNA repair (Figure 3). Thus, in these cells the absence of checkpoint recovery could result from a repair defect (Figure 2 and 3). The repair defect can be caused by the absence of Sae2's activity in processing MMS-induced lesions, which may be critical in the absence of Pph3. However, after induction of a single DSB, the extent to which repair was delayed in the double mutant was similar to that observed in the *sae2Δ* mutant, yet only the latter strain recovered from checkpoint arrest (Figure 4C-E). This suggests that besides its role in end-resection Sae2 also has a role in checkpoint recovery, which becomes of importance in the absence of Pph3. In the case of a DSB, it was proposed that Mec1 and Tel1 phosphorylate Sae2, which in turn may inhibit the MRX-dependent association of Mec1 and Tel1 with DSBs and abrogate the DNA damage checkpoint [17]. The combined absence of Rad53 dephosphorylation and of Sae2-dependent checkpoint inhibition (through Mec1 and Tel1 dissociation from DSBs) may result in the checkpoint recovery defect observed in *sae2Δpph3Δ* cells.

The second interesting checkpoint feature of *sae2Δpph3Δ* cells is the low but constitutive level of Rad53 phosphorylation observed in exponentially growing unchallenged cells. A previous study has demonstrated that in unchallenged S-phase cells the lack of Sae2 induces endogenous damage that triggers Mre11 phosphorylation (which could lead to checkpoint activation) [17]. On the other hand, it is possible that Pph3 constitutively de-phosphorylates Rad53 to prevent its hyper-phosphorylation. The loss of

Pph3 could therefore lead to low (yet undetectable) levels of activated Rad53 in unchallenged cells. Consistent with this idea, in mammalian cells, constitutive phosphorylation of Chk1 by ATR/Mec1 is reversed by the phosphatase PP2A in the presence and absence DNA damage [18]. Eventually, both the induction of endogenous damage and the inability to de-phosphorylate Rad53 efficiently may have led to the mild (detectable) checkpoint signal in unchallenged *sae2Δpph3Δ* cells.

The third intriguing checkpoint phenotype is the rapid checkpoint activation after DSB induction and MMS-induced damage. In line with the idea that *sae2Δpph3Δ* cells have a low constitutively active checkpoint, it is likely that a low dose of damage is enough to accumulate phosphorylated forms of Rad53. In addition Clerici et al. found that Sae2 negatively regulates checkpoint activation by preventing recruitment of the MRX complex to sites of DSBs [19]. The low threshold for Rad53 activation and the lack of negative regulation of the checkpoint could explain the activation of Rad53 observed rapidly after DNA damage induction.

Further analysis of the *sae2Δpph3Δ* phenotype showed that Exo1 over-expression was sufficient to rescue cell survival to wild-type levels in response to a DSB, while the rescue effect was only partial after exposure to MMS. This could indicate that the end-resection defect is mainly responsible for the sensitivity of *sae2Δpph3Δ* cells to a single DSB, while it does not fully explain the hypersensitivity of *sae2Δpph3Δ* cells to MMS-induced damage. A previous report showed that the two phosphatases Ptc2 and Ptc3 can also de-phosphorylate Rad53 and as such promote checkpoint recovery after DSB repair [20]. This could explain why the compensation in end-resection is sufficient for *sae2Δpph3Δ*

Sae2 and Pph3 cooperate to promote DNA repair and checkpoint recovery

cells to better survive a DSB, a situation in which the lack of Pph3 may potentially be taken over by Ptc2 and Ptc3 activities (Figure 5B). However, in S-phase, when DNA replication is perturbed, Rad53 activation and deactivation is critical for cells to restart and complete replication after repair. Rad53 activation inhibits firing of late origins of replication to facilitate DNA repair prior to arrival of the fork. On the other hand, Rad53 deactivation allows replication forks to restart in cells that have repaired their DNA [21]. Pph3 is the main phosphatase that deactivates Rad53, which implies that its activity is particularly crucial in S-phase. Consequently, constant Rad53 activation may block DNA replication in *sae2Δpph3Δ* cells. The incompletely replicated DNA could lead these cells to arrest at the G2/M transition with undivided nuclei (Figure 3B-D). It may be that the persistence of Rad52 foci in these cells reflects their inability to complete replication rather than repair (Figure 3B-D). The critical role of Pph3 in helping fork restart in cells having a perturbed S-phase may explain why additional end-resection activity is not enough to rescue survival of *sae2Δpph3Δ* cells to MMS.

To investigate further the link between checkpoint activation, end-resection and DNA repair in *sae2Δpph3Δ* cells, it would be interesting to know how Exo1 over-expression affects Rad53 phosphorylation as well as DNA repair. It is feasible that DNA repair is more efficient, thereby leading to attenuation of checkpoint activation, which may be enough for *sae2Δpph3Δ* cells to overcome the presence of DSBs, but not MMS-induced lesions.

## MATERIAL & METHODS

### *Cell survival assays*

Overnight cultures were diluted 1:20, grown for 3 h at 30 °C and diluted to  $1 \times 10^7$  cells/ml. 10-fold serial dilutions were spotted on

plates containing CPT or MMS and grown at 30 °C for 3 days.

### *Cell Cycle Profiling*

Exponentially growing cells were synchronized in G1 with  $\alpha$ -factor (7.5 $\mu$ M) and exposed to 0.02% MMS for 30 minutes after which cells were washed and released into fresh medium. Samples were taken every 30 min for 3h. Cells were stained with propidium iodide. Flow cytometry analysis was performed on a BD™ LSRII instrument. BD FACSDiva™ software was used for data analysis.

### *Checkpoint assays*

Exponentially growing cells were synchronized in G1 with  $\alpha$ -factor (7.5 $\mu$ M) and exposed to 0.02% MMS for 30 minutes after which cells were washed and released into fresh medium. Whole cell extracts were prepared for western blot analysis to examine Rad53 phosphorylation using an Anti-Rad53 (Santa-Cruz, sc-6749) antibody.

### *Analysis of Rad52 foci*

Cells containing a Rad52-YFP expression vector were synchronized in G1 with  $\alpha$ -factor (7.5 $\mu$ M) and exposed to 0.02% MMS for 30 minutes after which cells were washed and released into fresh medium. Cells were then washed and concentrated in 1% low melting agar (Cambrex) for Rad52-foci analysis. Images were captured using a Leica AF6000 LX microscope at 100-fold magnification using a HCX PL FLUOTAR 100x 1.3 oil objective lens.

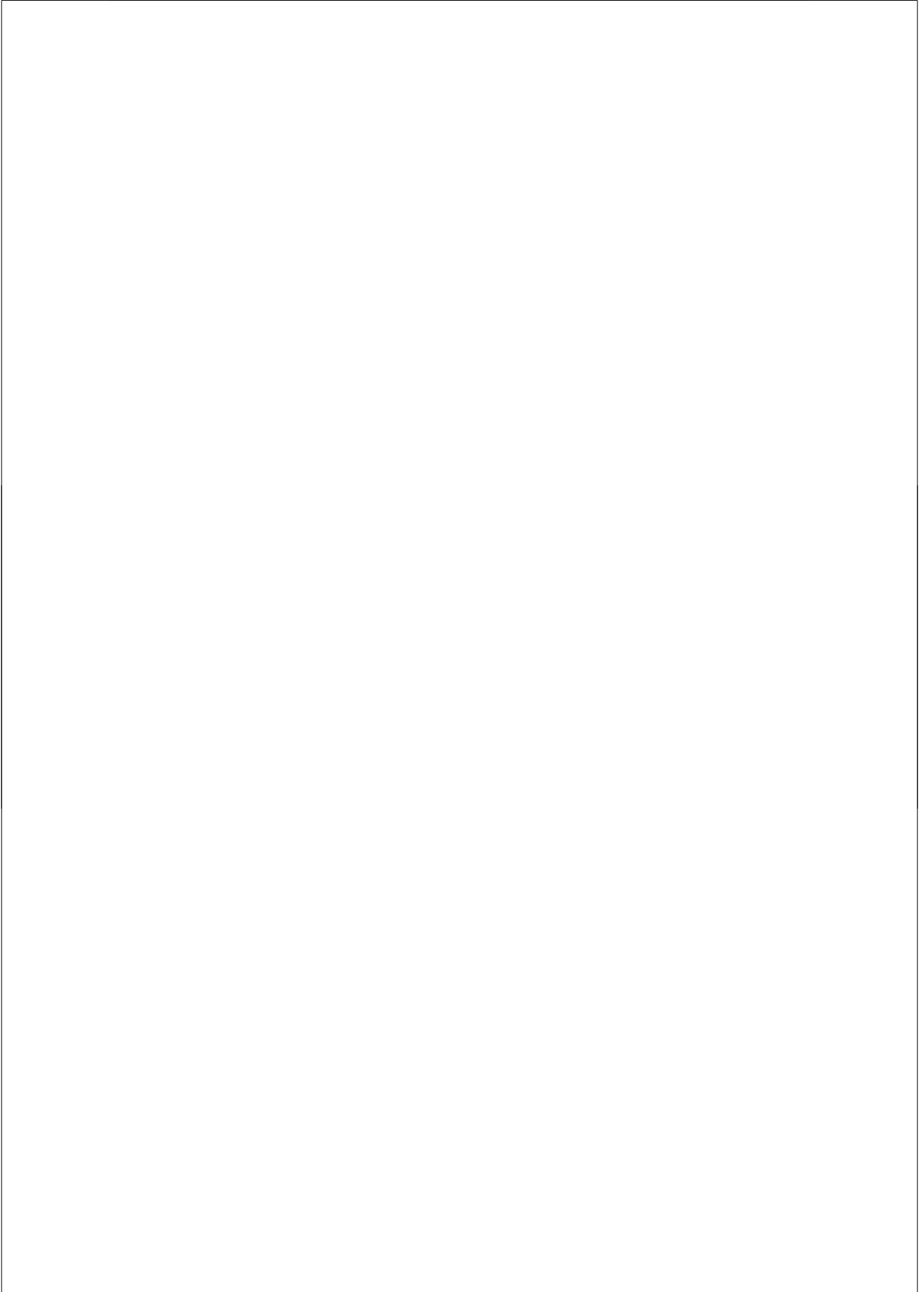
### *HO expression and Single strand annealing assay*

HO endonuclease was induced in the yHA-111 strain (also called YMV80; [15]) by adding 2% galactose to logarithmic-phase cultures ( $1 \times 10^7$  cells ml<sup>-1</sup>) grown in YPL-glycerol at 30°C. Genomic DNA was isolated at different time interval after HO induction,

digested with Asp718 restriction enzyme, separated on a 0.8% agarose gel and transferred to a nylon membrane (Hybond N+). The blot was probed with a  $^{32}\text{P}$ -labeled probe that was generated by PCR on genomic DNA using the forward primer oHA-921 (5'-ACGGGGATCTAAATAAATTC-3') and the reverse primer oHA-922 (5'-GGAGGTCGACTACGTCGTTAAG-3'). This probe detects a 1.5kb cut-product containing the LEU2 gene adjacent to the HO cut site (HOcs) on chromosome III before resection, or a 3.2kb product that covers the LEU2 gene and results from repair by SSA between the two LEU2 genes that flank the DSB site and that are separated by 25kb of intervening DNA sequences (see Figure 4A). The blots were analyzed by using the Cyclone® Plus Storage Phosphor System from PerkinElmer. The blots were quantified using the Quantity One® analysis software (by Bio-Rad). The repair efficiency was determined by measuring the intensity of the band reflecting the repair product. This was divided by the combined intensities of the bands for uncut, cut and repair products, and normalized to the cut efficiency, which is the intensity of the cut-product divided by the combined signals from cut and uncut bands.

## REFERENCES

1. Celeste, A., et al., Histone H2AX phosphorylation is dispensable for the initial recognition of DNA breaks. *Nat Cell Biol*, 2003. 5(7): p. 675-9.
2. van Attikum, H., O. Fritsch, and S.M. Gasser, Distinct roles for SWR1 and INO80 chromatin remodeling complexes at chromosomal double-strand breaks. *EMBO J*, 2007. 26(18): p. 4113-25.
3. Daley, J.M., et al., Nonhomologous end joining in yeast. *Annu Rev Genet*, 2005. 39: p. 431-51.
4. San Filippo, J., P. Sung, and H. Klein, Mechanism of eukaryotic homologous recombination. *Annu Rev Biochem*, 2008. 77: p. 229-57.
5. Mimitou, E.P. and L.S. Symington, DNA end resection: many nucleases make light work. *DNA Repair (Amst)*, 2009. 8(9): p. 983-95.
6. Mimitou, E.P. and L.S. Symington, Sae2, Exo1 and Sgs1 collaborate in DNA double-strand break processing. *Nature*, 2008. 455(7214): p. 770-4.
7. Lee, S.E., et al., *Saccharomyces* Ku70, mre11/rad50 and RPA proteins regulate adaptation to G2/M arrest after DNA damage. *Cell*, 1998. 94(3): p. 399-409.
8. Agarwal, R., et al., Two distinct pathways for inhibiting pds1 ubiquitination in response to DNA damage. *J Biol Chem*, 2003. 278(45): p. 45027-33.
9. Liang, F. and Y. Wang, DNA damage checkpoints inhibit mitotic exit by two different mechanisms. *Mol Cell Biol*, 2007. 27(14): p. 5067-78.
10. Keogh, M.C., et al., A phosphatase complex that dephosphorylates gammaH2AX regulates DNA damage checkpoint recovery. *Nature*, 2006. 439(7075): p. 497-501.
11. O'Neill, B.M., et al., Pph3-Psy2 is a phosphatase complex required for Rad53 dephosphorylation and replication fork restart during recovery from DNA damage. *Proc Natl Acad Sci U S A*, 2007. 104(22): p. 9290-5.
12. Collins, S.R., et al., A strategy for extracting and analyzing large-scale quantitative epistatic interaction data. *Genome Biol*, 2006. 7(7): p. R63.
13. Alvaro, D., M. Lisby, and R. Rothstein, Genome-wide analysis of Rad52 foci reveals diverse mechanisms impacting recombination. *PLoS Genet*, 2007. 3(12): p. e228.
14. Lisby, M., R. Rothstein, and U.H. Mortensen, Rad52 forms DNA repair and recombination centers during S phase. *Proc Natl Acad Sci U S A*, 2001. 98(15): p. 8276-82.
15. Vaze, M.B., et al., Recovery from checkpoint-mediated arrest after repair of a double-strand break requires Srs2 helicase. *Mol Cell*, 2002. 10(2): p. 373-85.
16. Mimitou, E.P. and L.S. Symington, Ku prevents Exo1 and Sgs1-dependent resection of DNA ends in the absence of a functional MRX complex or Sae2. *EMBO J*, 2010. 29(19): p. 3358-69.
17. Baroni, E., et al., The functions of budding yeast Sae2 in the DNA damage response require Mec1- and Tel1-dependent phosphorylation. *Mol Cell Biol*, 2004. 24(10): p. 4151-65.
18. Leung-Pineda, V., C.E. Ryan, and H. Piwnicka-Worms, Phosphorylation of Chk1 by ATR is antagonized by a Chk1-regulated protein phosphatase 2A circuit. *Mol Cell Biol*, 2006. 26(20): p. 7529-38.
19. Clerici, M., et al., The *Saccharomyces cerevisiae* Sae2 protein negatively regulates DNA damage checkpoint signalling. *EMBO Rep*, 2006. 7(2): p. 212-8.
20. Leroy, C., et al., PP2C phosphatases Ptc2 and Ptc3 are required for DNA checkpoint inactivation after a double-strand break. *Mol Cell*, 2003. 11(3): p. 827-35.
21. Szyjka, S.J., et al., Rad53 regulates replication fork restart after DNA damage in *Saccharomyces cerevisiae*. *Genes Dev*, 2008. 22(14): p. 1906-20.







### **Towards understanding the DDR network**

Previous work integrating protein interaction and genome-phenotyping data (which identify gene products that affect particular phenotypes such as sensitivity or resistance to DNA damaging compounds) has revealed connections between multiple pathways either related or unrelated that are required for cells to cope with DNA damage [1]. Thus, besides signaling and DNA repair pathways or transcription and chromatin remodeling, other processes such as RNA and protein metabolisms, protein transport or cytoskeleton organization appear to play key roles in response to DNA damage. One edifying example is the role of the proteasome, which degrades proteins to regulate cellular functions. It was found in numerous studies that the proteasome regulates the levels of DNA repair and transcription factors and thereby affects repair pathway choices [2-4].

In our analysis of the DDR network (Chapter 1, Figure 5) we also observed that the proteasome highly responds to DNA damage and engages connections with DNA damage signaling, chromatin remodeling or E2 ubiquitin-conjugating complexes. More challenging, we found new connections implicating pathways that were not yet identified to function in the DDR. For example, the SET3 histone deacetylase complex involved in transcription shows MMS-induced interactions with the E2 ubiquitin-conjugating Mms2-Ubc13 complex, which has been implicated in error-free post-replication repair. In addition, the membrane-associated retromer complex known to be essential for the endosome to golgi retrograde vesicle transport, is strongly connected to the DNA damage signaling 9-1-1 complex in response to camptothecin. In line with this, it was already suggested that the DNA damage checkpoint response involves cytoplasmic

processes to regulate cell cycle progression in presence of DNA damage. More recently, a study reported that mutations in the golgi-associated retrograde protein complex (GARP) block checkpoint adaptation and recovery in the presence of an irreparable DSB [5].

Interestingly, in human cells the golgi protein GOLPH3 was recently characterized as an oncogene [6]. In that particular study, the authors used yeast data from a large-scale chemical genomic profiling approach (which identify gene products that affect particular phenotypes such as sensitivity or resistance to chemicals) to connect GOLPH3 to the retromer complex, the mTOR signaling pathway and the response to rapamycin [7]. The common genetic network induced by MMS and CPT too revealed a link between the DDR and the mTOR pathway likely mediated by the cytochrome b5-like protein Irc21 (Chapter 4).

This clearly demonstrates that the connections between cellular processes that are triggered by DNA damage are conserved among eukaryotes and strengthens the utility of yeast data to further understand the human DDR. However, functional studies on the intriguing and unanticipated connections between these processes during the DDR are required to fully understand their relevance for DNA damage signaling and repair, as well as their utility for targeted anti-cancer strategies.

### **From yeast genetics to personalized cancer therapy**

The genetic instability leading to the onset of cancer originate in part from mutations in genome caretaker pathways such as cell cycle control, DNA damage signaling and repair. Yeast has been successfully used as a model organism to identify and dissect these key genetic pathways. The high similarities between yeast and mammalian cellular



processes and the ability to study the effect of a single gene deletion are characteristics that make yeast a perfect tool in cancer research.

Moreover, the recent development of genome-wide screening approaches led the yeast experimentations to focus on the findings of new drugs that would have therapeutic effects and new targets of these drugs [8]. For example, screening standard chemotherapeutic agents exploiting the yeast deletion library (a collection of nonessential gene disruption mutants covering the whole yeast genome) uncovered pathways that are required to protect cells against the toxic effects of these anticancer drugs [9]. The human homologues or orthologs of these genes when mutated in cancers are likely to specifically render cancer cells sensitive to the anticancer treatments. However, the fact that tumors tend to become resistance towards these targeted cancer treatments demands other strategies.

Another and complementary approach was to find synthetic lethal genes, whose combined mutations are lethal while neither single mutation is [10]. Conceivably, two genes may represent two redundant pathways that are necessary for cell survival, which implies that both pathways have to be inactivated to sensitize the tumor to treatment. Therefore, in human cancer, the combined inactivation of the orthologous genes may sensitize cells to anti-cancer drugs.

As a step forward in exploiting yeast genetics as a tool to study cancer, we merged the two genome-wide screening techniques described above. We successfully found DNA damage-induced synthetic lethal interactions between neddylation and checkpoints likely relevant in cancer as these interactions recapitulate

recent findings showing that neddylation inhibitors sensitize p53-deficient tumors to IR treatment (Chapter 3). Interestingly, in chapter 4, we depict a synthetic fitness interaction in which the combination of two mutations renders cells resistant to anti-cancer drugs. Extending these findings to the clinical context may help to understand the mechanisms of resistance that certain patients develop during the treatments.

We anticipate that our data contain essential information on gene deletions that are synthetic lethal in the absence or presence of (DNA damaging) anti-cancer drugs. This information can be very useful for a better understanding and elaboration of personalized cancer treatments.

#### **Linking EMAP approaches to promising anticancer targets**

Previous genome-wide genetic approaches demonstrated how genetic interactions can help to identify proteins that are in the same complex (positive interactions) or proteins that work in compensatory pathways (negative interaction) [11-14]. Besides identifying physical complexes, positive interactions were found to be successful at describing linear pathways such as those defined by enzymes and their substrates [15, 16]. Fiedler et al. observed an enrichment of positive interactions between kinases or phosphatases and their targets [15]. One explanation is that if the phosphorylation of a substrate is important for cellular growth, mutating the substrate and the kinase will not further affect cellular growth than either single mutation and give rise to a positive interaction (epistatic interaction). Thus, genetic interaction data can also inform on transient interactions, including those that are important for the post-translational modification of proteins [15, 16]. Indeed, our genetic screen allowed the identification of new proteins, such as Nhp10 and Mms22 that are regulated

by the yeast homologue of Nedd8, Rub1 (Chapter3) through neddylation.

In line with the aforementioned observations, we anticipate that epistatic interactions involving components of the neddylation pathway may help in finding other targets of neddylation. For example, in response to MMS, both RUB1 and RRI1, the latter encodes the Nedd8 de-neddylase (member of the COP9 signalosome), not only interact positively with other DNA repair factors such as RAD57, MMS2 or RMI1, but also with RPP2B and BUD21 components of the small ribosomal subunit, as well as with GIM3, PAC10 and YKE2, which are components of the prefoldin complex. This demonstrates that neddylation may for example impact on translational control or protein folding and that the EMAP is a powerful tool to identify and characterize the (de)neddylated proteins in these processes. Importantly, Fiedler et al. also found that two kinases working redundantly and affecting the same substrate are more likely to interact negatively (due to their redundant action on the same substrate). Extending this to the proteins involved in neddylation may help to find more cellular processes and proteins that are regulated by this pathway. Subsequently, biochemical and functional assays should confirm the neddylation status of the putative target proteins and the relevance of their modification for cellular processes, including the DDR.

In higher eukaryotes, the neddylation pathway is essential for cellular functions likely due to the fact that it regulates the activity of cullin-RING ubiquitin E3 ligases (CRL). Indeed, CRL targets are involved in various cellular processes such as DNA repair, cell cycle progression, cell growth and survival [17]. The expression of numerous CRL substrates such as the replication regulator Cdt-1 or the cell cycle

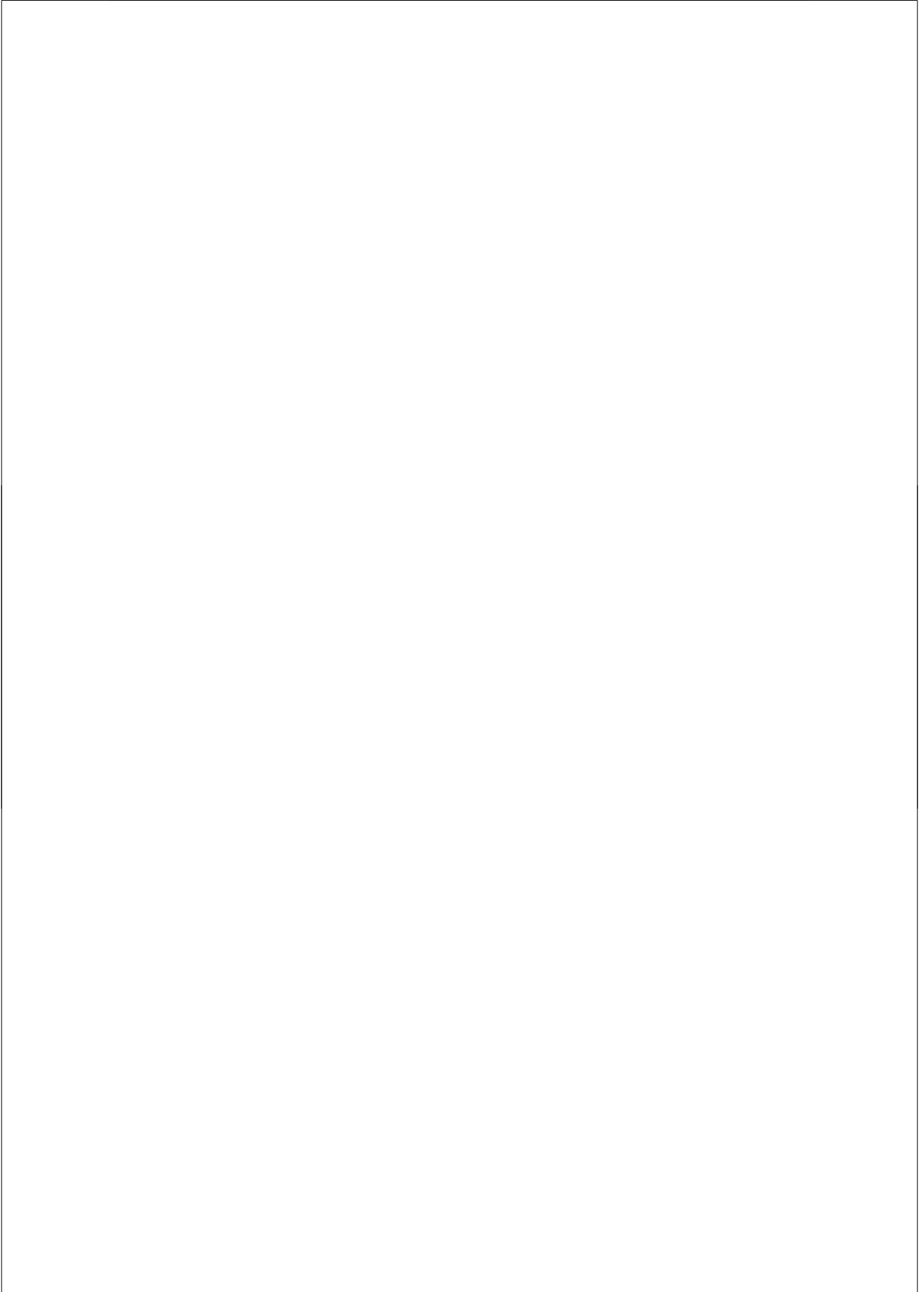
regulators cyclin E and p27 were found to be misregulated in various cancers. Although neddylation is largely known for controlling CRL activity, it was also found to modify the tumor suppressors p53 and VHL [18, 19]. Thus, it becomes clear that the neddylation pathway may be an attractive target for cancer treatment. Interestingly, MLN4924 an inhibitor of the Nedd8-activating enzyme (NAE) discovered by Millennium Pharmaceuticals, has recently been reported to be a potent anticancer drug. MLN4924-treated cells and human tumor xenografts were found to accumulate several CRL protein targets (e.g. NRF2, Cdt1 and p27). Importantly, tumor growth was inhibited in lung and colon tumor xenografts MLN4924-treated [20] and the phase 1 of a clinical trial with MLN4924 in patients with relapsed melanoma and non-hodgkin lymphoma demonstrated increased Cdt-1 levels in blood cells. Collectively these results suggest that MLN4924 may work as a potent anticancer drug by inhibiting protein neddylation and consequently the steady state levels of target proteins [20, 21]. Although promising in anticancer treatments, inhibitors of neddylation may have uncontrolled side effects due to the numerous cellular processes that neddylation regulates. Thus, it is critical to discover more, if not all neddylation targets to better understand the (side)effects of such inhibitors in cancer therapies. To this end, it will be of great importance to generate the neddylome under unchallenged conditions as well as after exposure to standard chemotherapeutic agents and that in both non-cancer and cancer cells. First, this will facilitate the finding of new targets of neddylation. Secondly, the new targets may aid to predict in which cases the patients can be treated with neddylation inhibitors in combination with standard anticancer drugs. For example, in MLN4924 treated cells, neddylation inhibition often leads to increased Cdt-1 levels, which induces

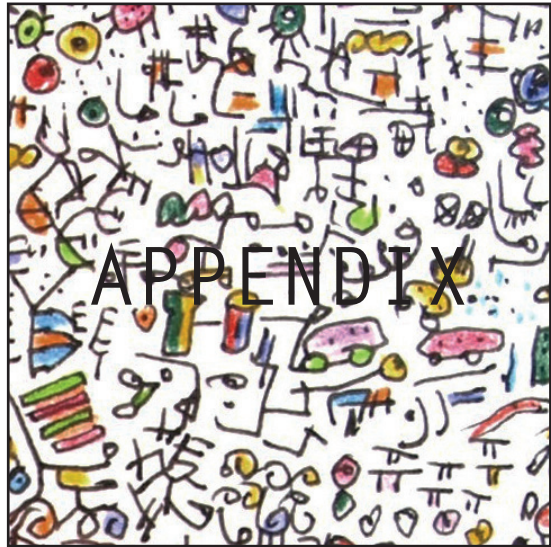
## Chapter 7

re-replication. Thus, combining MLN4924 treatment with a chemotherapeutic agent that blocks replication may lead to a reduced cell proliferation or increased apoptosis and in turn promote tumor growth inhibition in patients with elevated Cdt1 levels.

**REFERENCES**

1. Begley, T.J., et al., Damage recovery pathways in *Saccharomyces cerevisiae* revealed by genomic phenotyping and interactome mapping. *Mol Cancer Res*, 2002. 1(2): p. 103-12.
2. Ben-Aroya, S., et al., Proteasome nuclear activity affects chromosome stability by controlling the turnover of Mms22, a protein important for DNA repair. *PLoS Genet*, 2010. 6(2): p. e1000852.
3. Jelinsky, S.A. and L.D. Samson, Global response of *Saccharomyces cerevisiae* to an alkylating agent. *Proc Natl Acad Sci U S A*, 1999. 96(4): p. 1486-91.
4. Ju, D., et al., Inhibition of proteasomal degradation of rpn4 impairs nonhomologous end-joining repair of DNA double-strand breaks. *PLoS One*, 2010. 5(4): p. e9877.
5. Dotiwala, F., et al., DNA damage checkpoint triggers autophagy to regulate the initiation of anaphase. *Proc Natl Acad Sci U S A*, 2013. 110(1): p. E41-9.
6. Scott, K.L., et al., GOLPH3 modulates mTOR signalling and rapamycin sensitivity in cancer. *Nature*, 2009. 459(7250): p. 1085-90.
7. Xie, M.W., et al., Insights into TOR function and rapamycin response: chemical genomic profiling by using a high-density cell array method. *Proc Natl Acad Sci U S A*, 2005. 102(20): p. 7215-20.
8. Hartwell, L.H., Nobel Lecture. *Yeast and cancer*. *Biosci Rep*, 2002. 22(3-4): p. 373-94.
9. Lee, W., et al., Genome-wide requirements for resistance to functionally distinct DNA-damaging agents. *PLoS Genet*, 2005. 1(2): p. e24.
10. Pan, X., et al., A DNA integrity network in the yeast *Saccharomyces cerevisiae*. *Cell*, 2006. 124(5): p. 1069-81.
11. Kelley, R. and T. Ideker, Systematic interpretation of genetic interactions using protein networks. *Nat Biotechnol*, 2005. 23(5): p. 561-6.
12. Schuldiner, M., et al., Exploration of the function and organization of the yeast early secretory pathway through an epistatic miniarray profile. *Cell*, 2005. 123(3): p. 507-19.
13. Collins, S.R., et al., Functional dissection of protein complexes involved in yeast chromosome biology using a genetic interaction map. *Nature*, 2007. 446(7137): p. 806-10.
14. Roguev, A., et al., Conservation and rewiring of functional modules revealed by an epistasis map in fission yeast. *Science*, 2008. 322(5900): p. 405-10.
15. Fiedler, D., et al., Functional organization of the *S. cerevisiae* phosphorylation network. *Cell*, 2009. 136(5): p. 952-63.
16. Sharifpoor, S., et al., Functional wiring of the yeast kinome revealed by global analysis of genetic network motifs. *Genome Res*, 2012. 22(4): p. 791-801.
17. Tateishi, K., et al., The NEDD8 system is essential for cell cycle progression and morphogenetic pathway in mice. *J Cell Biol*, 2001. 155(4): p. 571-9.
18. Xirodimas, D.P., et al., Mdm2-mediated NEDD8 conjugation of p53 inhibits its transcriptional activity. *Cell*, 2004. 118(1): p. 83-97.
19. Stickle, N.H., et al., pVHL modification by NEDD8 is required for fibronectin matrix assembly and suppression of tumor development. *Mol Cell Biol*, 2004. 24(8): p. 3251-61.
20. Soucy, T.A., et al., An inhibitor of NEDD8-activating enzyme as a new approach to treat cancer. *Nature*, 2009. 458(7239): p. 732-6.
21. Soucy, T.A., P.G. Smith, and M. Rolfe, Targeting NEDD8-activated cullin-RING ligases for the treatment of cancer. *Clin Cancer Res*, 2009. 15(12): p. 3912-6.





*A  
p  
p  
e  
n  
d  
i  
x*

## NEDERLANDSE SAMENVATTING

De genetische informatie die nodig is voor de vorming en organisatie van cellulaire componenten ligt vast in onze genen. Het is daarom belangrijk voor het goed functioneren van alle cellen in het lichaam dat de genetische informatie intact blijft. Verschillende fysische en chemische agentia in het milieu (zoals UV-straling van de zon) en chemische entiteiten (zoals reactieve zuurstof radicalen) die door metabole processen in onze cellen gegenereerd worden, reageren met het drager-molecuul van de genetische informatie, namelijk het DNA. Deze agentia kunnen DNA-schade veroorzaken die kan leiden tot genetische veranderingen. De opeenstapeling van fouten in ons DNA kan in een cel leiden tot ongecontroleerde deling en uiteindelijk tot een kwaadaardige tumor. Om deze schadelijke effecten te voorkomen kunnen cellen na DNA schade inductie een reeks van afweermechanismen activeren, die gezamenlijk aangeduid wordt als de DNA schade respons (of met de Engelse term DNA damage response (DDR)). De DDR omvat verschillende DNA-herstelmechanismen en coördineert deze processen met de voortgang van de celcyclus. Dit leidt tot een efficiënte en nauwkeurige verwijdering van beschadigd DNA uit het genoom en voorkomt het ontstaan van genetische veranderingen. Echter, terwijl veel van de belangrijkste factoren die betrokken zijn bij de DDR zijn geïdentificeerd en gekarakteriseerd, is onze huidige visie op de wisselwerking tussen de verschillende factoren en processen die betrokken zijn bij de DDR beperkt. Het doel van dit proefschrift was dan ook om ons begrip van dit cruciale beschermingsprogramma te verbeteren. Om dit doel te bereiken, hebben we gebruik gemaakt van een genetische test genaamd Epistatic MiniArray Profiling (EMAP). Deze test kan epistatische (positieve) en synergistische (negatieve) interacties tussen paren van genen (en dus eiwitten) meten. Om de veranderingen in de genetische interacties veroorzaakt door bepaalde typen DNA-schade in kaart te brengen, hebben we EMAPs gegenereerd onder drie verschillende DNA-beschadigende omstandigheden. Deze genetische interactie netwerken brachten talrijke genen, waaronder bekende genen evenals nieuwe genen, aan het licht die samenwerken wanneer de cellen worden blootgesteld aan DNA-beschadigende middelen. Wij hebben genetische, biochemische en microscopische benaderingen gebruikt om de rol van een aantal van deze genen in de DDR te onderzoeken.

In hoofdstuk 2 beschrijven we het principe van EMAP, een technologie die we verder ontwikkeld hebben om genetische interacties te kunnen meten in de afwezigheid en aanwezigheid van verschillende agentia die DNA schade veroorzaken. We laten zien dat onze multi-conditionele EMAP een nuttige bron is die niet alleen vele bekende, maar ook een aantal nieuwe factoren en genetische paden betrokken bij de DDR onthult. Zo vonden we dat camptothecine (CPT), een chemische stof die dubbelstrengs-breuken (DSB) veroorzaakt tijdens de DNA-replicatie, de interacties van genen betrokken bij de reparatie van DSB verhoogde. Anderzijds vonden we dat methyl methaansulfonaat (MMS), een chemische stof die schade aan basen in het DNA veroorzaakt en daarmee DNA replicatie remt, interacties met post-replicatie herstel (PRR) genen verhoogde. Deze resultaten valideerden de kwaliteit van onze dataset. Van belang is dat deze vorm van screenen krachtiger is dan overlevings assays of expressie profilering in het vinden van associaties tussen DNA beschadigende agentia en DDR gerelateerde processen. Opmerkelijk is dat de drie afzonderlijke DNA beschadigende agentia elk een unieke set van genetische interacties induceerden, suggererend dat de DNA schade gegenereerd door elk van deze agentia specifieke DDR processen aanschakelde. Er zijn slechts enkele genetische interacties in een gemeenschappelijk netwerk gevonden die

A  
p  
p  
e  
u  
d  
i  
x



geïnduceerd werden door alle drie de geneesmiddelen. Vier sets van nieuwe genetische interacties werden verder onderzocht op moleculair niveau. We presenteren de resultaten in hoofdstuk 3 tot 6.

In hoofdstuk 3 beschrijven we de identificatie van genetische interacties tussen *RTT109*, een histon H3 acetyltransferase, en genen die coderen voor componenten van een van de translesie synthese (TLS) polymerases, namelijk Pol $\zeta$ . Deze waarnemingen spoorden ons aan om te testen of Rtt109 de mutagene en replicatieve bypass van DNA-beschadigingen door TLS polymerases beïnvloedt. Inderdaad vonden we dat het verlies van Rtt109 een afname in de mutatie frequentie na blootstelling van cellen aan UV licht veroorzaakte. Analyse van de UV-geïnduceerde mutatiespectra (op het *CAN1* gen) en de mutatie frequentie in stammen defect in Rtt109, een van de TLS polymerases of beiden suggereerde dat Rtt109 TLS beïnvloedt die gedreven wordt door Pol $\zeta$  en Pol $\eta$ . Zo identificeerden we Rtt109 als een nieuwe factor die de mutagene bypass van DNA-schade door verschillende TLS polymerases regelt.

In hoofdstuk 4 vonden we dat twee genen, *RUB1* en *UBC12*, die coderen voor de belangrijkste componenten van de neddylatie machinerie in gist, sterke negatieve interacties laten zien met tal van genen betrokken bij de celcyclus (cell cycle checkpoint genen), waaronder *RAD17*, *DDC1*, *RAD9* en *RAD24*, in reactie op CPT-geïnduceerde DNA schade. Derhalve onderzochten we een rol voor de neddylatie machinerie in de regulatie van cell cycle checkpoints na DNA schade. We vonden niet alleen dat het verlies van neddylatie leidt tot verstoringen in celcyclus progressie in aanwezigheid van CPT, maar ook tot verhoging van genominstabiliteit in cellen met een defect in cell cycle checkpoints. Neddylatie is een proces waarbij eiwitten worden gemodificeerd door de associatie met een peptide genaamd Rub1. In de groep van de belangrijkste eiwitten die gemodificeerd worden, bevinden zich Cullin RING ubiquitine ligasen (CRL), die verantwoordelijk zijn voor de afbraak van eiwitten betrokken bij vele cellulaire processen. Om verder te onderzoeken hoe neddylatie de cellulaire respons op CPT-geïnduceerde DNA-schade beïnvloedt, onderzochten we of DDR eiwitten gemodificeerd kunnen worden. Interessant genoeg, vonden we dat neddylatie invloed heeft op de steady-state niveaus van niet-CRL eiwitten zoals Mms22 en Nhp10, waarvan is aangetoond dat ze betrokken zijn bij de controle van de celcyclus en de reparatie van DNA. Wij stellen daarom voor dat neddylatie door het reguleren van de steady-state niveaus van verschillende DDR factoren van invloed is op de reparatie van DNA, celcyclus controle en stabiliteit van het genoom.

We toonden aan dat de genetische wisselwerkingen geïnduceerd door elk van de agentia zeer specifiek zijn (hoofdstuk 2). Dit suggereerde dat een unieke set van DDR gerelateerde processen wordt geactiveerd afhankelijk van het type DNA-schade dat wordt geïnduceerd. Wij vonden echter ook een groot aantal wijzigingen in de genetische interacties die werden geïnduceerd door minimaal twee van de genotoxische verbindingen. We noemden deze overlap tussen de genetische netwerken het gemeenschappelijke DDR-netwerk. In het gemeenschappelijke netwerk zaten niet alleen diverse bekende DDR factoren, maar ook onverwachte en slecht gekarakteriseerd genen zoals *IRC21*. Hoofdstuk 5 beschrijft de identificatie en karakterisering van Irc21 als nieuwe factor bij de respons op DNA-schade. We toonden aan dat de deletie van *IRC21* niet alleen de gevoeligheid van cell cycle checkpoint mutanten voor CPT en MMS onderdrukt, maar ook de geassocieerde genoom instabiliteit

en deficiënties in celcyclus regulatie en DNA-herstel. Verder vonden wij dat het verlies van IRC21 cellen overgevoelig maakt voor MMS in combinatie met de TOR-remmer rapamycine, een verbinding die kan leiden tot een verhoogde en verlaagde aanwezigheid van eiwitten (via het proces van autophagy), met inbegrip van factoren betrokken bij de DDR. Dit suggereert dat Irc21 invloed kan hebben op de DDR door het reguleren van de steady-state niveaus van verschillende DDR eiwitten.

Hoofdstuk 6 rapporteert over de negatieve interactie (MMS en CPT-geïnduceerd) tussen het DNA-reparatie-gen *SAE2* en een eiwitfosfatase coderend gen, *PPH3*. We hebben geprobeerd om te begrijpen hoe deze DNA reparatie factor en eiwitfosfatase samenwerken om de signalering en de reparatie van DNA-schade te coördineren. We vonden dat cellen deficiënt voor *SAE2* en *PPH3* ernstige gebreken in de regulatie van de cel cyclus in reactie op DNA-schade laten zien. Bovendien was het herstel van DNA schade geïnduceerd door de alkylerende stof MMS verminderd in deze cellen, terwijl die van nuclease-geïnduceerde DNA dubbelstrengs breuken onaangetast bleef in vergelijking met die in de reparatie-deficiënte *sae2* cellen. Wij stellen voor dat de samenwerking tussen *Sae2* en *Pph3* belangrijk is voor een efficiënte reparatie van DNA en activatie van cell cycle checkpoints in reactie op door MMS veroorzaakte schade in replicatievorken, maar dat die samenwerking geen rol speelt in de reparatie van DSB.

Concluderend blijkt onze multi-conditionele genetische interactie screen een extreem krachtige methode om de wisselwerking tussen factoren of signaalwegen die essentieel zijn voor de verdediging van de cel tegen de nadelige gevolgen van DNA-schade te ontrafelen. In combinatie met functionele studies van deze genetische interacties kan mechanistisch inzicht in de rol van nieuwe factoren in de orkestratie van de DDR worden verkregen. Gezien het feit dat de DDR sterk is geconserveerd van gist tot mens verwachten we dat onze genetische interactie kaarten ook kennis zullen verschaffen over de menselijke DDR en de bijbehorende ziektes.

*A  
p  
p  
e  
n  
d  
i  
x*

## ENGLISH SUMMARY

The genetic information required for the generation of cellular components and their organization is fixed in our genes. It is therefore important to ensure that all cells in the body function properly and that their genetic information remains intact. Various physical and chemical agents within our environment (such as UV radiation from the sun) or chemical entities (such as reactive oxygen species) generated by metabolic processes in our cells interact with the carrier-molecule of genetic information namely the DNA and cause DNA damage that can lead to mutations. The accumulation of errors in our DNA can cause a cell to divide uncontrollably and to become cancerous. Hence to avoid these adverse effects cells trigger a series of defense mechanisms upon DNA damage induction, which is collectively referred to as the DNA damage response (DDR). The DDR involves distinct DNA repair mechanisms and coordinates these processes with cell cycle progression to promote efficient and accurate removal of damaged DNA from the genome. However, while many of the key factors involved in the DDR have been identified and characterized, our current view on the interplay between the different factors and processes involved in the DDR is limited. The objective of this thesis is therefore to improve our understanding of this crucial protection program. To achieve this goal, we used a high throughput genetic screening approach called Epistatic MiniArray Profiling (EMAP). This technique can measure epistatic (positive) and synergistic (negative) interactions between pairs of genes. To assess the changes in genetic interactions induced by certain types of DNA damage, we generated EMAPs under three different DNA damaging conditions. These genetic interaction networks revealed numerous genes (and thus proteins), including well-known genes as well as several novel genes, that interact and collaborate when cells are exposed to DNA damaging agents. We have used genetic, biochemical and microscopical approaches to investigate the roles of some of these genes in the DDR.

In chapter 2, we describe the principle of EMAP, a technology that we further developed to be able to measure genetic interactions in unperturbed conditions, as well as in the presence of different DNA damaging agents. We show that our multi-conditional EMAP is a useful resource that not only reports on many well known, but also several novel factors and pathways involved in the DDR. For example, we found that camptothecin (CPT), an agent that causes double strand-breaks (DSB) during DNA replication, increase the interactions for genes involved in DSB repair. On the other hand, methyl methanesulfonate (MMS), a drug that induces base damages and the stalling of replication forks, increases interactions for post-replication repair (PRR) genes. These results validated the quality of our dataset. Importantly, we demonstrate that this type of screening is more powerful than single mutant sensitivity screens or expression profiling in highlighting associations between damaging agent and DDR pathway. Remarkably, the three distinct DNA damaging agents each induced a unique set of genetic interactions, suggesting that the lesions generated by each agent trigger a highly specific DDR. Only few genetic interactions were found in a common network induced by all three drugs. Four sets of novel genetic interactions were further investigated at the molecular level. We present the results of this work in chapter 3 to 6.

In chapter 3, we describe the identification of genetic interactions between *RTT109*, a histone H3 acetyltransferase, and genes encoding for components of one of the translesion synthesis polymerases (TLS) Pol $\zeta$ . These observations prompted us to test whether Rtt109

affects the mutagenic bypass of DNA lesions by TLS polymerase. Indeed, we found that the loss of *Rtt109* causes a decrease in the rate of mutations generated by TLS polymerases after exposure of cells to UV light. Analysis of the UV-induced mutation spectra (at the *CAN1* gene) and mutation rates in strains defective for either *Rtt109* or one of the TLS polymerases or both suggests that *Rtt109* affects translesion synthesis driven by Pol $\zeta$  and Pol $\eta$ . Thus, we identify *Rtt109* as a novel factor that regulates the mutagenic bypass of DNA lesions driven by different TLS polymerases.

In chapter 4, we found that two genes, *RUB1* and *UBC12* which encode key components of the yeast neddylation machinery, displayed strong negative interactions with numerous DNA damage checkpoint genes, including *RAD17*, *DDC1*, *RAD9* and *RAD24*, in response to CPT-induced DNA damage. Thus, we investigated a role for the neddylation machinery in DNA damage checkpoint control. We not only found that loss of neddylation leads to perturbations in cell cycle progression in the presence of CPT, but also increases genome instability in checkpoint-deficient cells. Neddylation is a process by which proteins are modified through the attachment of a peptide called Rub1. Among the prime targets are Cullin RING ubiquitin ligases (CRLs), which are responsible for the degradation of proteins involved in many cellular processes. To further explore how neddylation could affect the cellular response to CPT-induced DNA damage, we examined whether this process would target proteins involved in the DDR. Interestingly, we found that neddylation has an impact on the steady state levels of non-CRLs proteins such as *Mms22* and *Nhp10*, which been shown to be involved in cell cycle control and DNA repair. Thus, we propose that the neddylation by regulating the steady state levels of distinct DDR factors affects DNA repair, cell cycle control and genome stability.

We showed that the genetic interactions induced by each drug are very specific (chapter 2). This suggested that a unique set of DDR pathways is triggered depending on the type of DNA damage that is induced. However, we also found a significant number of changes in the genetic interactions that were induced by at least two of the genotoxic compounds. We called this overlap between the genetic networks the common DDR network. The common network not only included several known DDR factors, but also revealed unanticipated and poorly characterized genes such as *IRC21*. Chapter 5 describes the identification and characterization of *Irc21* as a novel factor involved in the response to DNA damage. We showed that deletion of *IRC21* not only suppresses the sensitivity of checkpoint mutants to CPT and MMS, but also their genome instability and their cell cycle and DNA repair defects. In addition, we observed that loss of *IRC21* renders cells hypersensitive to MMS when combined with the TOR inhibitor rapamycin, a compound that can lead to increased and decreased abundance of proteins (via the autophagy pathway), including factors involved in the DDR. This suggests that *Irc21* may affect the DDR by regulating the steady state levels of distinct DDR proteins.

Chapter 6 reports on the negative interaction (MMS and CPT-induced) between the DNA repair gene *SAE2* and a protein phosphatase encoding gene, *PPH3*. We attempted to understand how this DNA repair factor and protein phosphatase would interact to coordinate the signaling and repair of DNA damage. We found that cells deficient for *SAE2* and *PPH3* display severe checkpoint defects in response to DNA damage. Moreover, the repair of DNA damage induced by the alkylating agent MMS was impaired in these cells, whereas repair of

nuclease-induced DNA double stranded breaks remained unaffected when compared to that in the repair-deficient *sae2Δ* cells. We propose that the co-operation between Sae2 and Pph3 is important for efficient DNA repair and checkpoint activation in response to replication fork-associated damage induced by MMS, but is dispensable for DSB repair.

In conclusion, our multi-conditional genetic interactions screen has proven to be an extremely powerful method to unravel the interconnections between factors or signaling pathways that regulate cellular responses to various types of DNA damage. In combination with functional studies of these genetic interactions, mechanistic insight into the role of novel factors in the orchestration of the DDR can be obtained. Given that the DDR is highly conserved from yeast to man we anticipate that our genetic interaction map will also inform on the human DDR and its associated diseases.

*A  
p  
p  
e  
n  
d  
i  
x*

## RESUME EN FRANCAIS

L'information génétique nécessaire à la production de composants cellulaires et à leur organisation est fixée dans nos gènes. Il est donc important, pour que toutes cellules du corps fonctionnent correctement, que leur information génétique reste intacte. Divers agents physiques et chimiques dans notre environnement (comme les rayonnements UV du soleil) ou des entités chimiques (tels que les espèces réactives de l'oxygène) générés par les processus métaboliques dans nos cellules endommagent la molécule support de l'information génétique, l'ADN. Ces dommages de l'ADN peuvent conduire à des mutations. Hors, l'accumulation d'erreurs (ou mutations) dans notre ADN peut amener une cellule à se diviser de manière incontrôlée et donc à devenir cancéreuse. Par conséquent, pour éviter ces effets néfastes, les cellules déclenchent une série de mécanismes de défense lors de l'induction de dommages de l'ADN. Ces mécanismes de défense sont collectivement appelés réponses aux dommages de l'ADN (ou DNA damage response-DDR-en anglais). Le DDR coordonne l'activité des différentes voies de réparation de l'ADN avec la progression du cycle cellulaire afin de promouvoir l'élimination efficace et précise des lésions de l'ADN. Cependant, alors que bon nombre des facteurs clés impliqués dans le DDR ont été identifié et caractérisé, notre point de vue actuel sur les interactions entre les différents facteurs et les processus impliqués dans le DDR est limité. L'objectif de cette thèse est donc d'améliorer notre compréhension de ce programme de protection crucial. Pour atteindre cet objectif, nous avons utilisé une approche de criblage génétique à haut débit appelé Epistatic MiniArray profiling (EMAP). Cette technique permet de mesurer les interactions épistatiques (positives) et synergiques (négatives) entre des paires de gènes. Afin de savoir si ces interactions entre gènes changent lors de l'induction de certains types de lésions de l'ADN, nous avons généré des EMAPs sous trois conditions induisant différents types de lésions dans l'ADN. Ces réseaux d'interactions génétiques ont révélé de nombreuses interactions entre gènes déjà connus ou nouveaux lorsque les cellules sont exposées à des agents endommageant l'ADN. Nous avons utilisé des approches génétiques, biochimiques et microscopiques afin d'explorer le rôle de certains de ces gènes (et interactions) dans les réponses aux dommages de l'ADN.

Dans le chapitre 2, nous décrivons le principe de l'EMAP, une technologie que nous avons développé pour pouvoir mesurer des interactions génétiques dans des conditions normales ainsi qu'en présence de différents agents endommageant l'ADN. Nous montrons que notre EMAP multi-conditionnelle est une ressource très utile pour révéler les facteurs et voies de signalisations impliqués dans le DDR. Cette technique a permis de retrouver des éléments connus du DDR mais elle en a aussi mis en évidence de nouveaux. Ainsi, nous avons constaté que la camptothécine (CPT), un agent qui provoque des cassures double-brins (CDB) lors de la réplication de l'ADN, augmente les interactions des gènes impliqués dans la réparation des CDB. D'autre part, le métyl méthanesulfonate (MMS), une drogue qui provoque des dommages des bases de l'ADN et le blocage des fourches de réplication, augmente les interactions des gènes impliqués dans les mécanismes de réparation post-réplicatifs (RPR). Ces résultats valident la qualité de nos données. Et surtout, nous avons démontré que ce type de criblage est statistiquement plus puissant pour révéler des associations entre agents endommageant l'ADN et voies de réparations que les criblages de sensibilité ou analyse de profile d'expression fait avec des simples mutants. De façon remarquable, les trois agents qui endommagent l'ADN de manières distinctes, induisent chacun un ensemble unique d'interactions génétiques. Ceci suggère que les lésions produites par chaque agent

A  
p  
p  
e  
u  
d  
i  
x



déclenchent une DDR très spécifique. Seulement quelques interactions génétiques ont été trouvés dans le réseau commun, c'est à dire induit par les trois agents. Nous avons choisi de poursuivre l'étude de quatre séries de nouvelles interactions génétiques. Nous présentons ces résultats dans les chapitres 3 à 6.

Dans le chapitre 3, nous décrivons l'identification des interactions génétiques entre *RTT109*, une histone H3 acétyltransférase, et les gènes codant pour des composants de l'une des polymérase de synthèse translésionnelle (TLS) Pol $\zeta$ . Ces observations nous ont amené à tester si *Rtt109* affecte le contournement mutagène des lésions de l'ADN par les polymérase TLS. En effet, nous avons constaté que la perte de *Rtt109* entraîne une diminution du taux de mutations générées par les polymérase TLS après l'exposition des cellules à la lumière UV. L'analyse des spectres de mutations induits par les UV (au niveau du gène *CAN1*) et les taux de mutation dans les souches défectueuses soit pour *Rtt109* ou pour l'une des polymérase TLS ou les deux suggèrent que *Rtt109* affecte la synthèse translésionnelle médiée par Pol $\zeta$  et Pol $\eta$ . Ainsi, nous avons identifié *Rtt109* comme un nouveau facteur qui régule le contournement mutagène des lésions de l'ADN effectué par différentes polymérase TLS.

Dans le chapitre 4, nous avons constaté que deux gènes, *RUB1* et *UBC12*, qui codent pour des éléments clés de la machinerie de neddylation chez la levure, montrent de fortes interactions négatives avec de nombreux gènes signalant la présence de dommages dans l'ADN (ou gène du checkpoint des dommages de l'ADN), comme *RAD17*, *DDC1*, *RAD9* et *RAD24*, en réponse aux lésions induites par la CPT. Ainsi, nous avons étudié le rôle du mécanisme de neddylation dans le contrôle du checkpoint des dommages de l'ADN. Nous avons non seulement constaté que la perte de neddylation conduit à des perturbations dans la progression du cycle cellulaire en présence de CPT, mais aussi augmente l'instabilité du génome dans les cellules déficientes en checkpoint. La neddylation est un processus par lequel les protéines sont modifiées par l'attachement d'un peptide appelé Rub1. Les cibles principales du processus de neddylation sont les Cullin RING ubiquitine ligases (CRL). Elles sont responsables de la dégradation de protéines impliquées dans de nombreux processus cellulaires. Pour explorer davantage comment le processus de neddylation pourrait affecter la réponse cellulaire aux dommages de l'ADN induits par CPT, nous avons regardé s'il cible des protéines impliquées dans le DDR. De façon intéressante, nous avons constaté que la neddylation a un impact sur les niveaux de protéines non-LCR comme *Mms22* et *Nhp10*, deux protéines impliquées dans le contrôle du cycle cellulaire et la réparation de l'ADN. Ainsi, nous proposons que la neddylation régule les niveaux protéiques de facteurs impliqués dans la DDR et par conséquent affecte réparation de l'ADN, le contrôle du cycle cellulaire et la stabilité du génome.

Nous avons montré que les interactions génétiques induites par chaque agent endommageant l'ADN sont très spécifiques (chapitre 2). Cela suggère qu'un ensemble unique de voies de la DDR est déclenché en fonction du type de lésion induit dans l'ADN. Cependant, nous avons également constaté un nombre important de changements dans les interactions génétiques qui ont été induites par au moins deux des composés génotoxiques. Nous avons appelé cette intersection entre les réseaux génétiques: le réseau DDR commun. Le réseau commun comprend non seulement plusieurs facteurs connus de la DDR, mais révèle également des gènes non-caractérisés comme *IRC21*. Le chapitre 5 décrit l'identification et la caractérisation de *Irc21* comme un nouveau facteur impliqué dans la réponse aux dommages

de l'ADN. Nous avons montré que l'absence de *IRC21* non seulement supprime la sensibilité des mutants du checkpoint à la CPT et au MMS, mais aussi leur instabilité génomique, leurs défauts de progression dans le cycle cellulaire et de réparation de l'ADN. En outre, nous avons observé que la perte de *IRC21* rend les cellules hypersensibles au MMS lorsqu'il est combiné avec la rapamycine, un inhibiteur de TOR. La rapamycine est un composé qui peut conduire à une augmentation et une diminution de l'abondance de protéines (par la voie de l'autophagie). Ceci suggère que *Irc21* peut affecter la DDR en régulant l'abondance de certaines protéines de la DDR.

Le chapitre 6 rapporte sur l'interaction négative (MMS et CPT-induite) entre le gène de réparation de l'ADN, *SAE2* et un gène codant pour une phosphatase, *PPH3*. Nous avons tenté de comprendre comment ce facteur de réparation de l'ADN et la protéine phosphatase interagissent pour coordonner la signalisation et la réparation des dommages à l'ADN. Nous avons constaté que les cellules déficientes pour *SAE2* et *PPH3* présentent de graves défauts de signalisation des lésions de l'ADN (checkpoint). Par ailleurs, la réparation des lésions de l'ADN, induites par le MMS, est altérée dans ces cellules doubles mutantes, tandis que la réparation des cassures double brins (CDB) induites par une nucléase se fait normalement, au contraire des cellules simple mutante pour *SAE2*. Nous proposons que la coopération entre *Sae2* et *Pph3* est importante pour la réparation de l'ADN et l'activation du checkpoint en réponse aux lésions induites par le MMS, mais est dispensable pour la réparation des CDB.

En conclusion, notre criblage génétique multi-conditionnel s'est avérée être une méthode extrêmement puissante pour mettre en évidence les interconnexions entre les facteurs ou les voies de signalisation qui régulent les réponses cellulaires à divers types de dommages de l'ADN. Les études fonctionnelles de ces interactions génétiques permettront de comprendre le rôle de nouveaux facteurs dans les mécanismes impliqués dans la DDR. Étant donné que la DDR est hautement conservée de la levure à l'homme, nous prévoyons que notre carte d'interactions génétiques informera également sur la DDR humaine et ses maladies associées.

*A  
p  
p  
e  
n  
d  
i  
x*

**ACKNOWLEDGEMENTS**

It was a long way with ups and downs but eventually the trip is over. This work would not have been feasible without the help and the support of a lot of people that I would like to thank.

Haico, you gave me the chance to start and complete this work successfully. I am very grateful for your trust and persistence in trying to get the best science out of me.

Leon, thank you for being so helpful and supportive in pushing me to complete my thesis.

Rohith, you have been a great collaborator. It was a pleasure to work with you. I learned a lot from your perseverance and scientific skills. Nevan and Trey, the generation and the interpretation of the EMAP data would have been impossible without you.

Dear present or former members of the van Attikum crew, you have been so patient and encouraging when I was so gloomy. I hope you will also remember our good time. To all of you and to the other people of the Toxicogenetics department, a big thanks for your help, technical and scientific advices and more importantly for your smiles during these 5 years.

I crossed the way of a lot of people during my PhD time in Leiden. To all of you that I met in the Netherlands or in the US, who are still in the Netherlands or already having a new life somewhere else in the world, you made my life beside work very enjoyable. Thanks a lot.

I have a great family! Maman, Sam, Ben et Dam, je n'aurais pas pu tenir si dans mes moments de doutes, de fatigue ou de désespoir, vous n'aviez pas été là pour croire en moi. Melou et Anso, votre amitié pendant cette longue période de thèse a été très importante pour moi. Akim, Na gbeï. Papa, cette thèse est beaucoup pour toi.

*A  
p  
p  
e  
u  
d  
i  
x*

*A  
p  
p  
e  
n  
d  
i  
x*

**CURRICULUM VITAE**

Aude Guérolé was born the 31st of October 1983 in Léon, France. In September 2002, she entered the classes préparatoires aux grandes écoles of Chateaubriant in Rennes, which consisted of 2 years of preparatory courses to join schools for Science & Engineering. In September 2004, she decided to continue her studies with a bachelor in Life Sciences at the Pierre and Marie Curie University in Paris. Then, she completed a Master in Molecular and Cellular Genetics. It was during this part of her studies that she got particularly interested in the field of DNA damage repair. To confirm her sensibility for this field, she first did an internship of 6 months in the Lab of Nico Dantuma at the Karolinska Institut in Stockholm, where she studied the yeast repair and shuttling factor Rad23. Her second internship on the mammalian repair factor Rad54 was done in the laboratory of Roland Kanaar at the Erasmus MC in Rotterdam. In February 2008, she joined the laboratory of Haico van Attikum to begin her PhD with the aim of investigating how the DNA damage response is coordinated in the context of chromatin. For her PhD research she worked for about 6 months in the laboratory of Nevan Krogan at the University of California, San Francisco (UCSF), where she performed a genetic interaction screen called the EMAP technology. Then, she was invited for 3 months to work in the laboratory of Trey Ideker at the University of California, San Diego (UCSD) to analyze the EMAP dataset generated in the laboratory of Nevan Krogan. She recently obtained a prestigious grant from the French Foundation for Cancer Research (ARC), which she will use to continue her carrier in the laboratory of Bijan Sobhian at the Cancer Research Institut of Montpellier (IRCM).

*A  
p  
p  
e  
n  
d  
i  
x*

**PUBLICATIONS**

1. **Guéno**lé A, Srivas R, Vreeken K, Wang ZZ, Wang S, Krogan NJ, Ideker T, van Attikum H. Dissection of DNA damage responses using multiconditional genetic interaction maps. *Mol Cell*. 2013 Jan 24;49(2):346-58.
2. Hegnauer AM, Hustedt N, Shimada K, Pike BL, Vogel M, Amsler P, Rubin SM, van Leeuwen F, **Guéno**lé A, van Attikum H, Thomä NH, Gasser SM. An N-terminal acidic region of Sgs1 interacts with Rpa70 and recruits Rad53 kinase to stalled forks. *EMBO J*. 2012 Sep 12;31(18):3768-83.
3. Ryan C, Greene D, **Guéno**lé A, van Attikum H, Krogan NJ, Cunningham P, Cagney G. Improved functional overview of protein complexes using inferred epistatic relationships. *BMC Syst Biol*. 2011 May 23;5:80.
4. Agarwal S, van Cappellen WA, **Guéno**lé A, Eppink B, Linsen SE, Meijering E, Houtsmuller A, Kanaar R, Essers J. ATP-dependent and independent functions of Rad54 in genome maintenance. *J Cell Biol*. 2011 Mar 7;192(5):735-50.
5. Bandyopadhyay S, Mehta M, Kuo D, Sung MK, Chuang R, Jaehnig EJ, Bodenmiller B, Licon K, Copeland W, Shales M, Fiedler D, Dutkowski J, **Guéno**lé A, van Attikum H, Shokat KM, Kolodner RD, Huh WK, Aebersold R, Keogh MC, Krogan NJ, Ideker T. Rewiring of genetic networks in response to DNA damage. *Science*. 2010 Dec 3;330(6009):1385-9. 21127252.
6. Hannum G, Srivas R, **Guéno**lé A, van Attikum H, Krogan NJ, Karp RM, Ideker T. Genome-wide association data reveal a global map of genetic interactions among protein complexes. *PLoS Genet*. 2009 Dec;5(12):e1000782.



